20th Real Time Conference

Padova, Italy, June 5-10, 2016

Evolution of Data Acquisition and Processing in Medical Imaging with Radiation

Roger Lecomte, Ph.D.

CIMS Centre d'imagerie moléculaire de Sherbrooke

CENTRE DE RECHERCHE | CHUS

Medical Imaging Axis

GRAMS

UNIVERSITÉ DE SHERBROOKE

Department of Nuclear Medicine & Radiobiology

Outline

- Background
- Historical review of PET
- Preclinical PET scanner developments
  - 1st APD PET system
  - LabPET™ developments
- Current and future directions
  - Multimodality PET/CT
  - Time-of-flight PET

Medical Imaging Modalities

Using ionizing radiation:

- X-ray
  - Radiography
  - Computed Tomography (CT)
  - Spectral CT
- Nuclear medicine
  - Planar scintigraphy (gamma camera)
  - Single Photon Emission Computed Tomography (SPECT)
  - Positron Emission Tomography (PET)

Using non-ionizing radiation:

- Ultrasound (US)
- Magnetic Resonance Imaging (MRI)
- Optical
- ...

Imaging Modalities using Radiation

CT

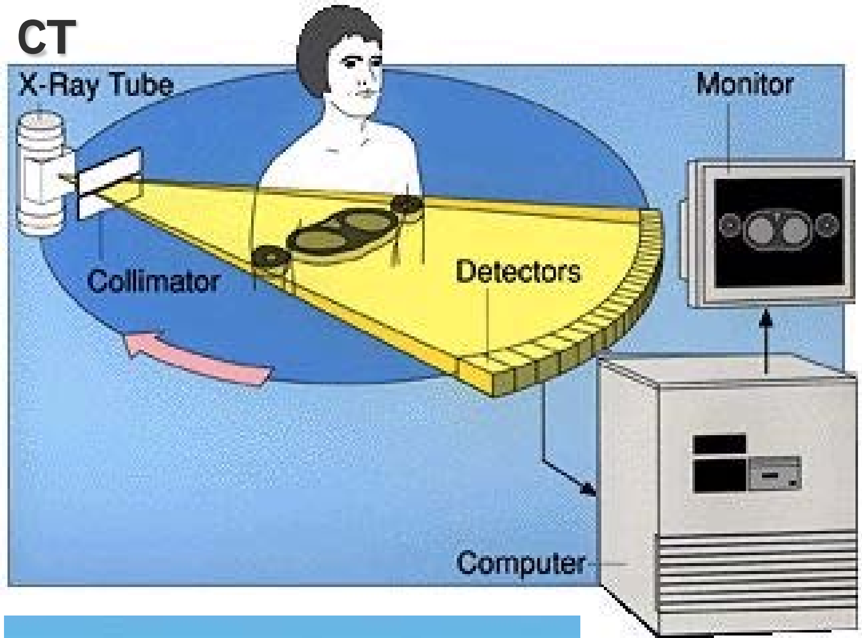

PET

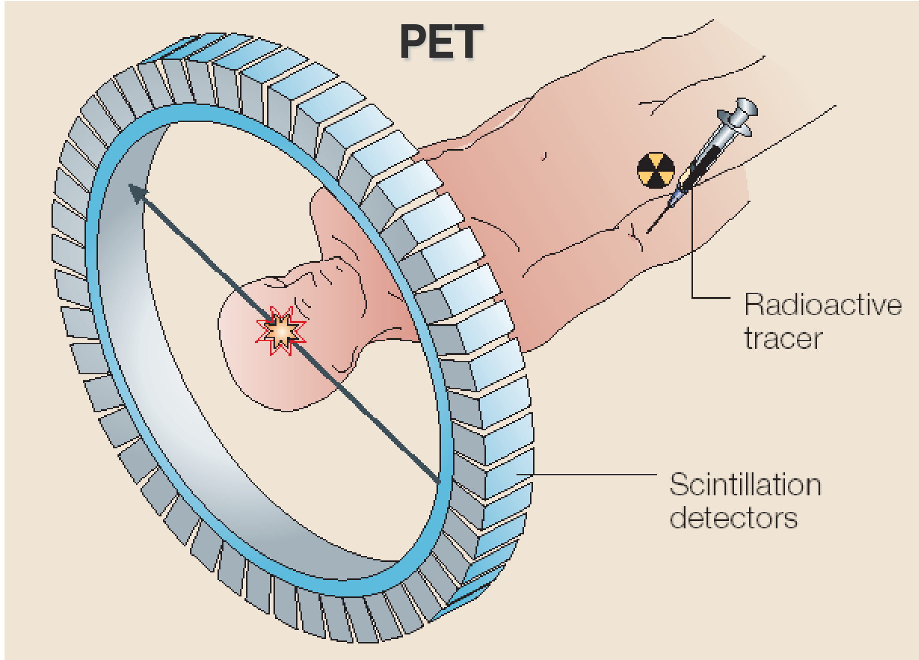

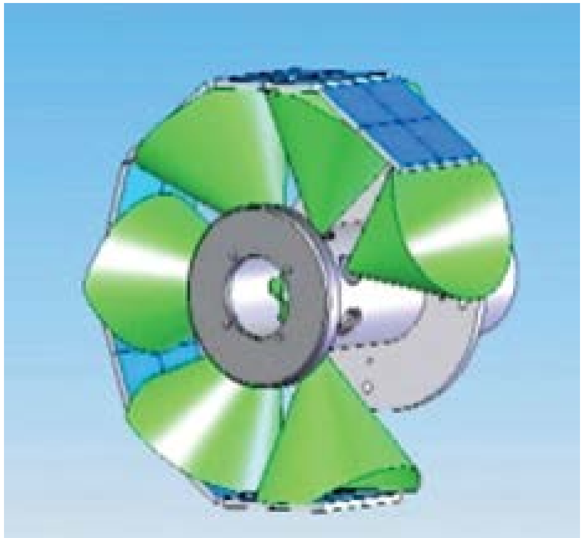

SPECT

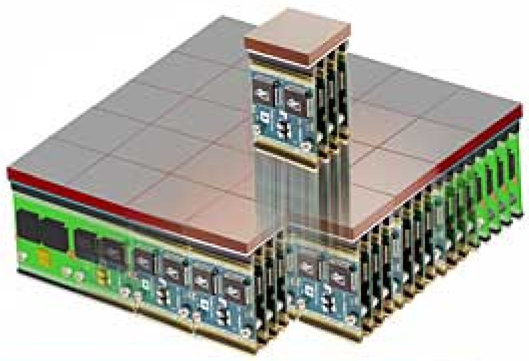

Panel detectors

- **Compact arrays of pixel detectors**

Information Required for Medical Imaging

Parameter	CT	SPECT	PET
Position	✓✓	✓	✓*
Energy	(✓)**	✓✓	✓
Time	Frame rate	-	✓✓ ToF***

* (x,y) + Depth-Of-Interaction (DOI)

** Spectral counting CT

*** Time-of-flight

Positron Emission Tomography (PET)

Patient in PET scanner

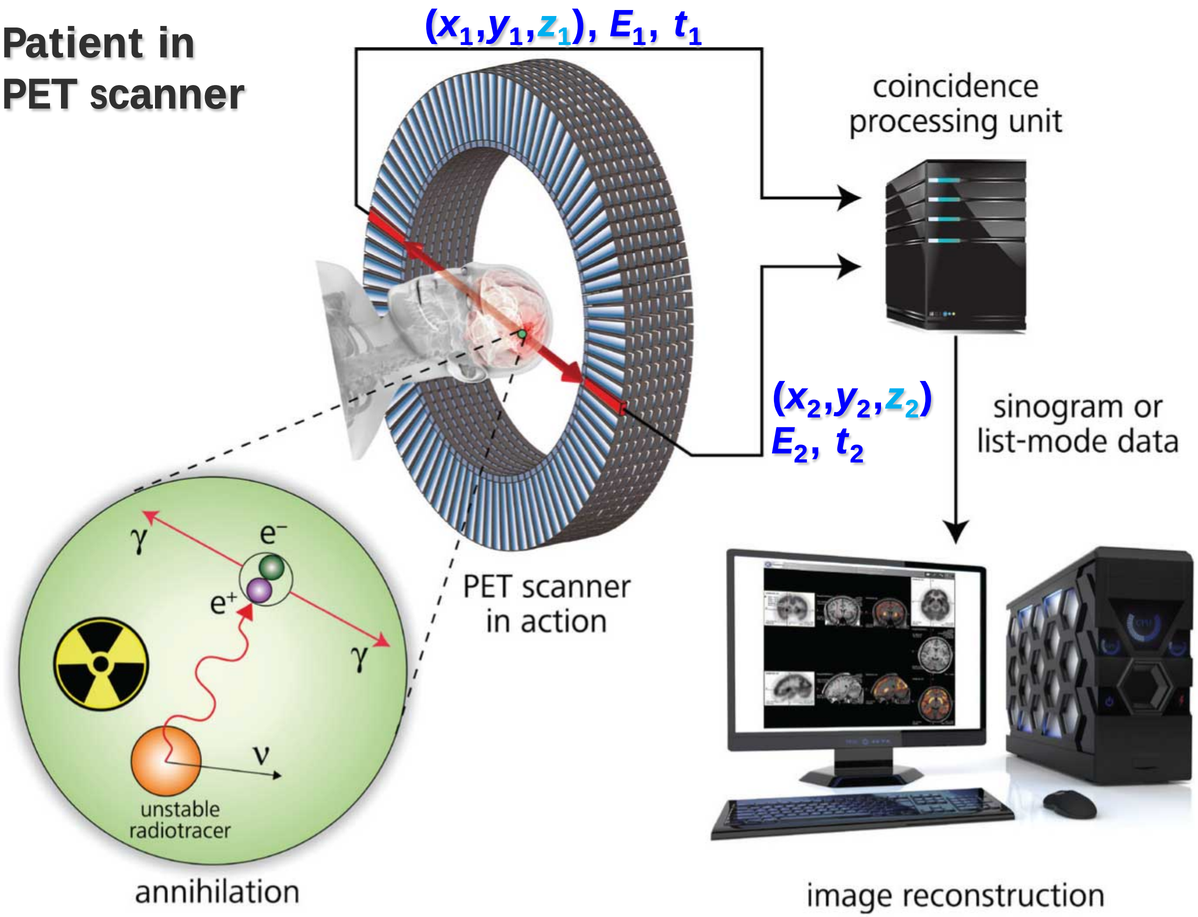

Brain PET Image

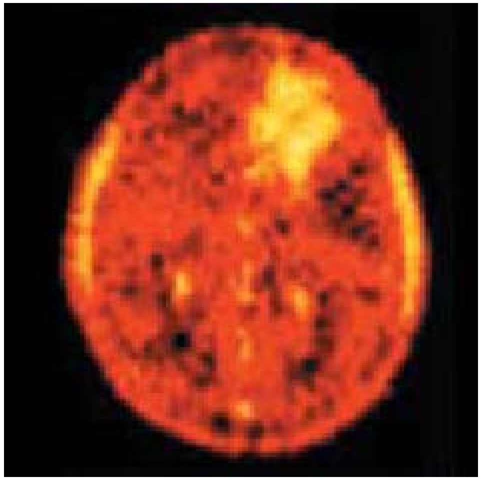

Time-Activity curves

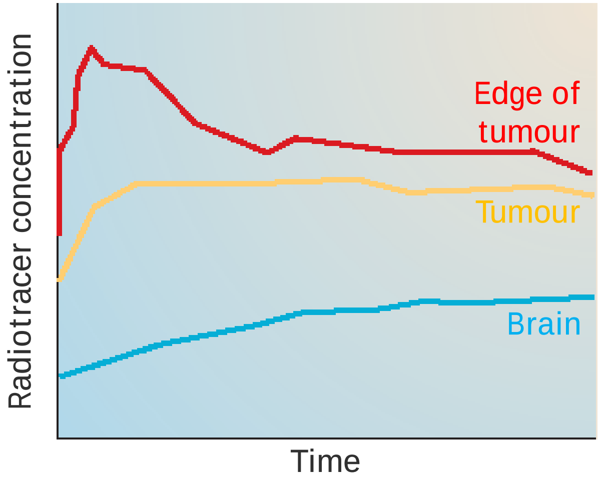

- ✓ **Dynamic imaging of *in vivo* processes**
- ✓ **Tracer concentration *vs* Time**

First Medical Application of Positrons - 1952

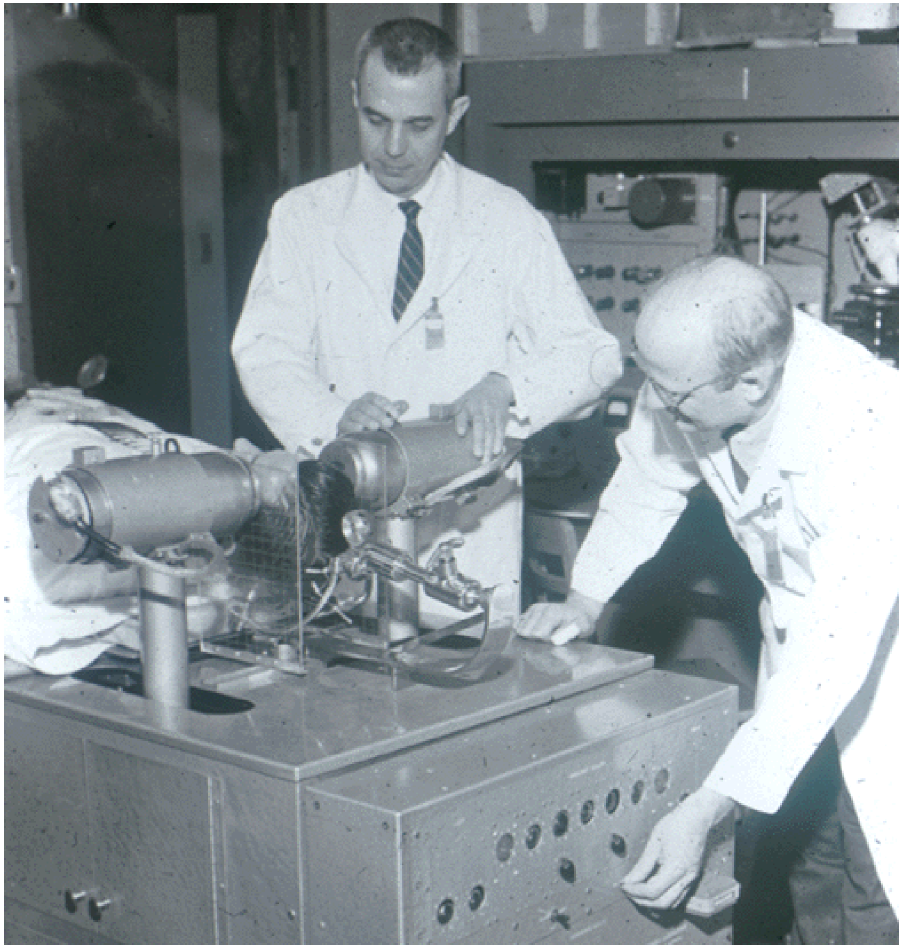

- Idea to use annihilation radiation for measuring internal structures first proposed in 1951 by Sweet[1] and Wrenn[2].
- First clinical positron imaging device, two coincident NaI(Tl)-PMT detectors with 2-D scanning motion, used in 1952 to obtain images of radiotracer distribution in the brain by Brownell at Massachusetts General Hospital.[3]

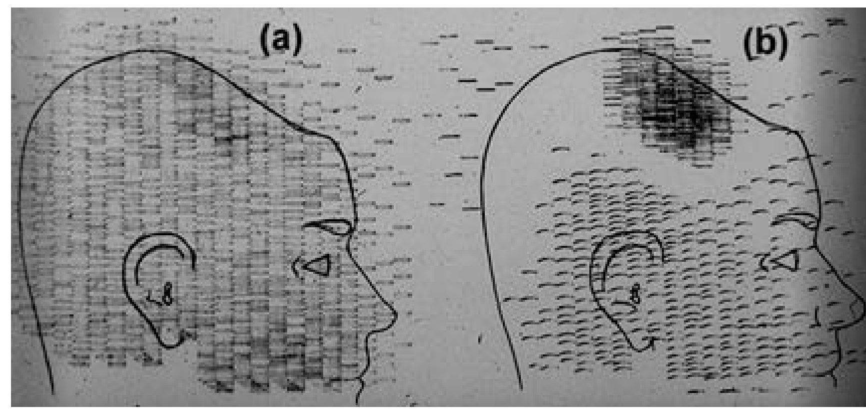

[1] Sweet, W.H. The use of nuclear disintegration in diagnosis and treatment of brain tumors. *N Engl J Med* 245:875–878; 1951.

[2] Wrenn, F.R. Jr., Good, M.L., Handler, P. The use of positron emitting radioisotopes for localization of brain tumors. *Science* 113:525–527; 1951.

[3] Brownell, G.L., Sweet W.H. *Nucleonics* 11:40-45; 1953.

Early Positron Imaging Devices

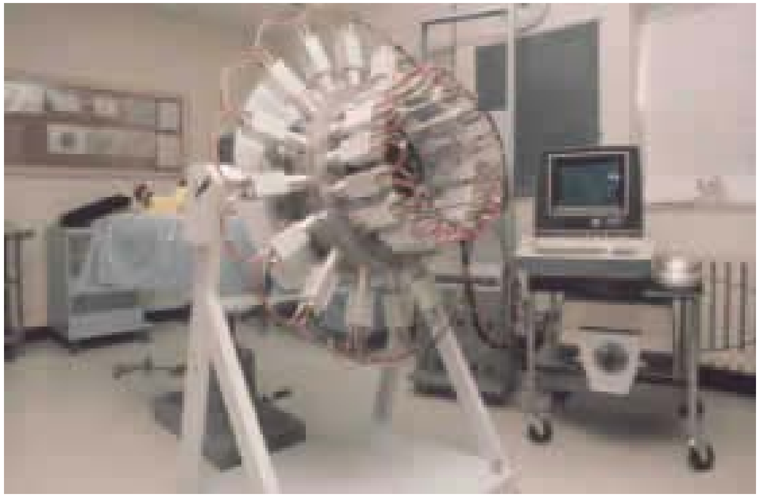

1973: "Positome I", first circular ring PET scanner, 32 NaI(Tl) detectors. Built at BNL and used for blood flow studies with ^{77}Kr. Transferred to Montreal Neurological Institute in 1975.

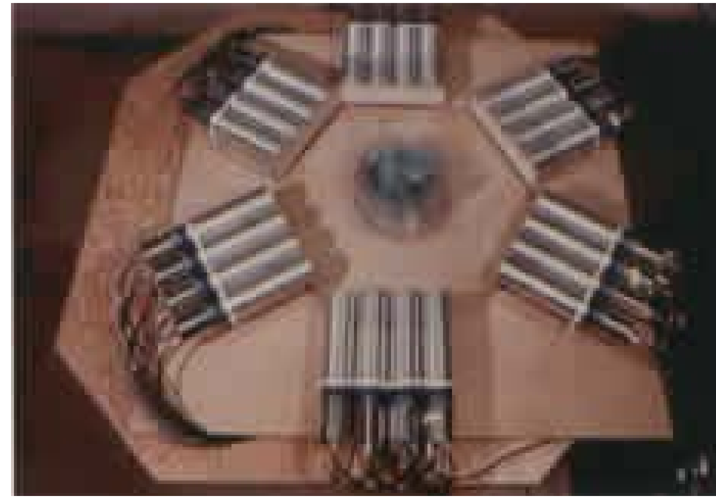

1973-74: "PETT II" hexagonal array, 24 NaI(Tl) detectors, Ter-Pogossian et al., Washington University, St.Louis.

1977-78: Positome II
First BGO PET scanner
64 BGO detectors
C.J. Thompson, Montreal Neurological Institute.

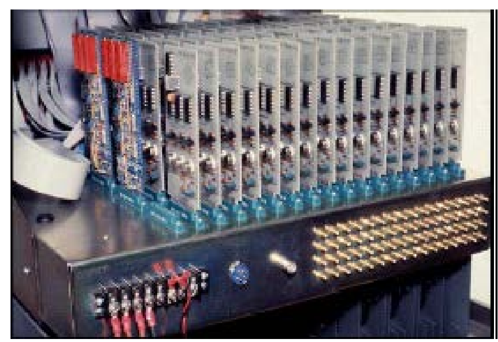

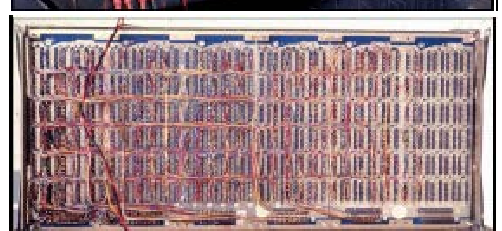

The Race to Higher Resolution

- 1977: Positome II-IIIp: 64-128 BGO detectors → ~1.5 cm FWHM
- 1978: PETT III / Ortec ECAT II (1st commercial PET scanner)
  - 96 NaI(Tl) detectors → 9.5 mm FWHM
- 1981: Donner-280: 280 NaI(Tl) → BGO detectors
  - 8 mm NaI(Tl) / 9.5 mm BGO → ~8 mm FWHM
- 1986: Donner-600: 600 BGO detectors
  - ✓ 3 mm BGO → 2.6 mm FWHM
  - ✗ Single detector ring

? ***Semiconductor detectors***

? ***Solid state photodetectors***

✓ ***Crystal coding***

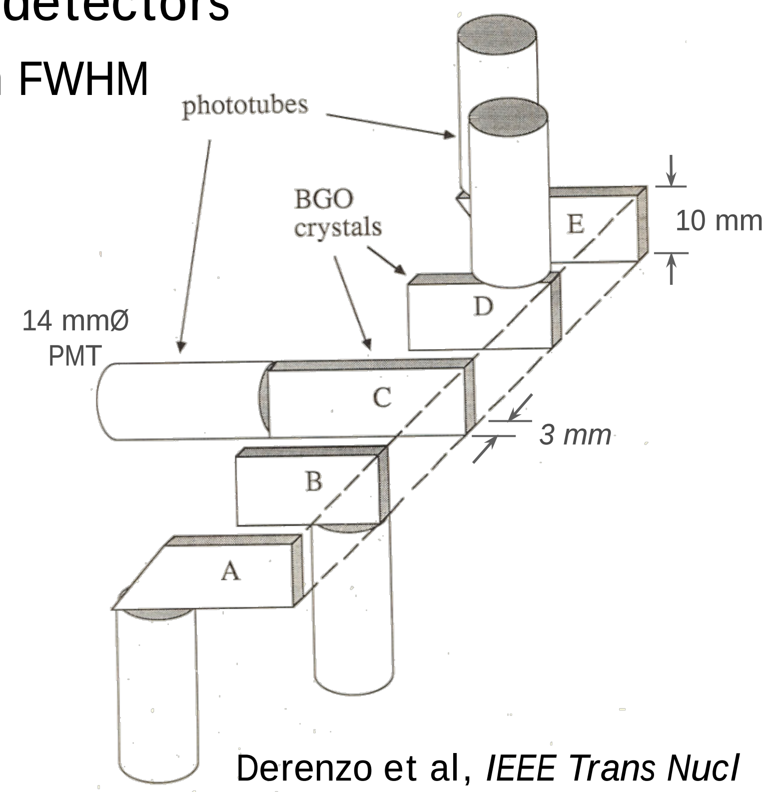

Derenzo et al, *IEEE Trans Nucl Sci* 34:321-5, 1987

The Race to Higher Resolution

- 1977: Positome II-IIIp: 64-128 BGO detectors → ~1.5 cm FWHM
- 1978: PETT III / Ortec ECAT II (1st commercial PET scanner)
  - 96 NaI(Tl) detectors → 9.5 mm FWHM
- 1981: Donner-280: 280 NaI(Tl) → BGO detectors
  - 8 mm NaI(Tl) / 9.5 mm BGO → ~8 mm FWHM
- 1986: Donner-600: 600 BGO detectors
  - 3 mm BGO → 2.6 mm FWHM
- 1990: BGO block detectors
  - 4 mm BGO → 3.8 mm FWHM
- 1998: LSO quadrant sharing detectors
  - 4 mm LSO → 2.8 mm FWHM

Casey & Nutt, *IEEE Trans Nucl Sci* 33:460-3, 1986

Block Detectors for PET Scanners

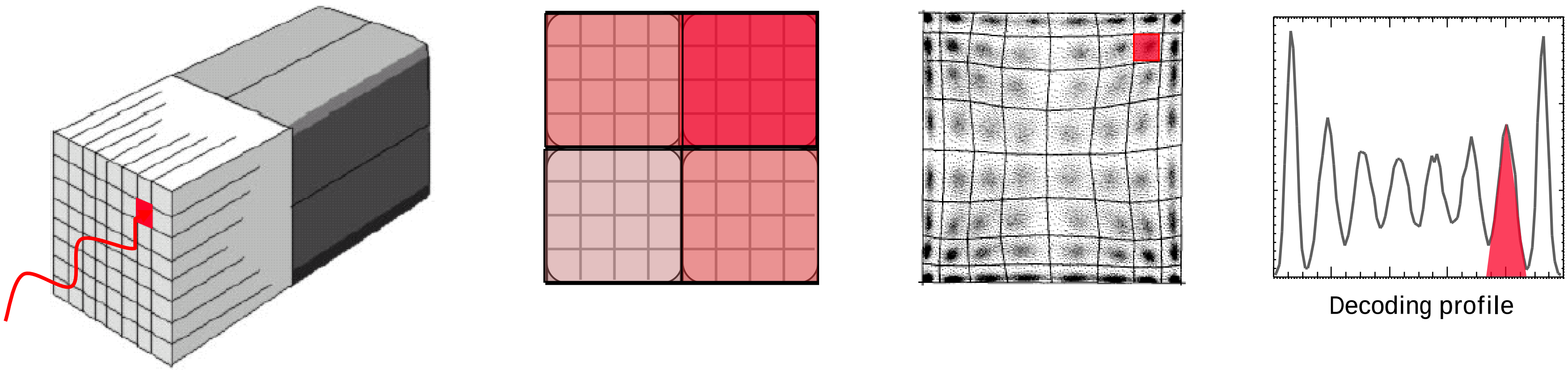

$$R_x = \frac{A+B}{A+B+C+D}$$

$$R_y = \frac{A+C}{A+B+C+D}$$

- Up to 361 (19×19) pixels in 4 electronic channels
- Can be processed by analog or digital electronics

Evolution of PET Image Quality

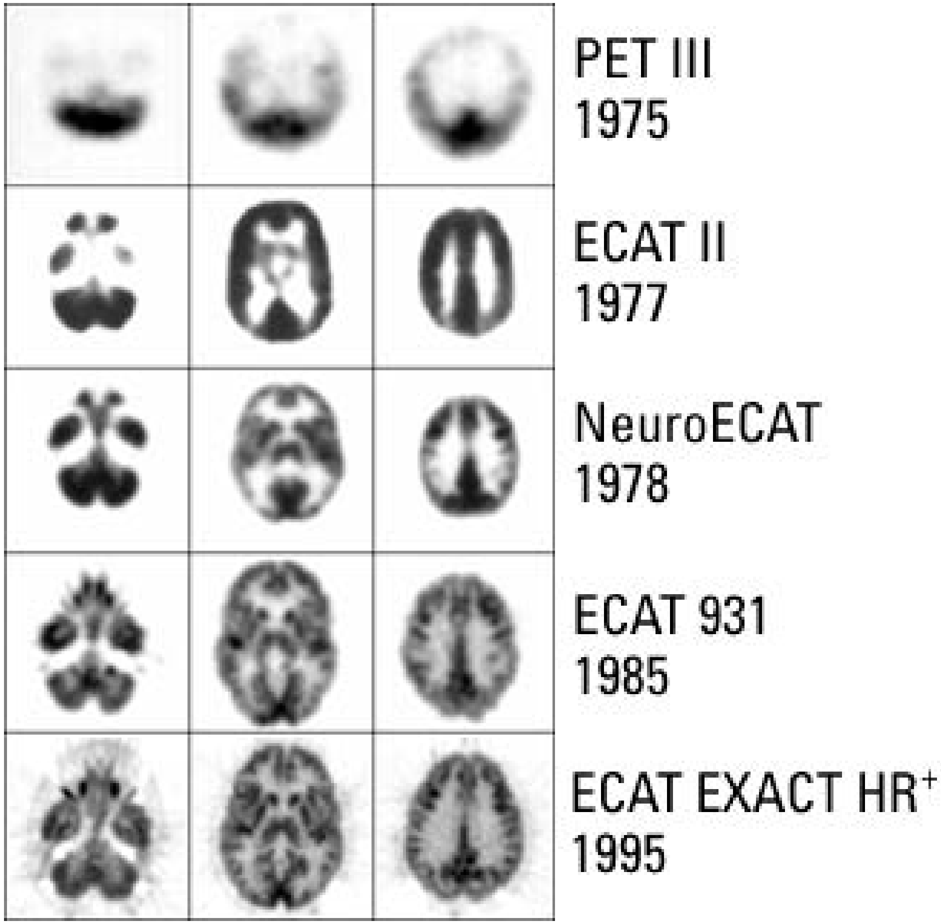

[18F]-FDG

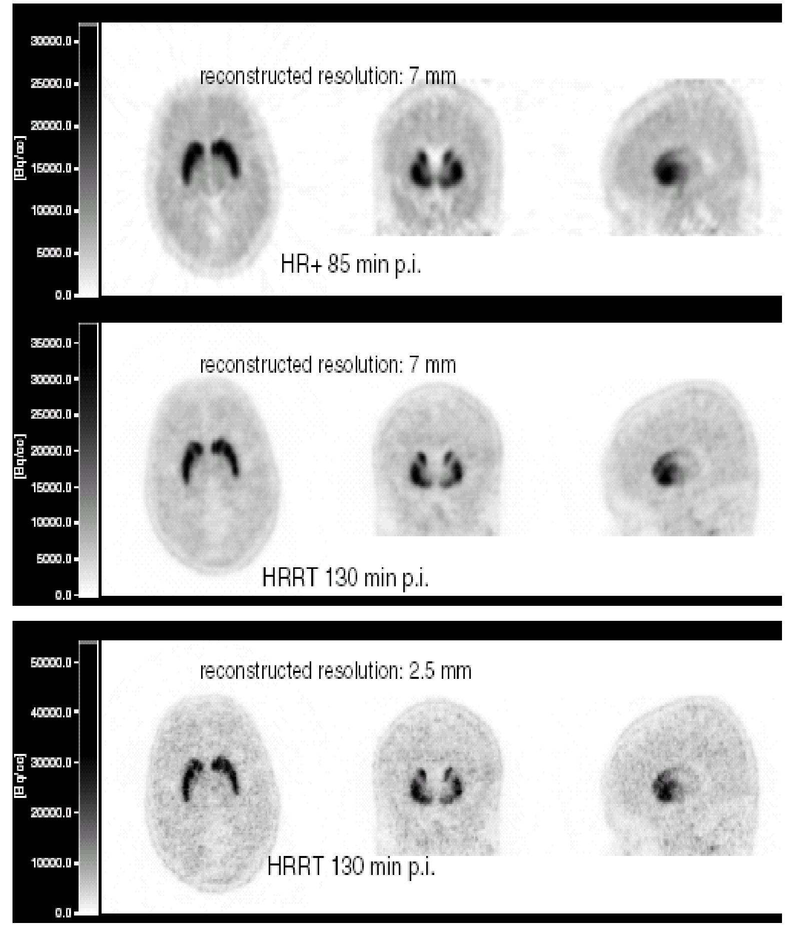

[18F]-FP-ß-CIT

De Jong et al, *Phys Med Biol* **52** (2007) 1505–1526

The Race to Higher Sensitivity

2D → 3D Configuration of PET Scanners

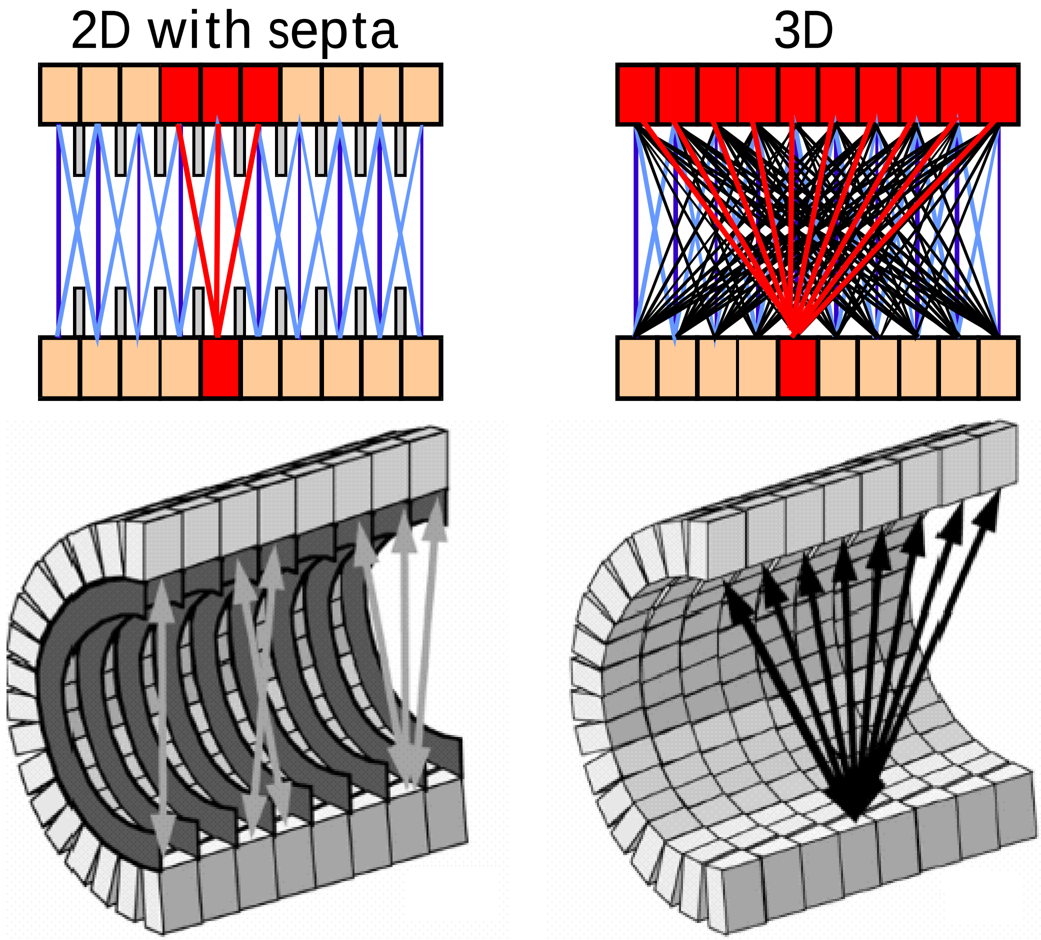

- ✓ 5 to 7-fold gain in absolute sensitivity
- ✗ Increased scatter, randoms, deadtime

The Race to Higher Sensitivity

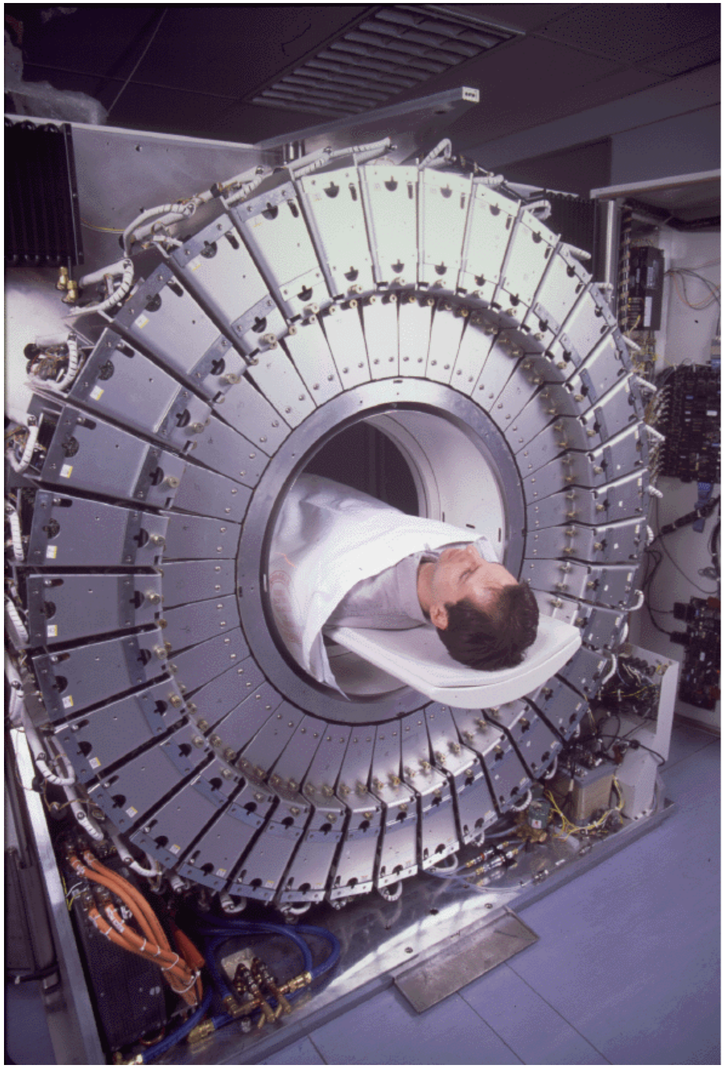

ECAT EXACT (1993)

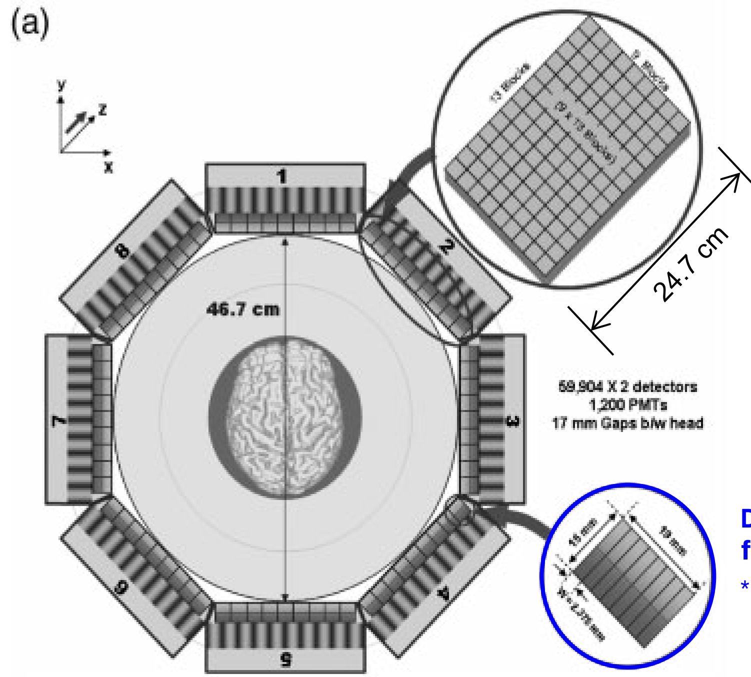

Dual-layer phoswich for DOI measurement*

* R. Lecomte, "Scintillation detector for tomographs", US Patent 4,843,245 (1989)

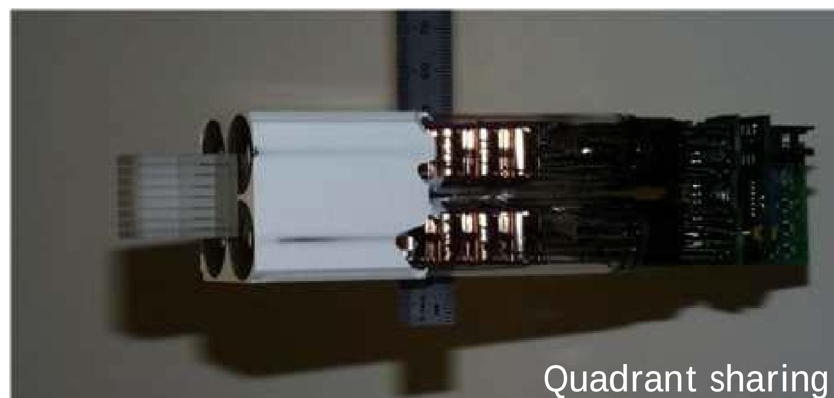

HRRT (1998)

Evolution of Technology

Electronic devices

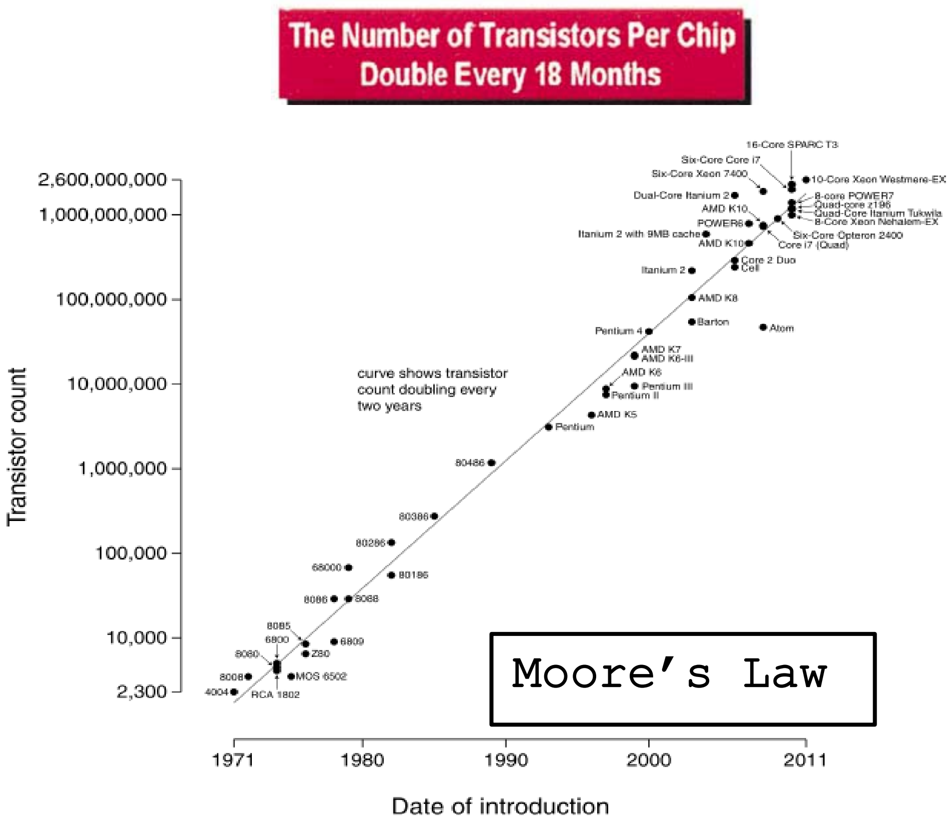

PET scanners

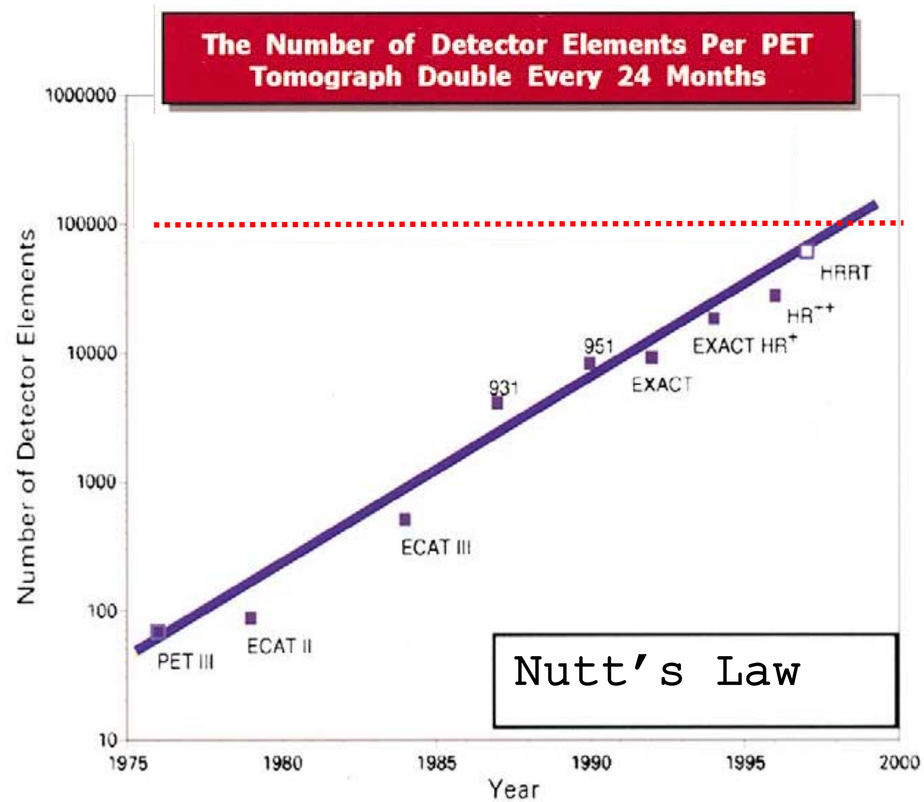

Evolution of Technology

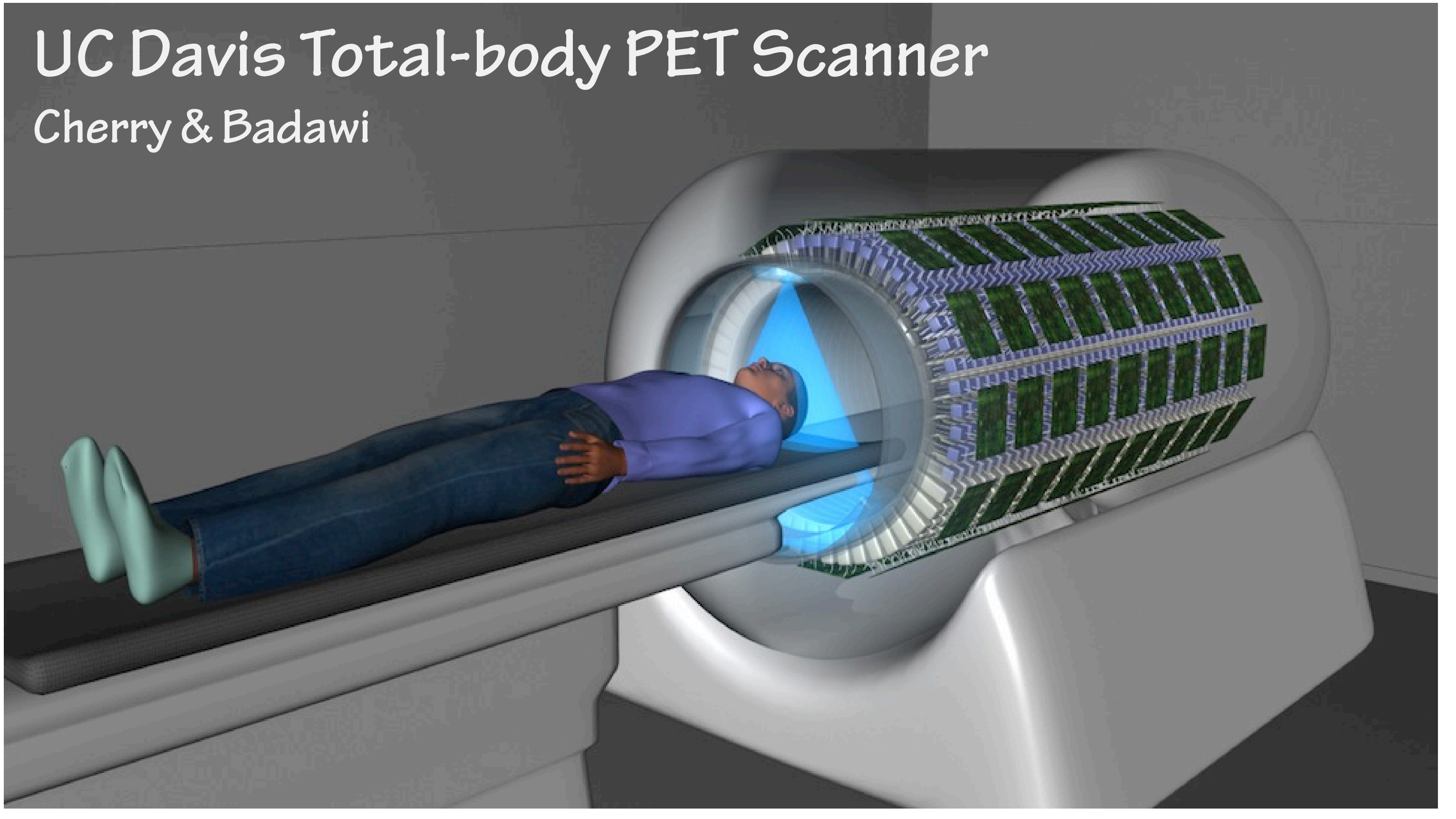

JOE PROUDMAN / UC DAVIS

- ✓ Total-body PET scanner (~2 m long)
- ✓ ~40-fold gain in sensitivity, 30 s scans
- ? 8x more detectors (~10^6 crystals)
- ! $15.5M

Spatial Resolution in PET*

$$FWHM = a\sqrt{(d/2)^2 + b^2 + (0.0022D)^2 + r^2}$$

Tomographic reconstruction
1.1<a<1.3
(a=1: no recons.)

Geometric
Detector size (triangular)

Coding
?

Non-colinearity
Ring diameter:
***D*=10-80 cm**
~0.2-2 mm

Positron range
^{18}F:
~0.1 mm FWHM
~0.5 mm *rms*

Detector

Physical limit
≈ 0.4 - 0.7 mm

FWHM : Full Width at Half Maximum
a : Factor accounting for resolution degradation due to tomographic reconstruction
d : Detector size
b : Detector positioning accuracy
D : Distance between coincident detectors (~ring diameter)
r : Positron range in tissues

*Derenzo & Moses, “Critical instrumentation issues for resolution <2mm, high sensitivity brain PET”, in *Quantification of Brain Function, Tracer Kinetics & Image Analysis in Brain PET*, ed. Uemura et al, Elsevier, 1993, pp. 25-40.

Spatial Resolution in PET

$$FWHM = a\sqrt{(d/2)^2 + b^2 + (0.0022D)^2 + r^2}$$

Coding

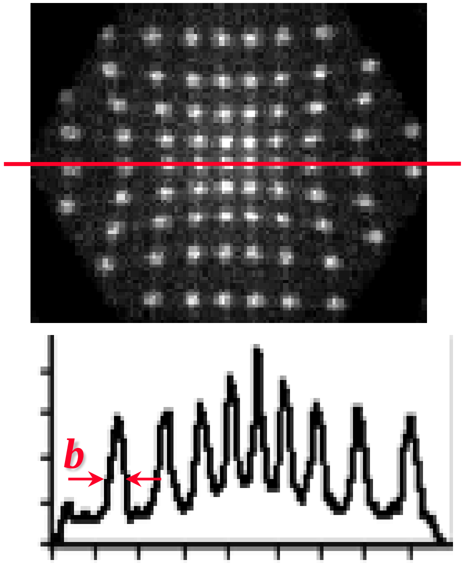

Positioning accuracy ≠ Intrinsic (geometric) resolution!!

Coding effect in PET Scanners

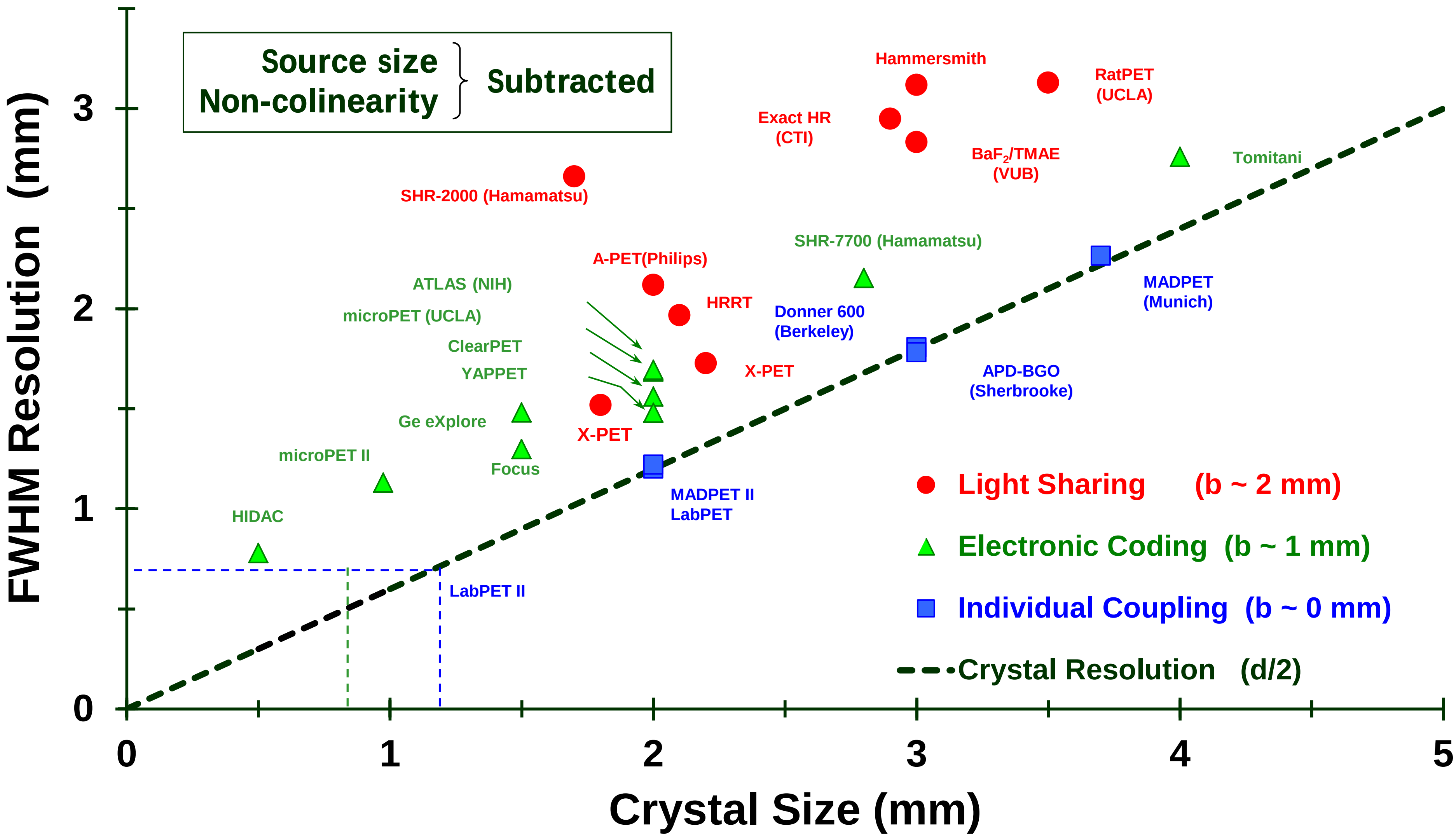

* Adapted from: Lecomte, "Technology challenges in small animal PET imaging", *Nucl. Instrum. Meth. Phys. Res. A*527:157-165, 2004

Coding *vs* Non-Coding

Analog coding

- ✓ Large area photodetectors
- ✓ Low channel nb
- ✓ Mature technology (PMT)
- ✓ High gain (>10^6), low noise
- ✓ Inexpensive

- ✗ Limited spatial resolution
- ✗ Spatial distortion
- ✗ High dead time
- ✗ Low max count rate

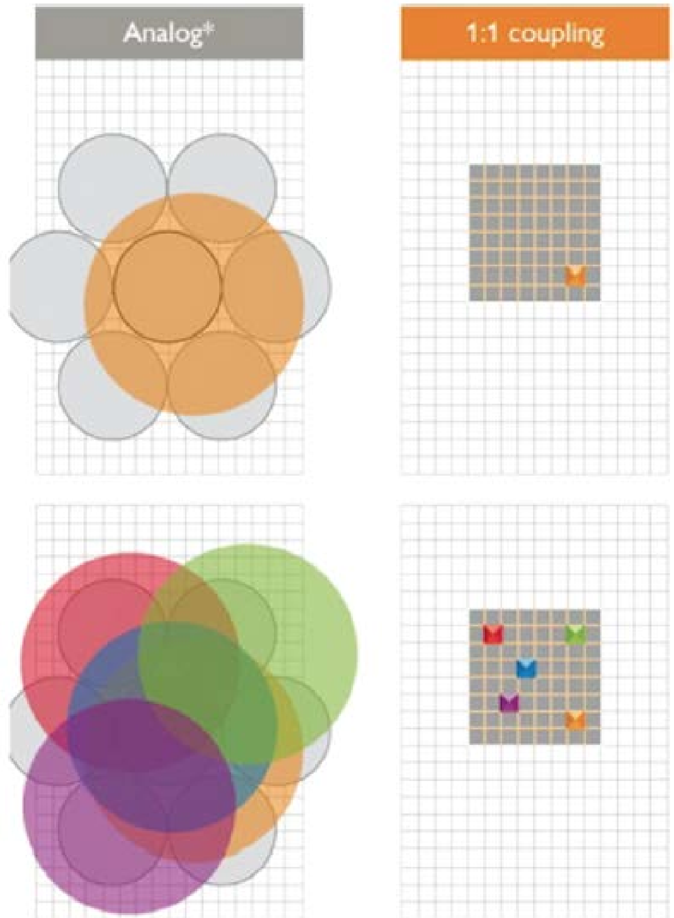

Image courtesy of Philips Healthcare

Direct 1:1 coupling

- ✓ No coding effect
- ✓ No spatial distortion
- ✓ High intrinsic spatial resolution
- ✓ Low dead time
- ✓ High max count rate

- ✗ Pixelated readout
- ✗ High channel nb
- ✗ High cost

Signals from Detectors

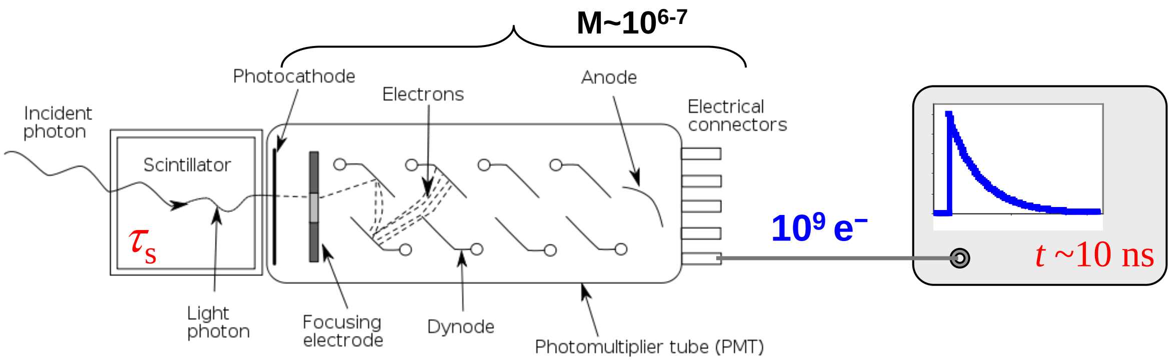

$$I(t) = I_0 e^{-t/\tau_s}$$

τ_s : Scintillator decay time

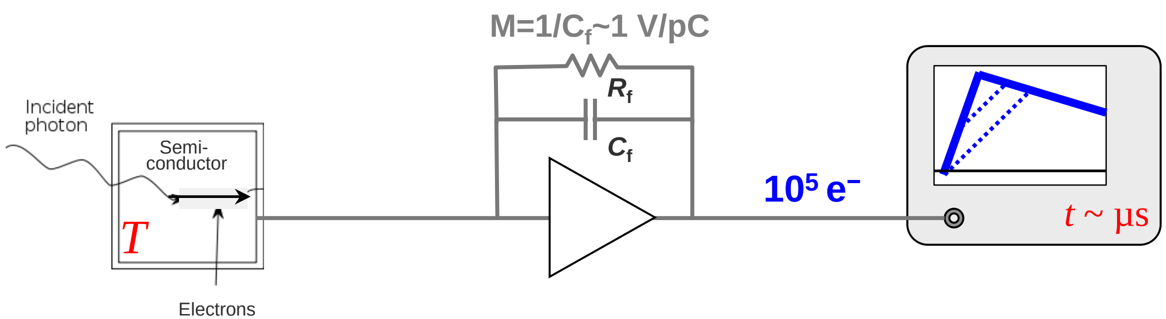

$$I(t) = \begin{cases} I_0 f(t) & t < T \\ I_0 e^{-t/R_f C_f} & t > T \end{cases}$$

T : Electron collection time

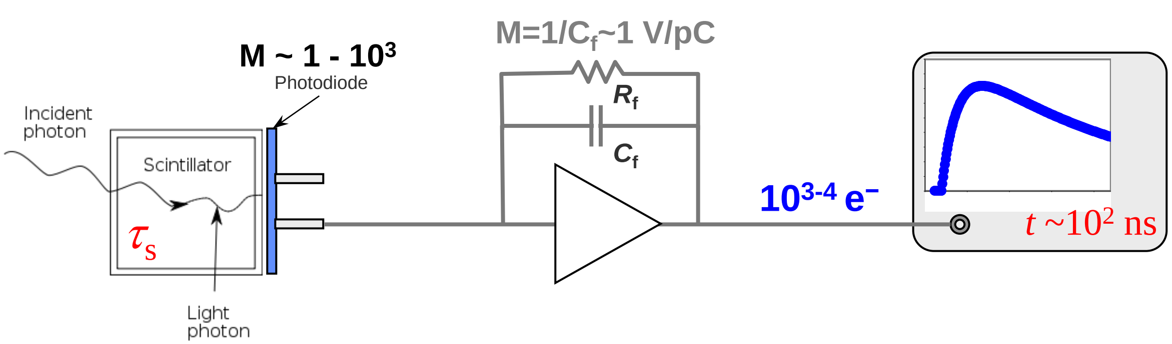

$$I(t) = I_0\left(e^{-t/R_f C_f} - e^{-t/\tau_s}\right)$$

$R_f C_f$: Preamplifier time constant

Technology Developments

- 1986: APD-based detector module for PET
  – AW Lightstone, RJ McIntyre, R Lecomte, D Schmitt. A BGO-APD module designed for use in high resolution PET. *IEEE Trans Nucl Sci* 33:456-9, 1986
- 1987: Dedicated preamplifier for APD
  – D Schmitt, R Lecomte, M Lapointe, C Martel, C Carrier, B Karuta, F Duval. Ultra-low noise charge sensitive preamplifier for scintillation detection with APDs in PET applications. *IEEE Trans Nucl Sci* 34(1): 91-96, 1987
- 1989: Patent on Depth-of-Interaction (DOI)
  – R Lecomte. Scintillation detector for tomographs. US PTO 4,843,245, registered 4 June 1986, delivered 27 June 1989

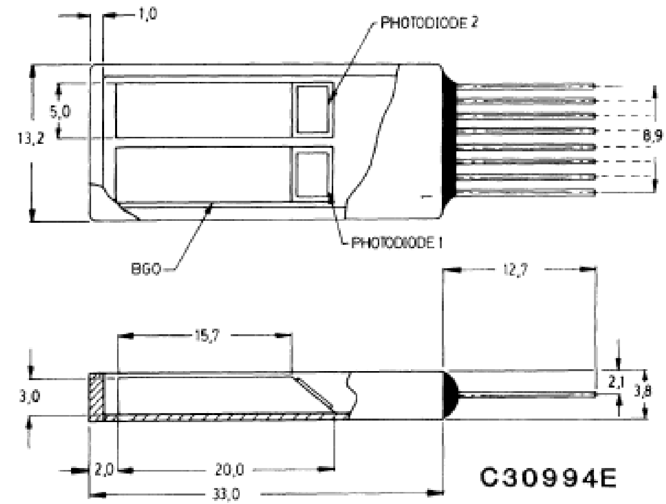

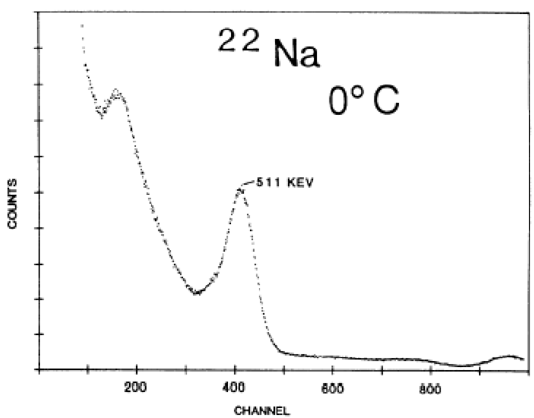

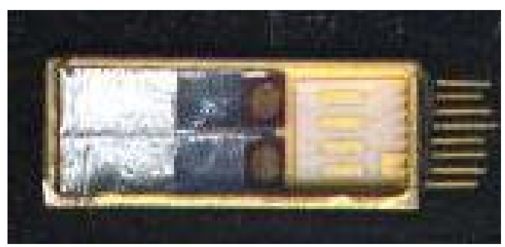

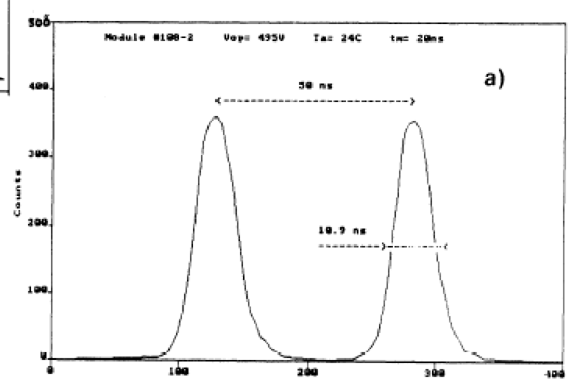

✓ BGO or BGO/GSO crystals
✓ Commercial product
✓ Custom analog electronics

✗ Advent of "block" detector (Casey & Nutt, 1986)
✗ Nobody could reproduce timing results

⇒ APD detector module unnoticed…

1995: Sherbrooke Animal PET Scanner

Lecomte et al, *IEEE TNS* 43 (1996) 1952-7

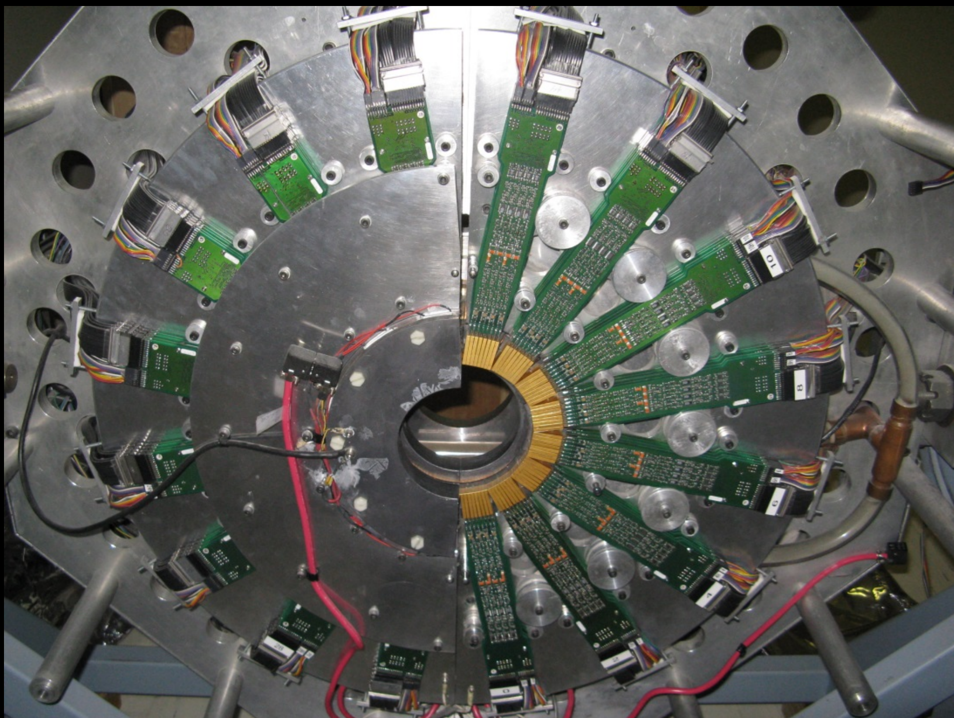

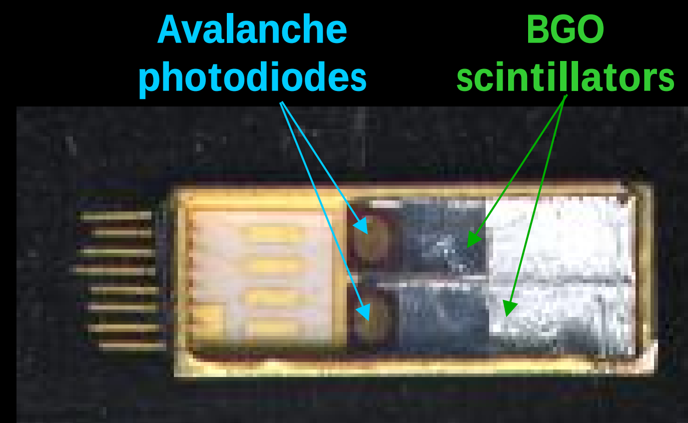

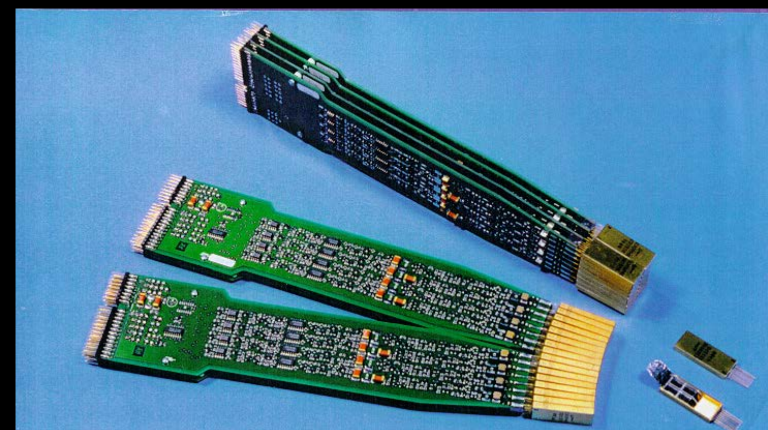

Detectors	**512 BGO 3 × 5 × 20 mm³**
Resolution	**1.75 mm (intrinsic)** **2.1 × 2.1 × 3.1 mm³ *or* 14 µl**
Efficiency	**200 cps/µCi (0.51%)**
Sensitivity	**2 kcps/µCi/ml/cm**
Timing window	**50 ns**

- ✓ Individual readout
- ✓ Parallel electronic channels
- ✓ Mostly analog processing

UNIVERSITÉ DE SHERBROOKE

APD PET Electronics

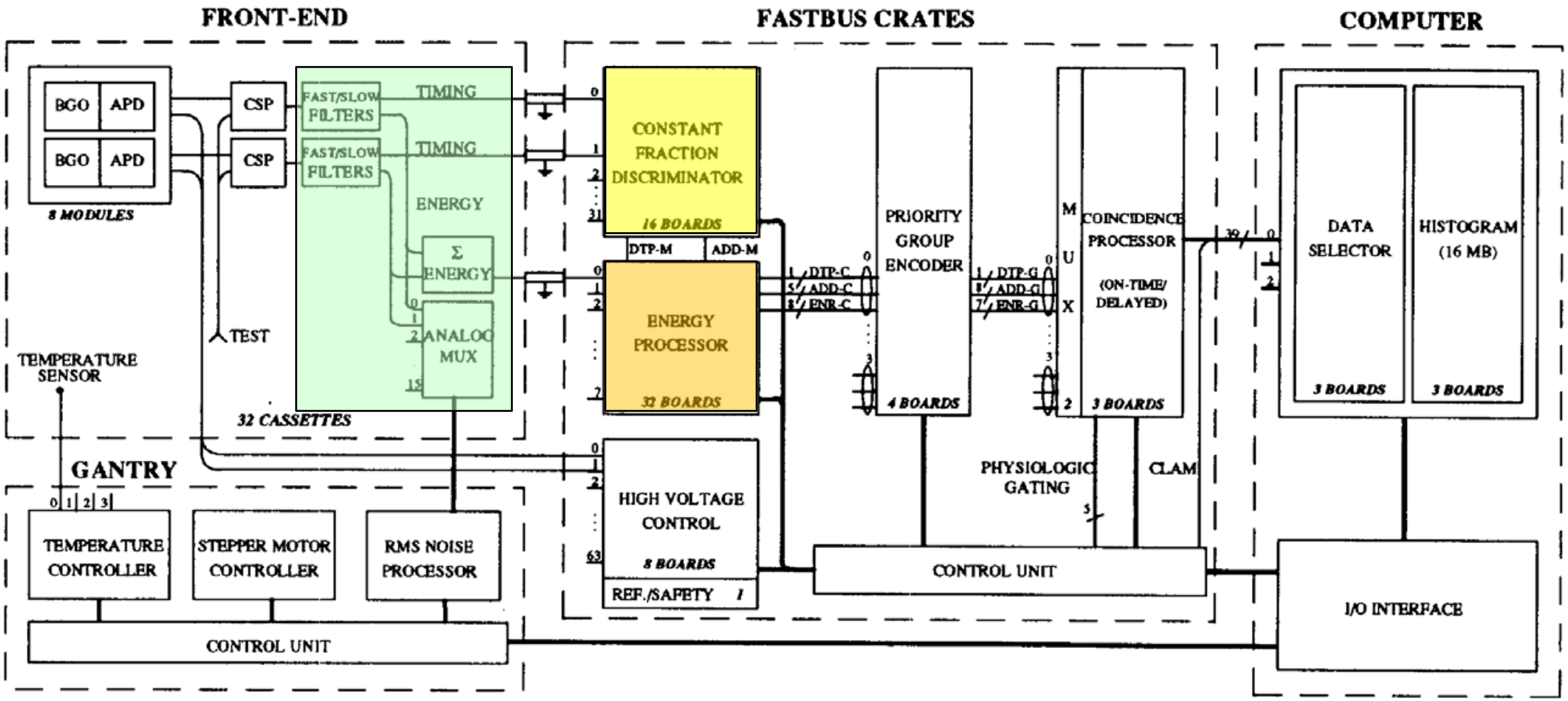

- All discrete components
- Front-end in scanner
- Data processing & acquisition in separate crates

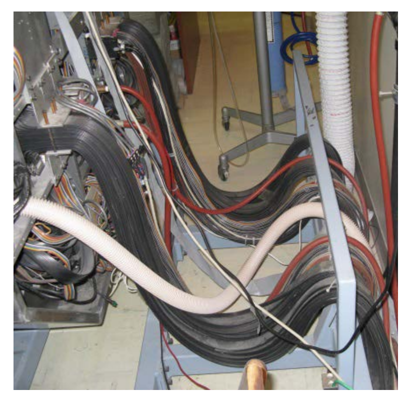

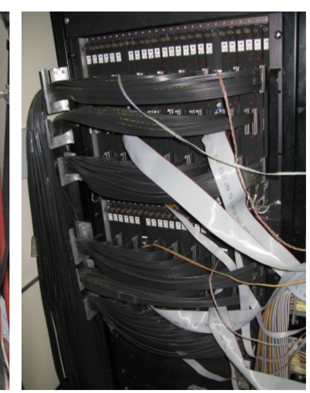

2001: 2nd Most Active Preclinical PET Center

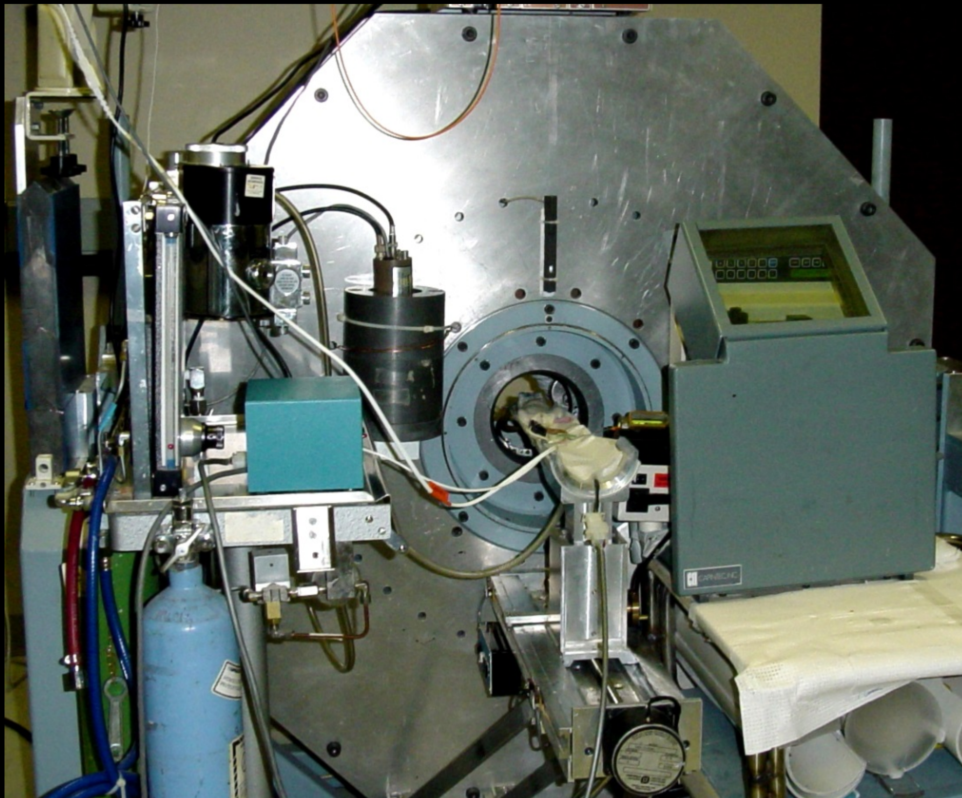

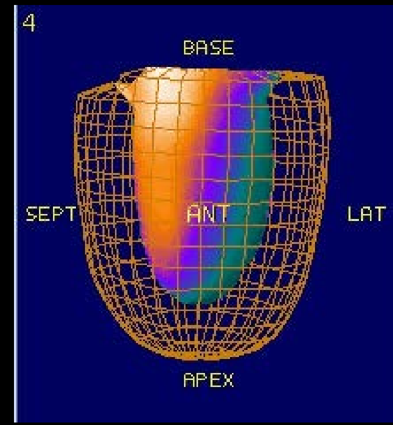

Cardiac PET Imaging
Normal rat (270 g)
3.8 mCi ^{18}FDG 60 min
ECG-gated acquisition

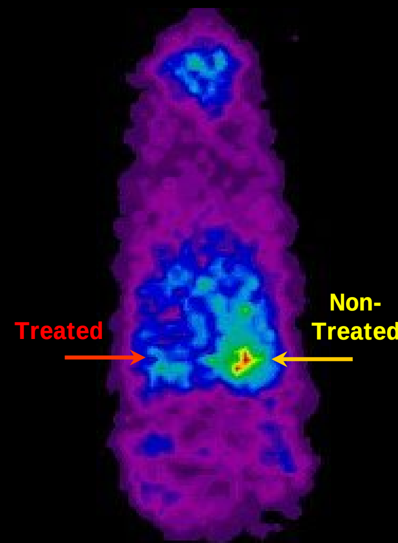

PET Imaging in Oncology
EMT-6 mammary tumors treated by PhotoDynamic Therapy (PDT)
BALB/c mouse (20 g)
400 µCi ^{18}FDG 60 sec

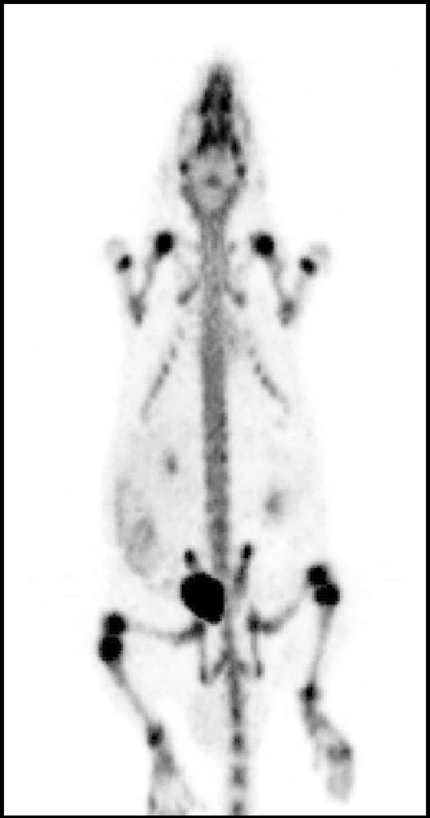

Whole-Body PET Scan
$^{18}F^{-}$ + ^{18}FDG, 250 g rat

UNIVERSITÉ DE SHERBROOKE

Next step?

- APD technology still a laboratory development
- Further dissemination of technology not possible
  - Major upgrade necessary
  - Cost reduction mandatory

⇒ **Options:**

- Redesign detectors
- Update electronics → Integrate front-end
- Marketing agreement with major medical equipment manufacturer ?
- Launch start-up ??

APD Detector Module

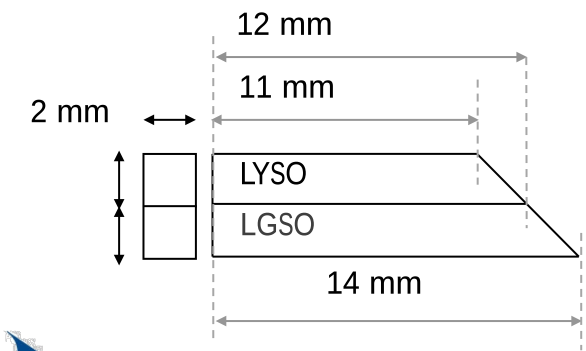

- Quad APD
- Dual LYSO/LGSO Phoswich
- 8-pixel detectors / module
- 2 mm × 2 mm pixels

PerkinElmer precisely.

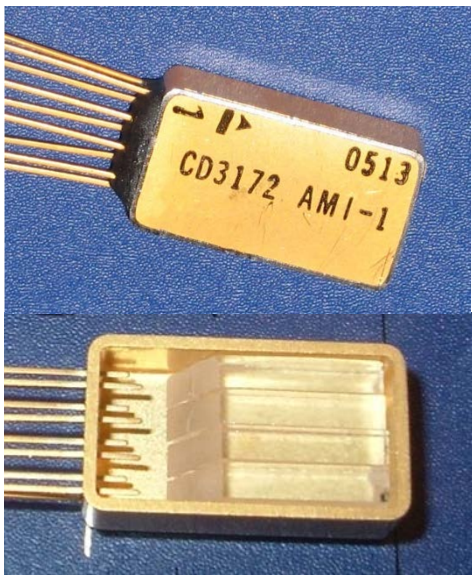

	LYSO	LGSO
Scintillation constant (ns)	40	65
Light yield (% NaI(Tl))	85	40
Emission maximum (nm)	420	420
Refraction index	1.81	1.85
Density (g/cm^3)	7.19	6.5
Effective Z	65	61-65
Probability of PE (%)	33	30

Pepin et al. *NSS/MIC* 2007

Yousefzadeh et al. *IEEE Trans Nucl Sci* 2008

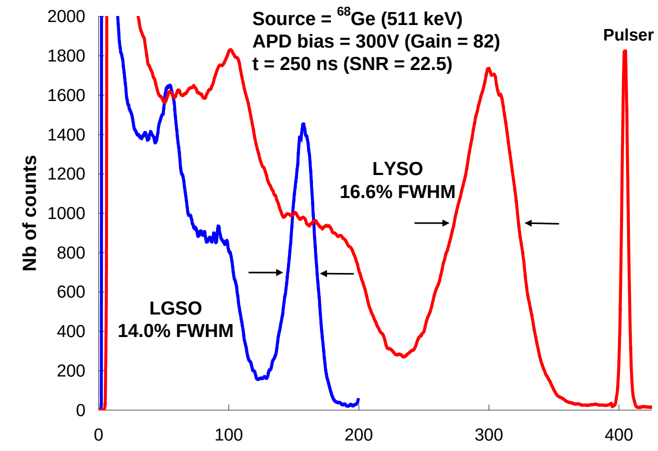

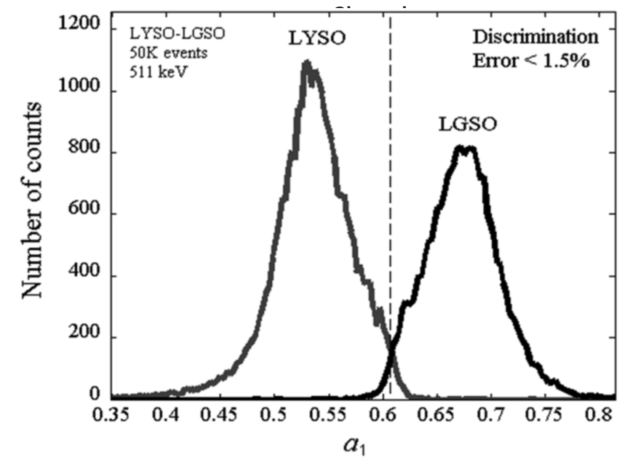

Preamplifier ASIC

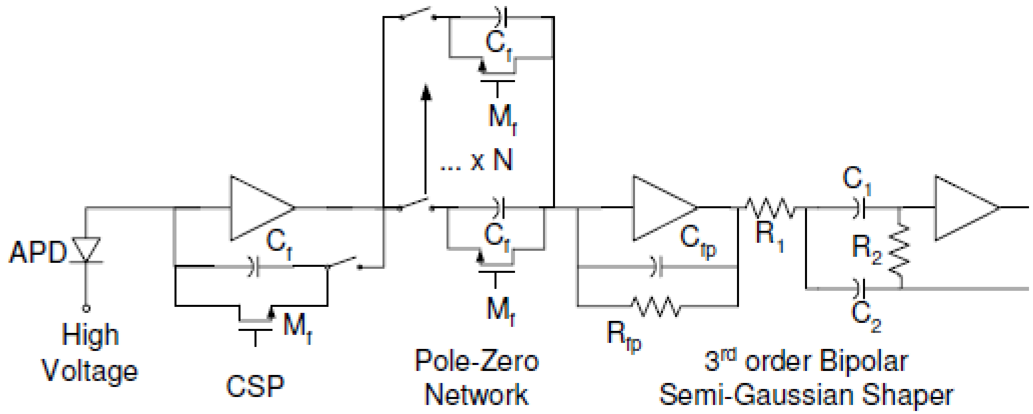

- 16/32 channels
- 80 ns peaking time
- 650 e⁻rms
- 117 mW
- TSMC CMOS 0.81 µm
- Shared with RatCAP development (BNL)

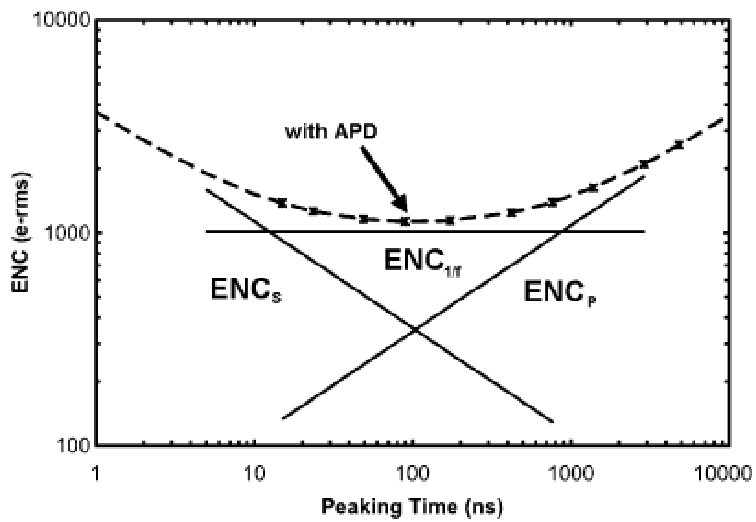

Robert et al. *NSS/MIC* 2003
Pratte et al. *IEEE Trans Nucl Sci* 2004
Pratte et al. *IEEE Trans Nucl Sci* 2008

Signal Processing

4 main sub-systems

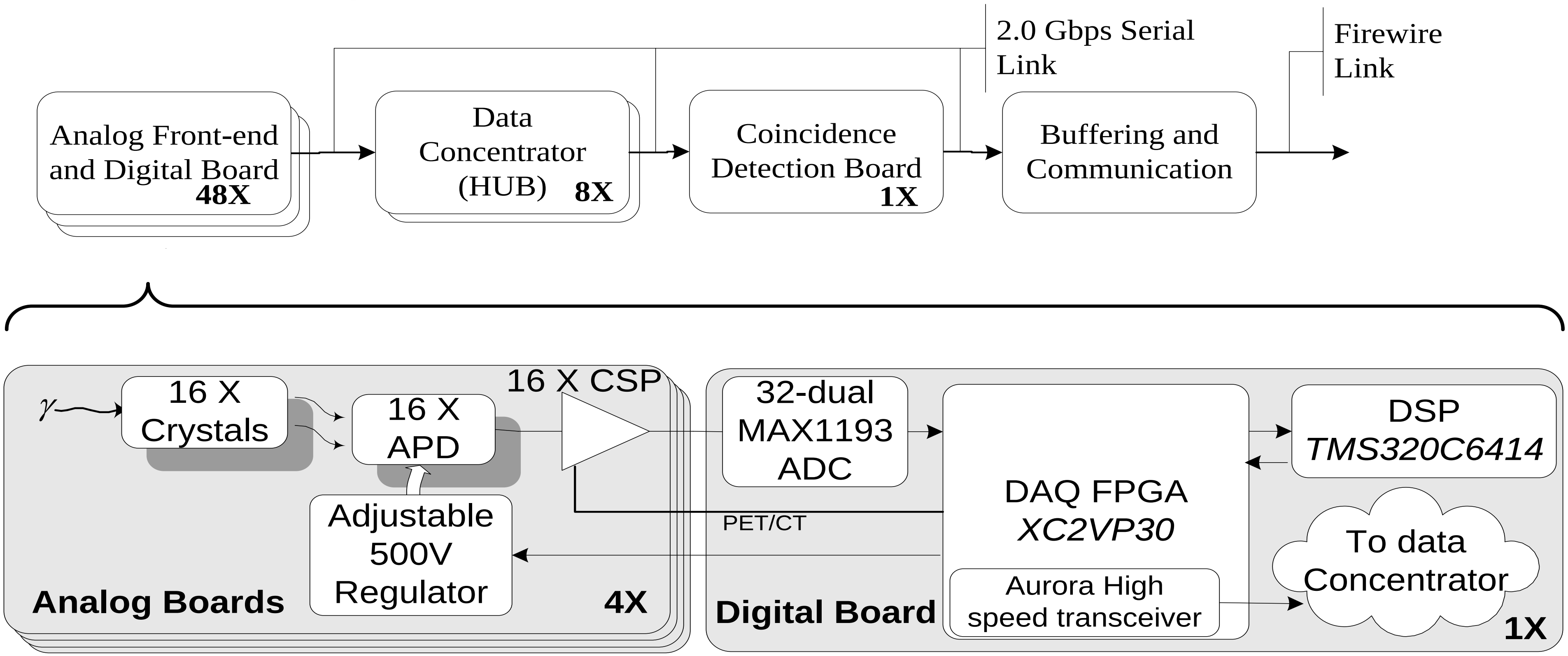

Fontaine et al. *IEEE Trans Nucl Sci* 2005

Tétreault et al. *IEEE Trans Nucl Sci* 2008

Fontaine et al. *IEEE Trans Nucl Sci* 2009

CF Timing Discrimination

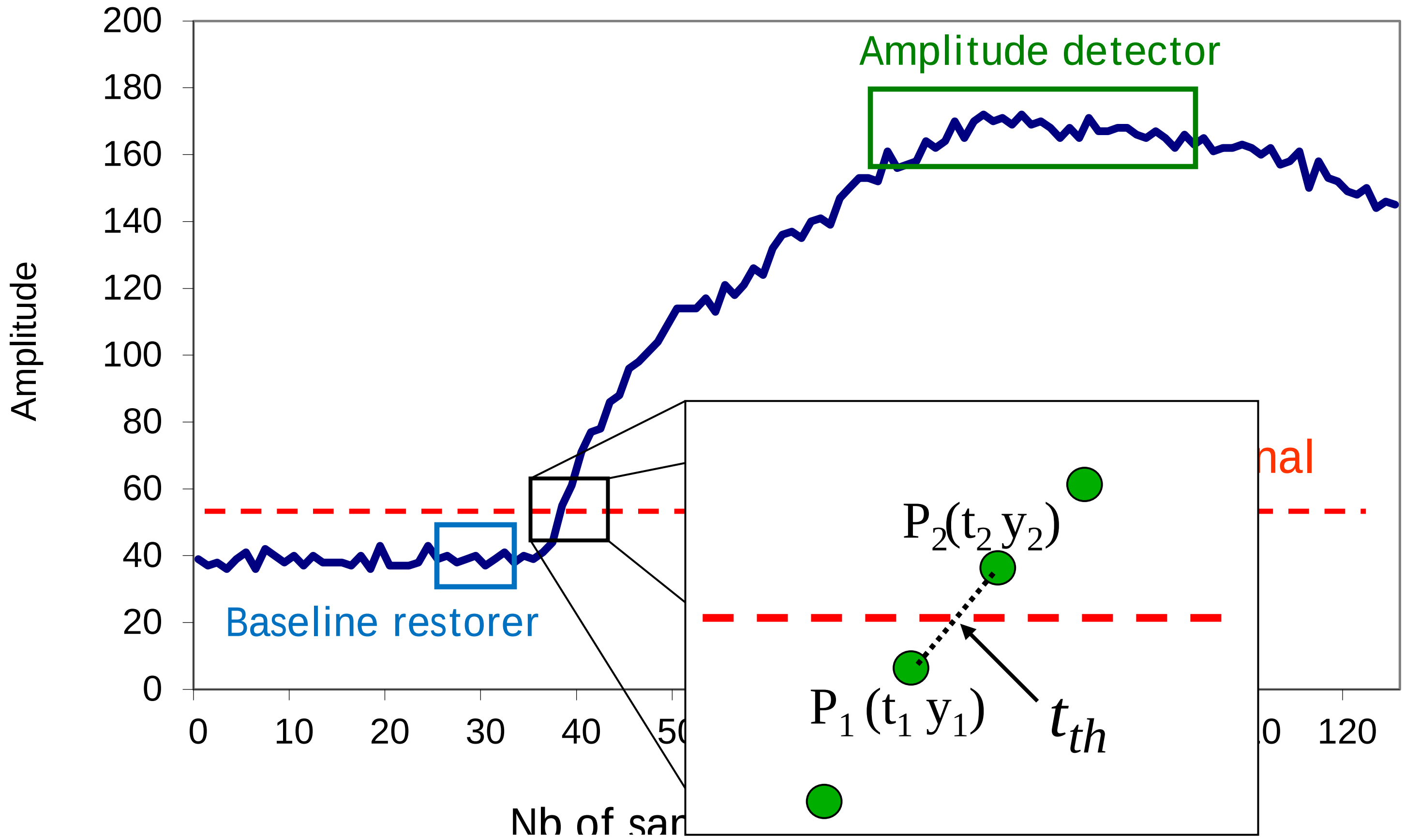

Time at threshold: $$t_{th} = t_1 + (y_{th} - y_1)\left(\frac{t_2 - t_1}{y_2 - y_1}\right)$$

Fontaine et al. *IEEE Trans Nucl Sci* 2008
Leroux et al. *IEEE Trans Nucl Sci* 2009

Crystal Identification

- Several analog pulse shape discrimination techniques
- Digital implementation:
  - Auto-Regressive Moving Average with eXogenous variable (ARMAX)
  - Vector quantization

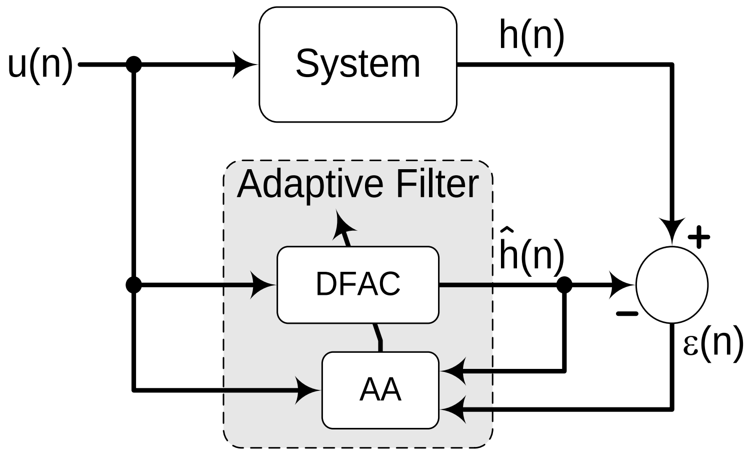

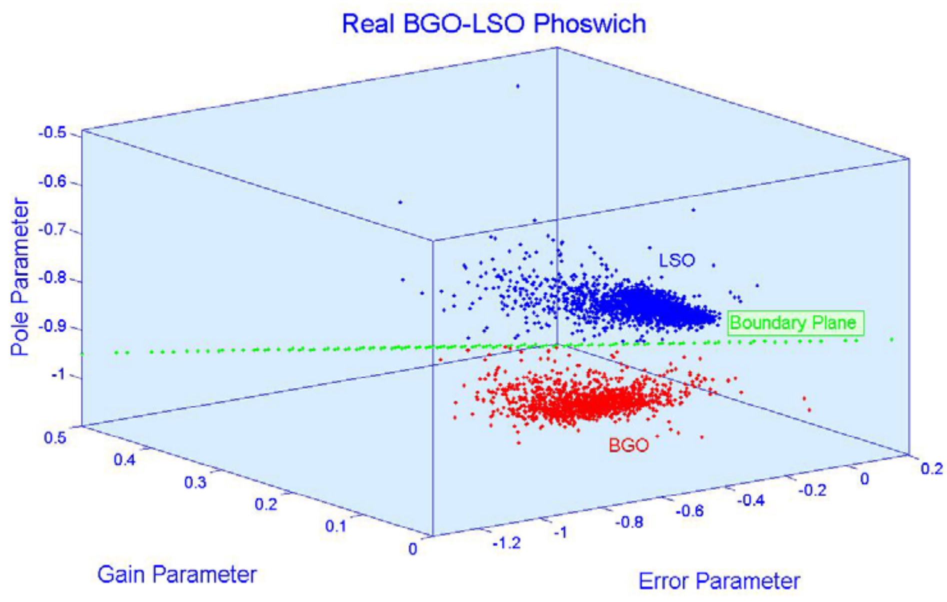

Michaud et al. NSS/MIC 2003

Michaud et al. IEEE Trans Nucl Sci 2010

LabPET Pre-commercial Prototype

Digital APD-based PET Scanner

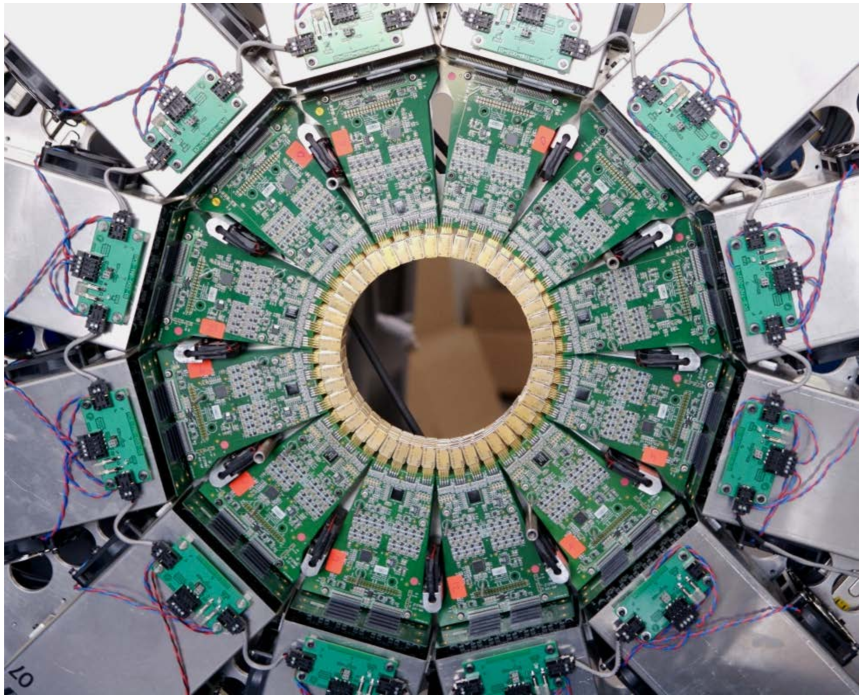

Detectors: LYSO/LGSO phoswich
$2 \times 2 \times$ 12-14 mm^3 pixels
Reach-through UV-enhanced APD

Individual readout & fully parallel electronics

- Integrated 16-ch CMOS front-end
- 40 MHz sampling
- Real-time digital signal processing

Quad APD, 8-pixel, Phoswish detector module

PerkinElmer precisely.

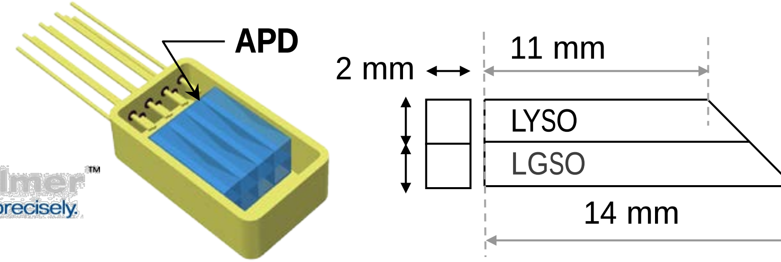

Scintillation crystals: 3072 to 9216
APDs & electronic channels: 1536 to 4608
FOV: 3.75 to 11.4 cm axial ×16.2 cm∅
Timing window: 22 ns

GMS GRAMS BIOMÉDICAL

R Fontaine et al. Architecture of a dual-modality, high-resolution, fully digital PET/CT scanner for small animal imaging. *IEEE TNS* 52: 691-696, 2005
R Fontaine et al. The hardware and signal processing architecture of LabPET™, a small animal APD-based digital PET scanner. *IEEE TNS* 56:3-9, 2009

Light/Charge Sharing vs *Individual Pixels*

Same resolution can be achieved with pixels twice as large!

microPET II prototype

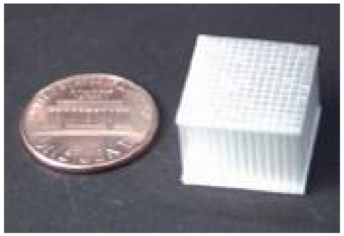

(Tai et al, PMB 2003)

0.975 mm LSO
64-ch PMT + F.O.
X-Y Analog decoding

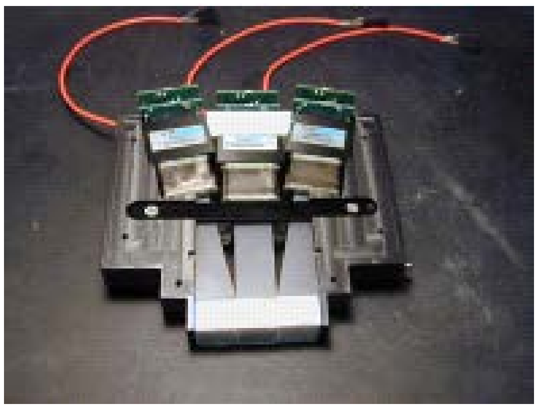

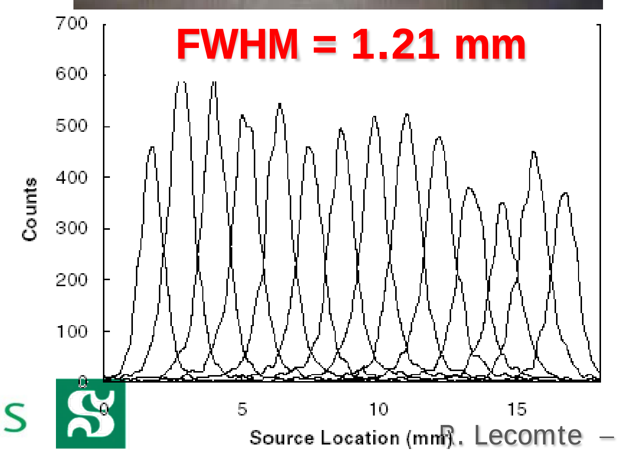

LabPET

2 mm pixels
APD readout
Parallel digital signal processing

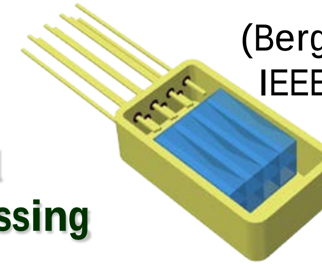

(Bergeron et al, IEEE TNS 2008)

FWHM = 1.22 mm

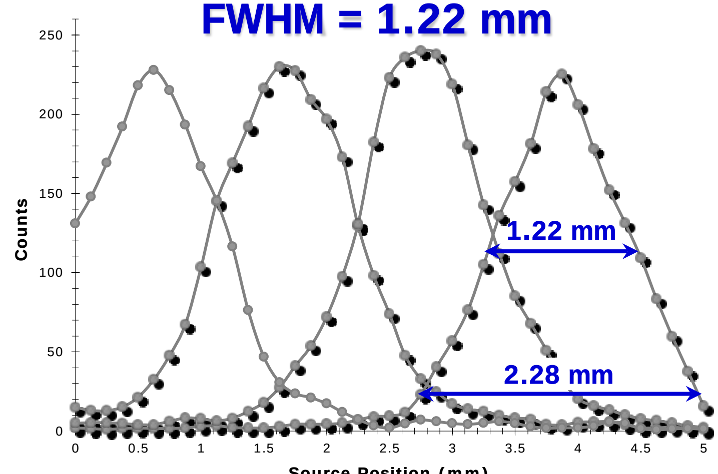

LabPET™ (2005)

1st commercial APD-based PET scanner

Advanced Molecular Imaging

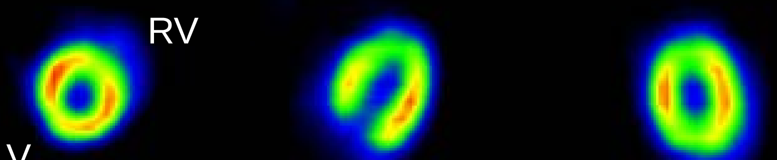

20 g mouse, 24 MBq ^{18}FDG,
30 min acquisition @ 30 min post-injection

200 g rat brain
77 MBq FDG

20 g mouse
28 MBq $^{18}F^{-}$
60 min

Detector	**LYSO/LGSO 2 × 2 × 12-14 mm³**
Resolution	**1.22 mm (intrinsic)**
	1.35 mm isotropic *or* 2.4 µl
Efficiency*	**200 cps/µCi (2.5%)**
Peak NEC*	**252 kcps (mouse phantom)**
	*** LabPET8: 7.5 cm axial FOV**

Lecomte et al,
IEEE MIC 2004 2006
SNM 2006
Fontaine et al,
IEEE MIC 2004 2005 2006
Bergeron et al,
IEEE MIC 2007 2008 2009
SNM 2008
IEEE TNS 2009

Scanner Triumph™/LabPET™ (2009)

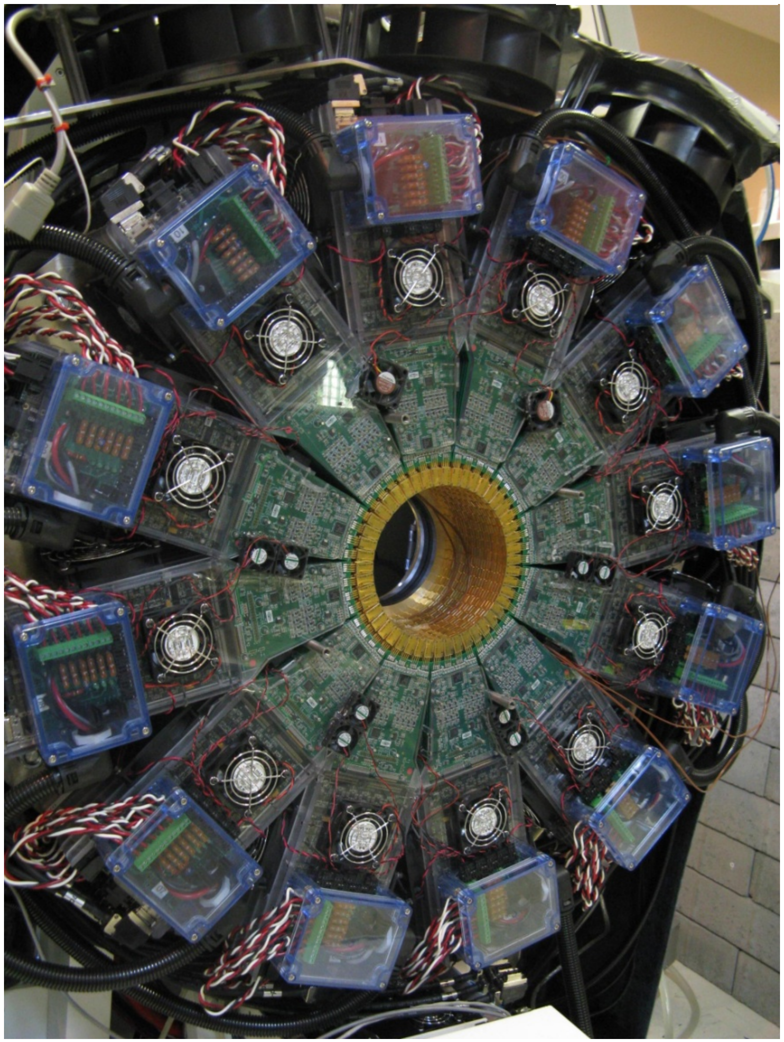

Resolution 1.2 mm / 1.8 µl
Reconstruction 3D + Physics modeling[1]

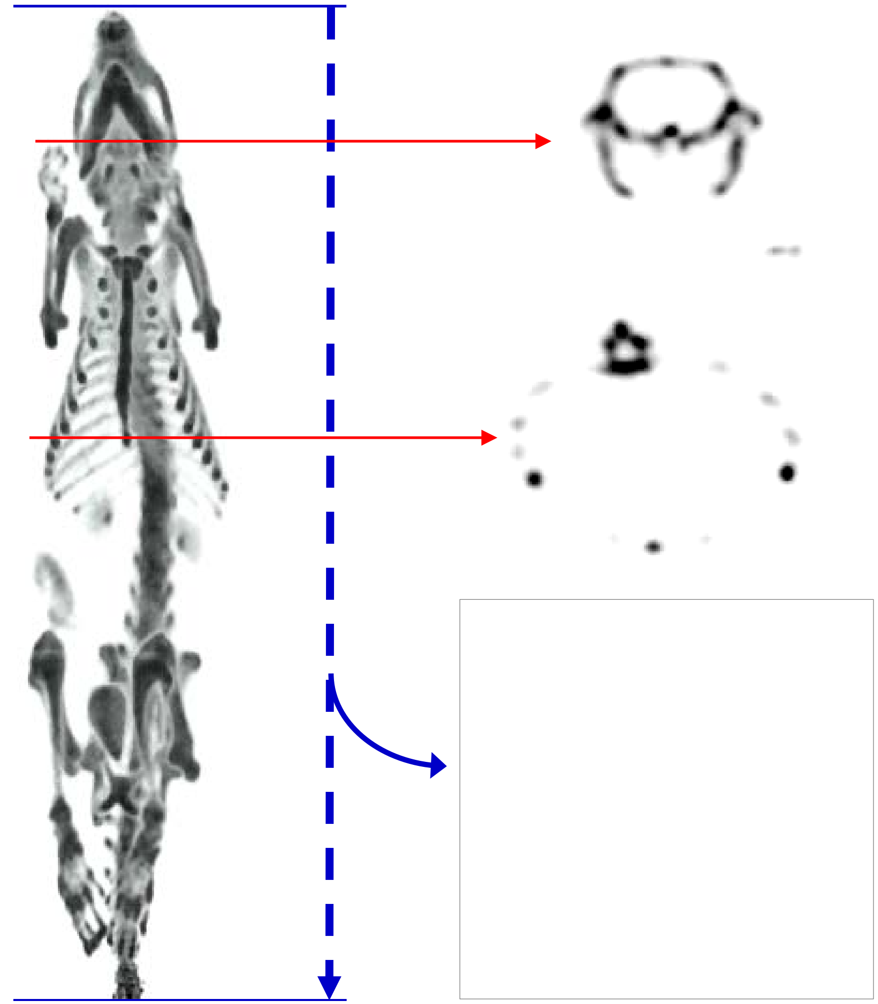

Rat 185 g, 31 MBq Na^{18}F (Bone tracer), 60 min acq @ 68 min p.i.

[1] Selivanov et al, “Detector response models for statistical iterative image reconstruction in high resolution PET”, *IEEE TNS* 47(3):1168-1175, 2000

Image Definition in PET

Na^{18}F Bone Scans

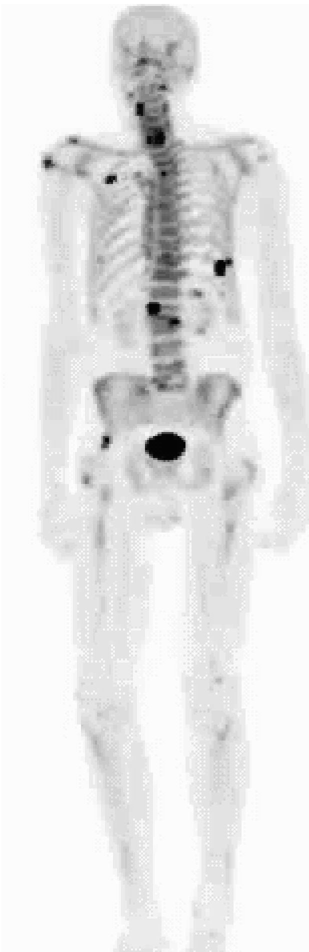

×1/300

×1/10

75 kg human
Clinical PET scanner
(5-6 mm or ~1 cc)

185 g rat
LabPET™ (2009)
(1.2 mm or 1.8 µl)

20 g mouse
LabPET™
(1.2 mm or 1.8 µl)

Spatial Resolution in PET*

$$FWHM = a\sqrt{(d/2)^2 + b^2 + (0.0022D)^2 + r^2}$$

Tomographic reconstruction
1.1<a<1.3
(a=1: no recons.)

Geometric
Detector size (triangular)

~~Coding~~
~~Individual: ~0 mm~~
~~Charge: ~1 mm~~
~~Light: ~2 mm~~

Non-colinearity
Ring diameter

Positron range
Source size

Detector (Geometric, Coding)

Physical limit (Non-colinearity, Positron range)

$\leq$ 1.0 mm $\Rightarrow$ $\approx$0.7 mm (Detector) $\approx$0.4 - 0.7 mm (Physical limit)

$b \sim 0$
$d \approx 1.2$ mm

$b \sim 0.5$ (*scaled*)
$d \leq 0.5$ mm

* Derenzo & Moses, "Critical instrumentation issues for resolution < 2 mm, high sensitivity brain PET", in *Quantification of Brain Function, Tracer Kinetics & Image Analysis in Brain PET*, Elsevier, 1993, pp. 25-40.

Challenges

- Channel density x10
- Photodetector & front-end electronics packaging
- Power management (digital processing)
- Digital electronics prohibitively costly for large scale applications
  - ✘ Power consumption/channel must be decreased
  - ✘ Cost reduction mandatory

$\Rightarrow$ **Solutions:**

- Redesign detectors
- Update electronics $\rightarrow$ Integrate analog front-end
  $\rightarrow$ Simplify signal processing to integrate

LabPET II Detector Development

- 4 × 8 APD/LYSO array
- 1.12 × 1.12 mm^2 pixels
- One-to-one coupling
- FWHM/FWTM = 0.82/1.54 mm
- FWTM < 2×FWHM (Δ shape)
- Detector resolution: 0.73 mm
- ***Sub-mm image resolution expected!***

AGILE TECHNOLOGIES

EXCELITAS TECHNOLOGIES

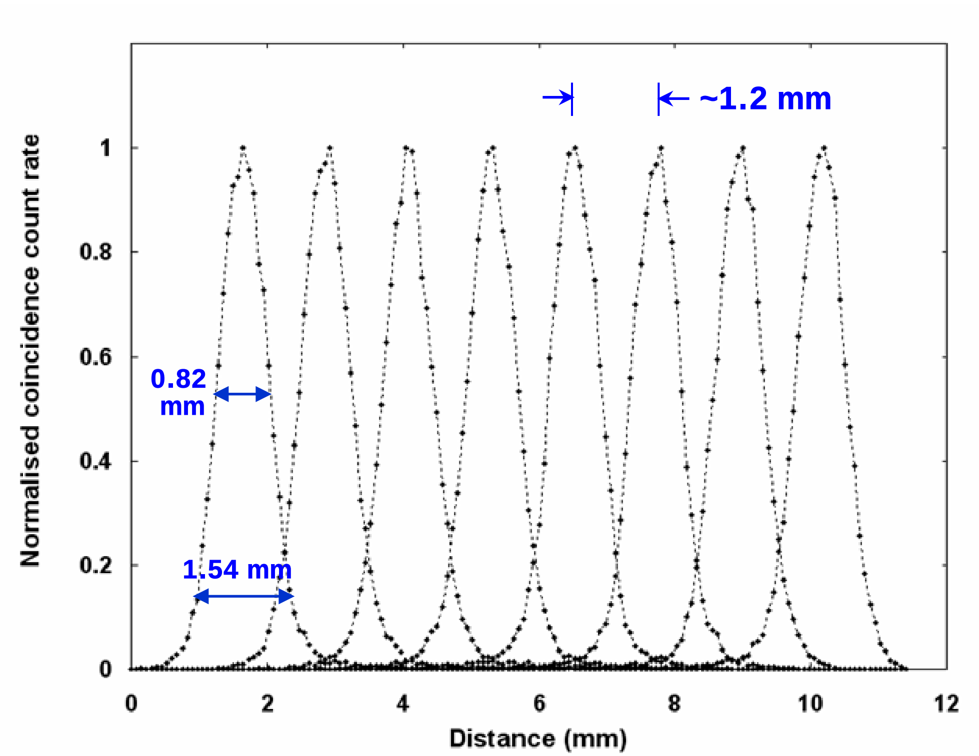

Gaudin et al, *Conf. Rec. IEEE NSS/MIC 2015*, N2AP-102

Bérard et al, *Nucl Instrum Meth Phys Res A* 610:20-23, 2009

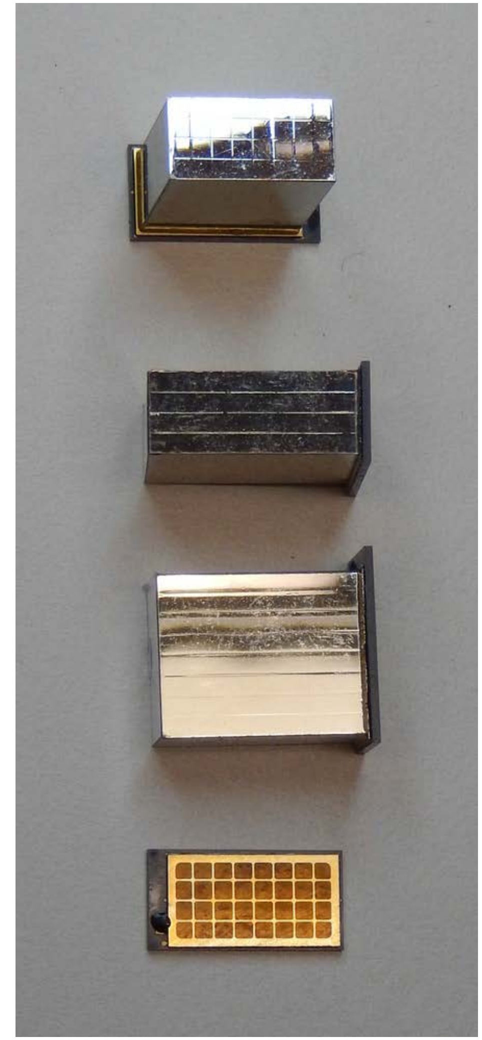

✓ ***Counting CT*** imaging capability
✓ Can be made MR-compatible

Information in Signal from Detectors

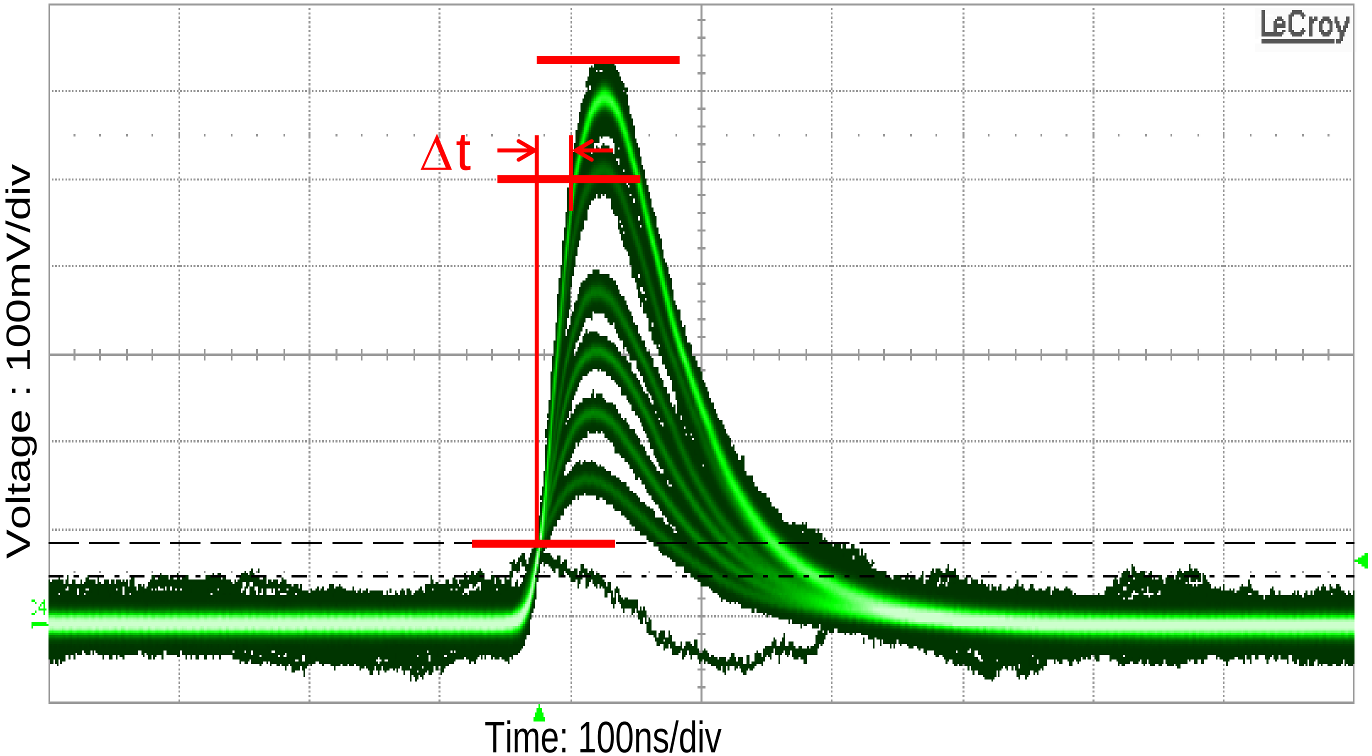

Characteristics:

- Polarity
- Rise/Fall time
- Amplitude
- Area
- Baseline
- Noise
- Rate

Amplitude → peak detector + ADC ⇒ Energy

Pulse start → LE/CF discriminator ⇒ Time

Pulse shape (e.g. rise time) ⇒ Positioning

Complex, hi-power, costly electronics!

Time over Threshold (ToT)

✓ Dual thresholds to achieve better precision

Detector signal

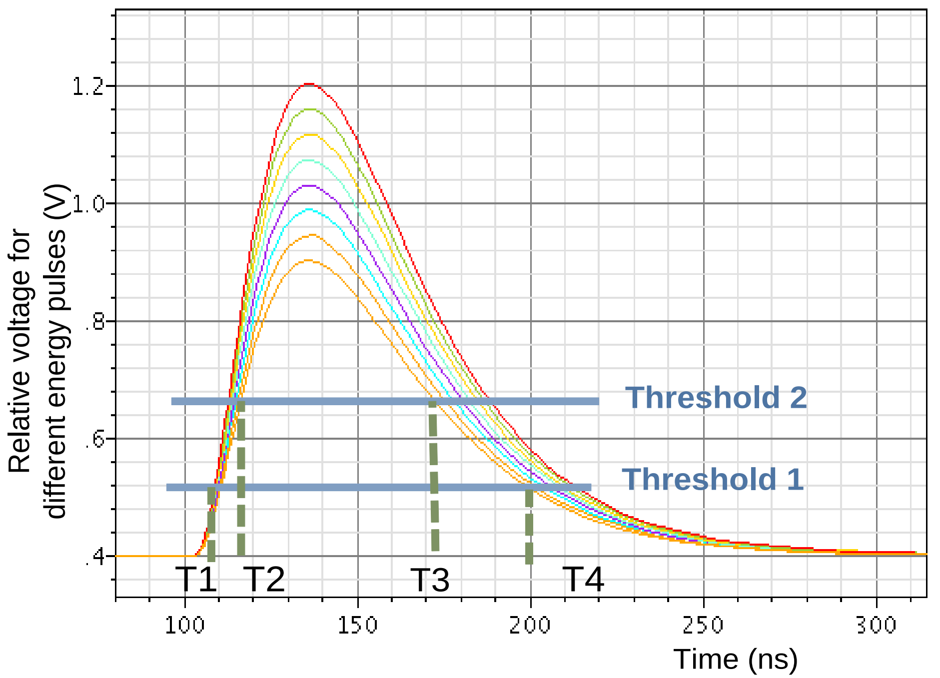

Noise analysis of signal

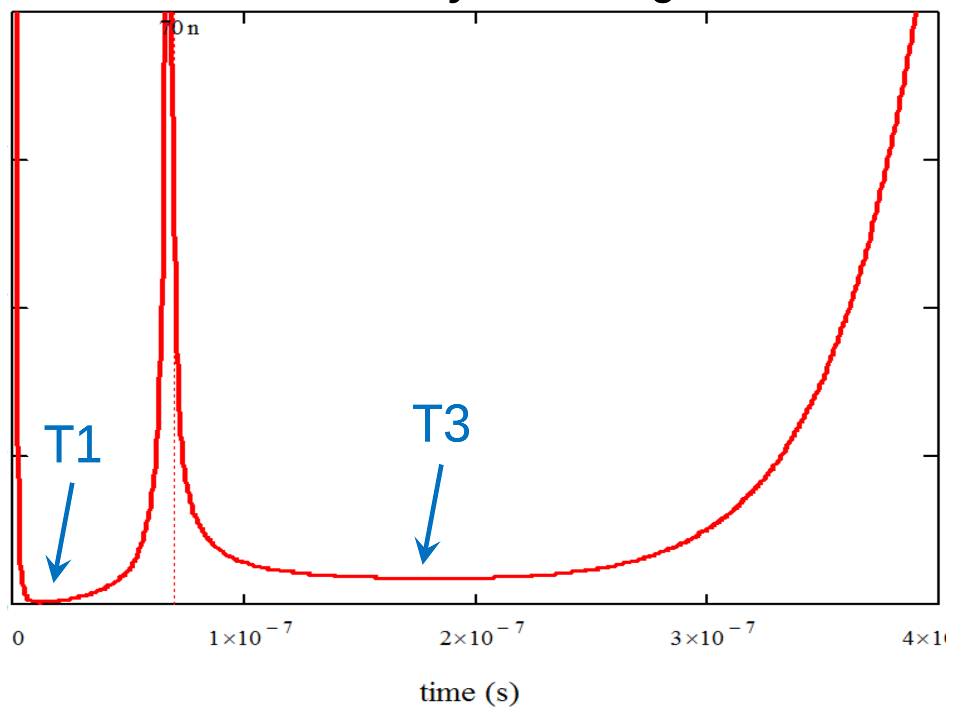

LabPETII 64-channel Front-End ASIC

HV regulator

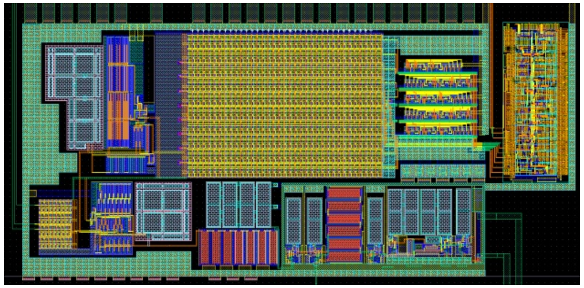

0 to -450 V
0.5 V increment

DLL (312.5 ps)

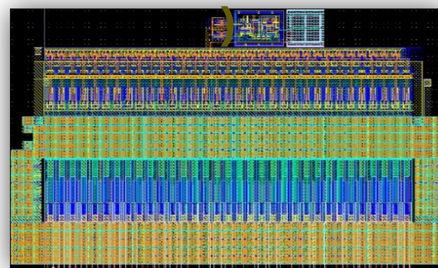

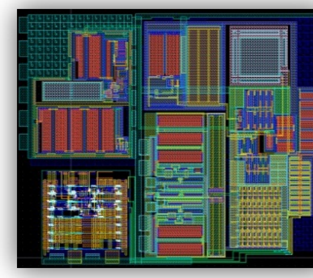

Programmable charge injector:

- **ASIC functionality test before assembly**
- **Automated channel gain calibration**

Temperature sensor

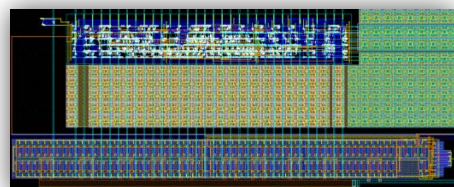

0 to 100°C
1°C accuracy

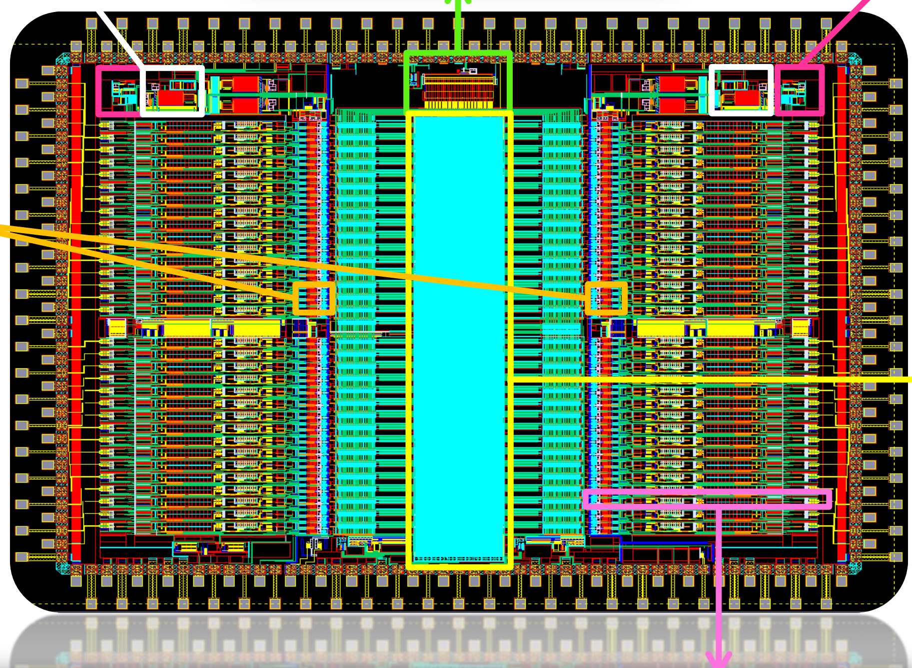

Digital data processing

TSMC 0.18 µm
5.9 mm × 4.6 mm
~ 480 mW

Analog channel (×64)

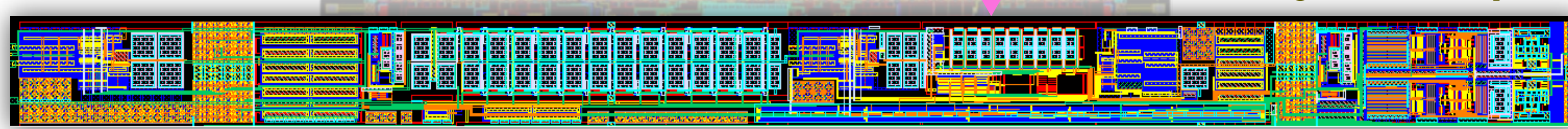

Arpin et al, *IEEE NSS/MIC* 2011

64-channel Mixed Signal ASIC

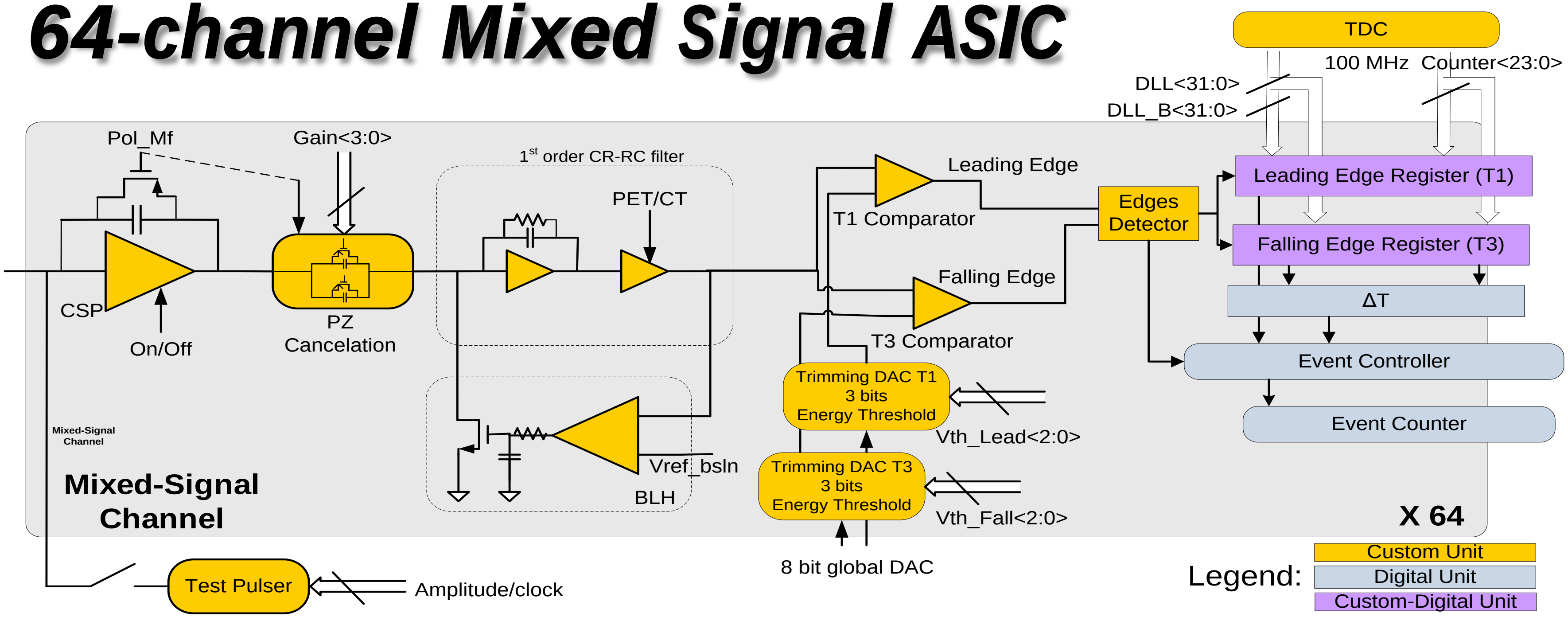

- **64-channel analog/digital processing**
- **Time-over-Threshold (ToT) scheme**
- **Dual threshold, 64 on-chip counters**
- **100 MHz clock rate**
- **2 Mevents/s LVDS data transfer rate**
- **400 mW**
- **TSMC 0.18 µm CMOS technology**
- **Prototypes made through CMC Microsystems**

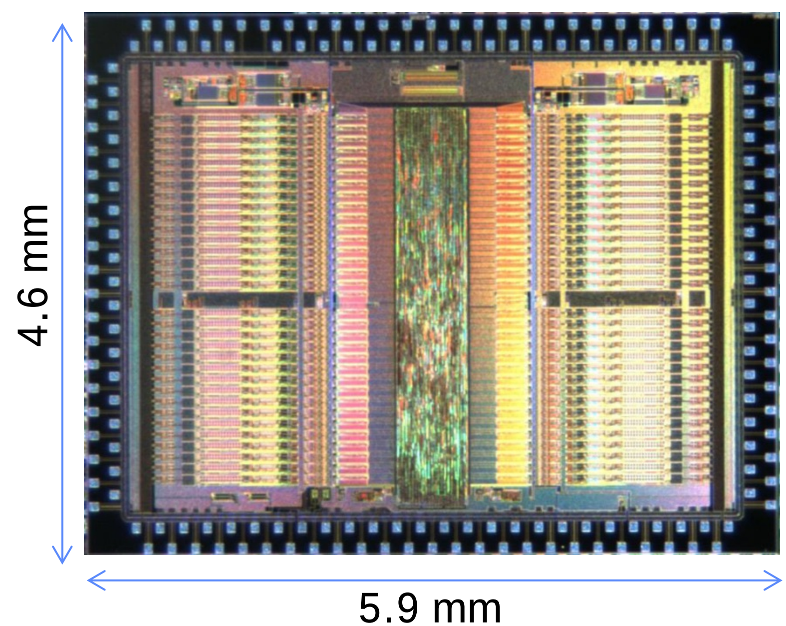

Arpin et al,
IEEE NSS/MIC 2011

CIMS
CMC MICROSYSTEMS

ToT Results

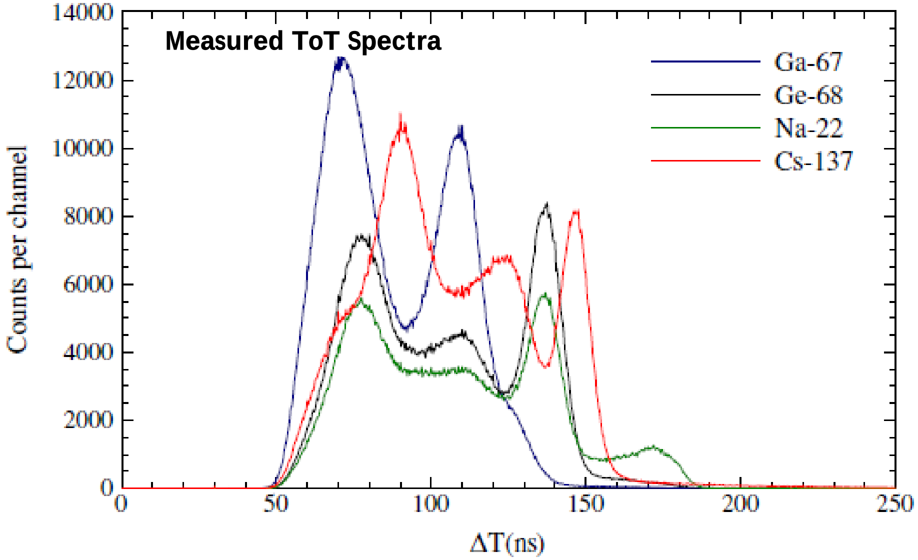

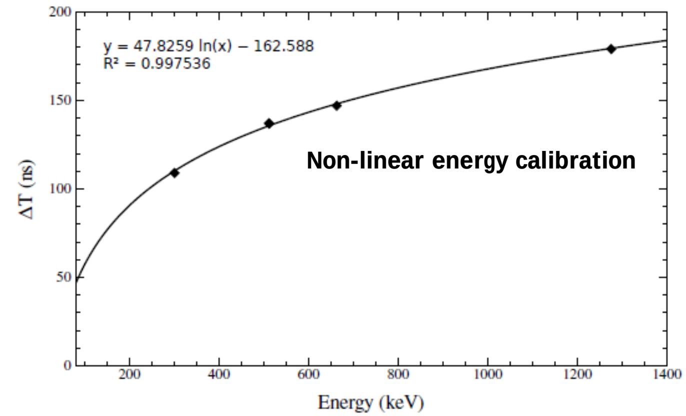

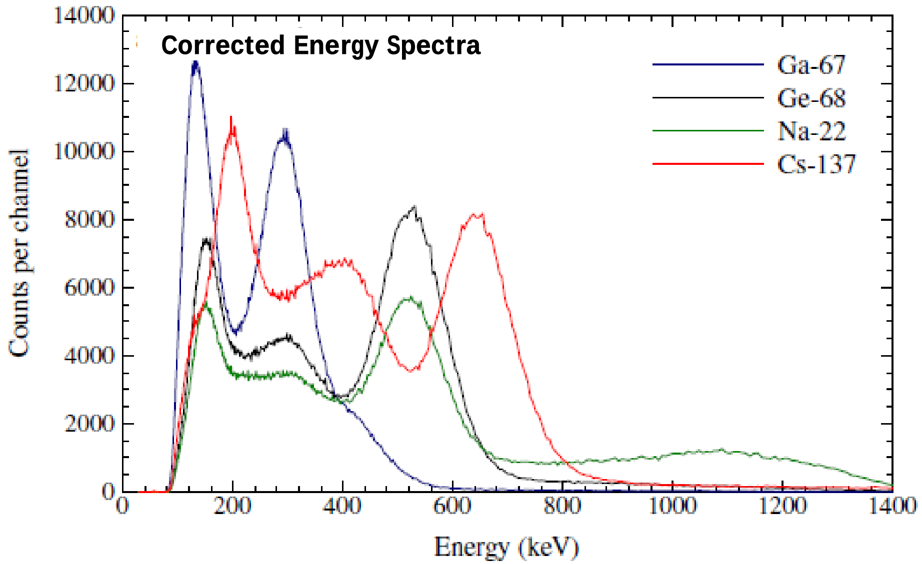

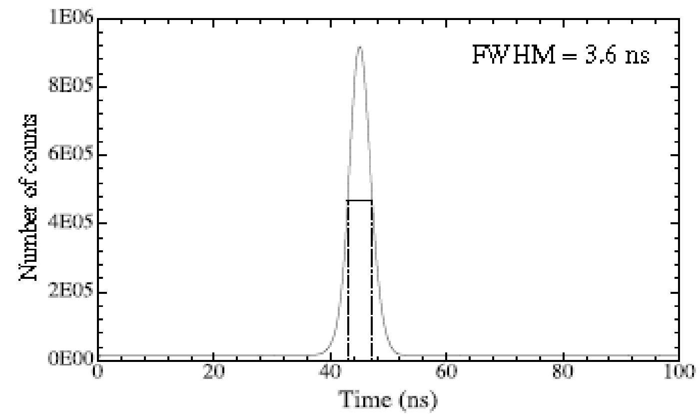

	^{67}Ga	^{68}Ge	^{22}Na	^{137}Cs
Energy (keV)	300	511	511	662
Mean photopeak position (ns)	105±10	135±9	136±9	146±10
Mean ToT resolution (%)	16±1	9±1	7±1	9±1
Mean photopeak position (keV)	293±5	526±8	526±2	659±8
Mean energy resolution (%)	32±3	24±2	25±2	20±2

E Gaudin *et al*. Performance characteristics of a dual-threshold Time-over-Threshold APD-based detector front-end module for PET imaging. *IEEE TNS/MIC 2015*, N2AP-102

LabPETII Detector Front-End

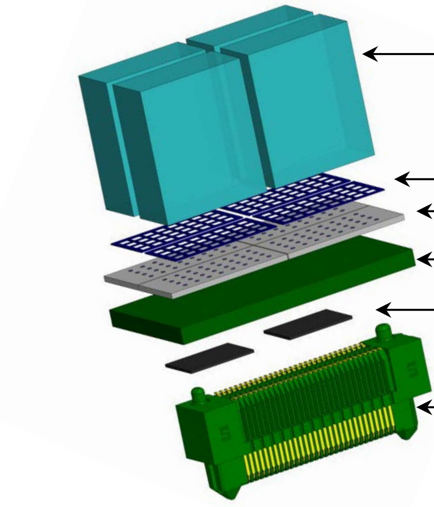

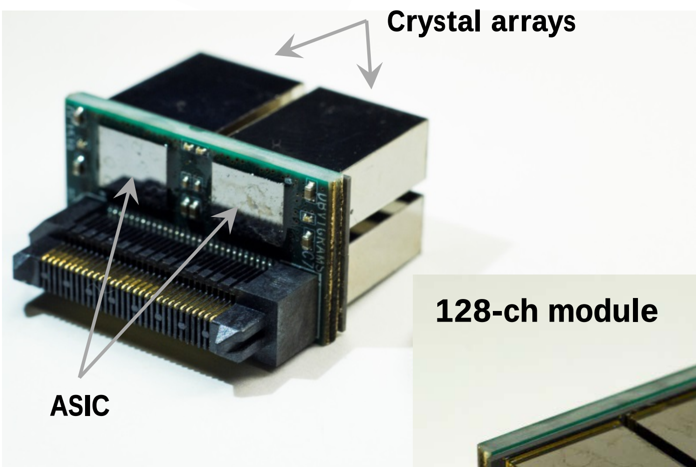

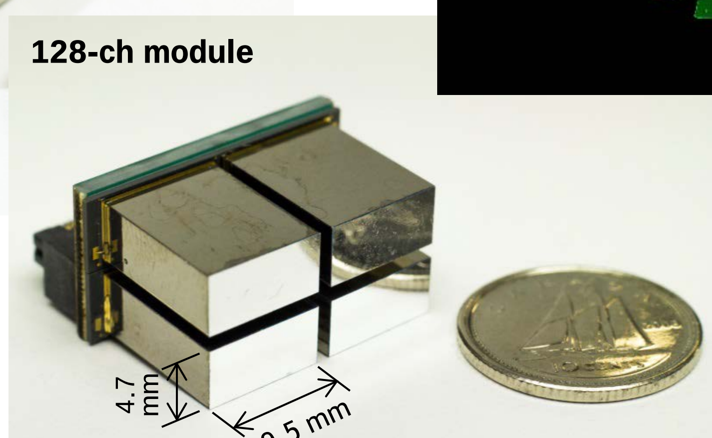

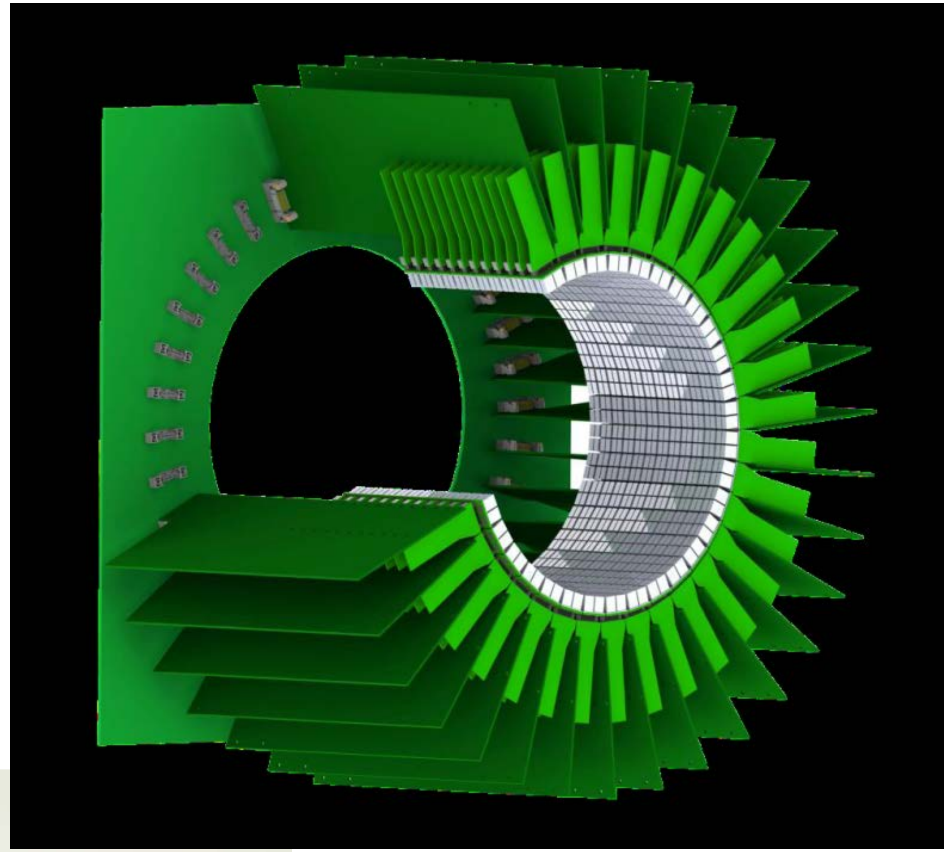

Modular design

CMC MICROSYSTEMS

AGILE TECHNOLOGIES

EXCELITAS TECHNOLOGIES

CIMS

LabPETII DAQ System

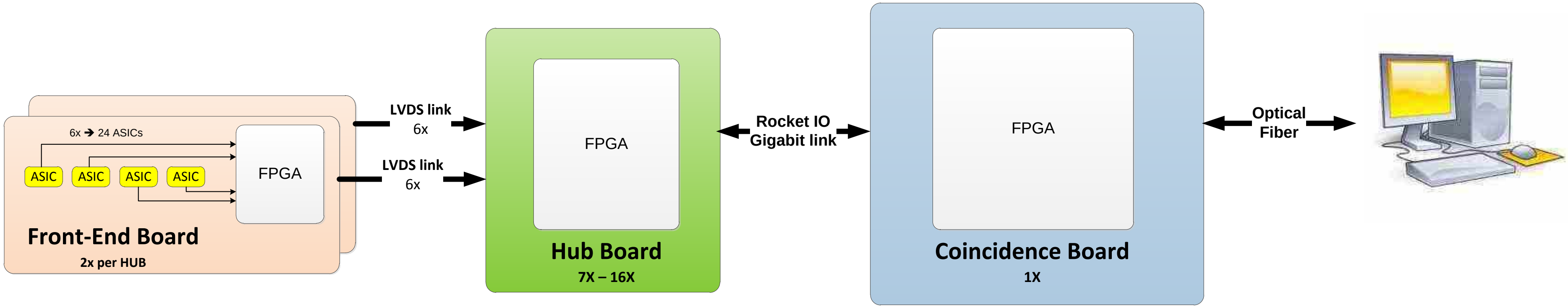

L Njejimana et al. Design of a real-time FPGA-based DAQ architecture for the LabPET II, an APD-based scanner dedicated to small animal PET imaging. *IEEE Transactions on Nuclear Science* 60:3633-3638, 2013

LabPETII DAQ System

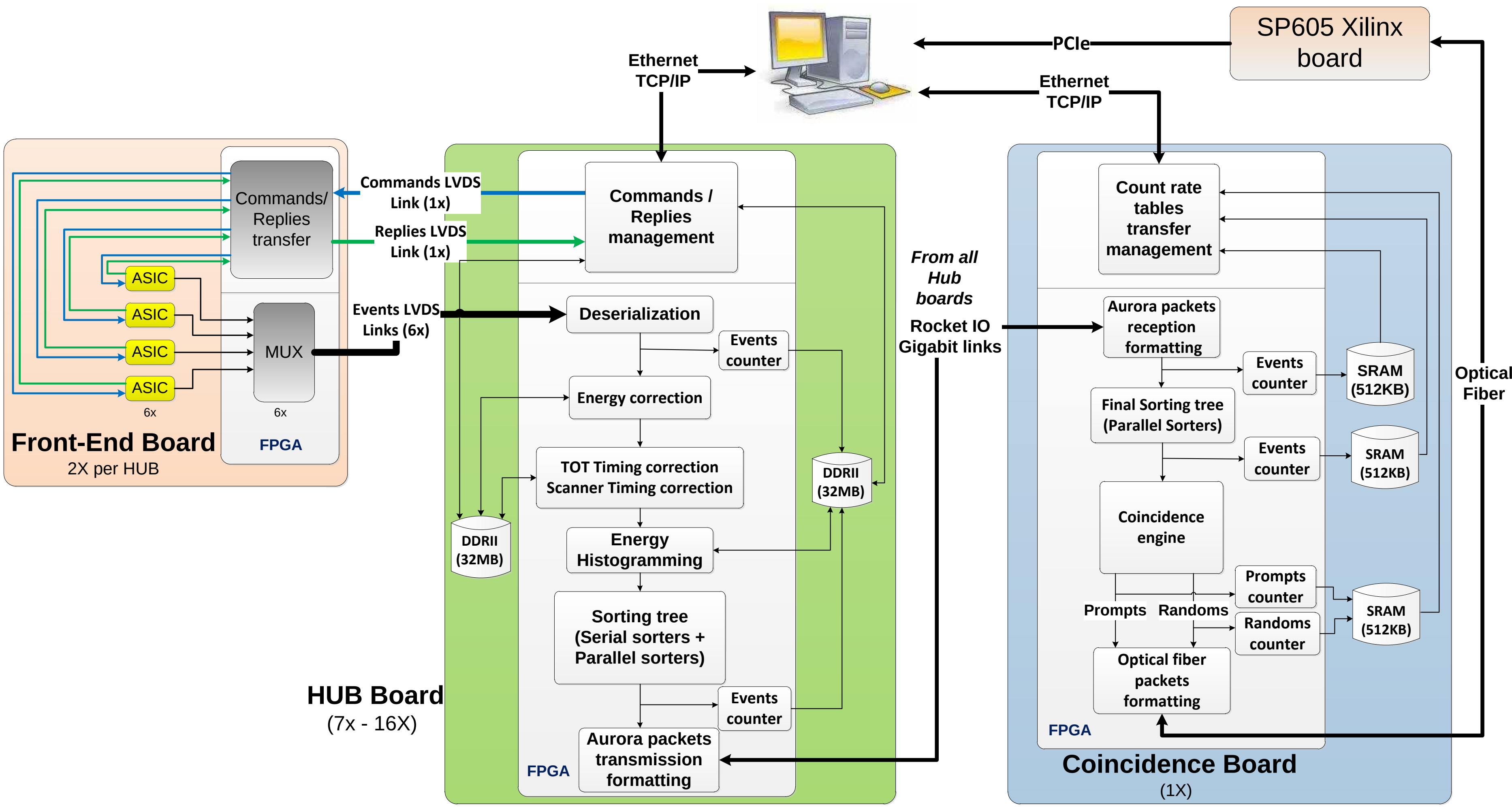

L Njejimana et al. Design of a real-time FPGA-based DAQ architecture for the LabPET II, an APD-based scanner dedicated to small animal PET imaging. *IEEE Transactions on Nuclear Science* 60:3633-3638, 2013

LabPET II Generic Detector Technology

Mouse Scanner

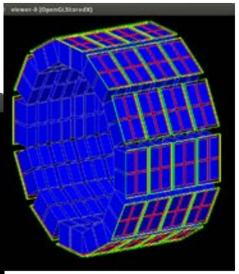

6,144 channels

Rat Scanner

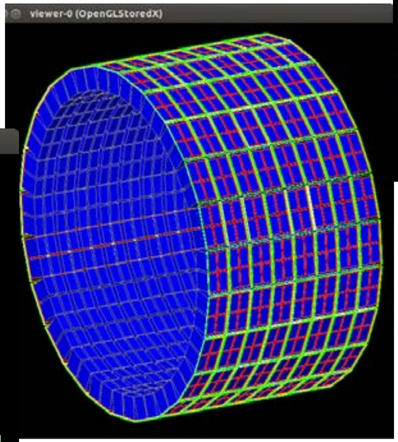

24,576 channels

Rabbit Scanner

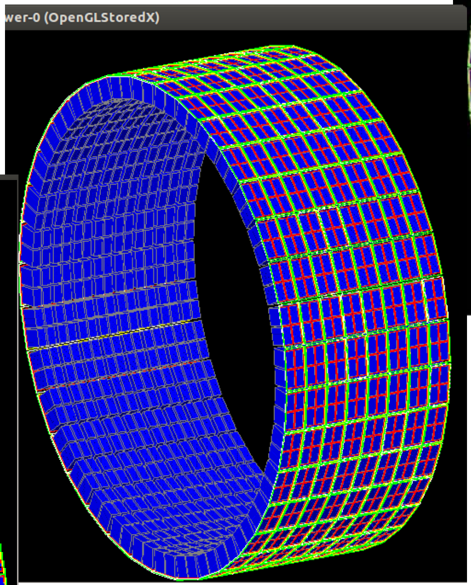

49,152 channels

Human Brain Scanner

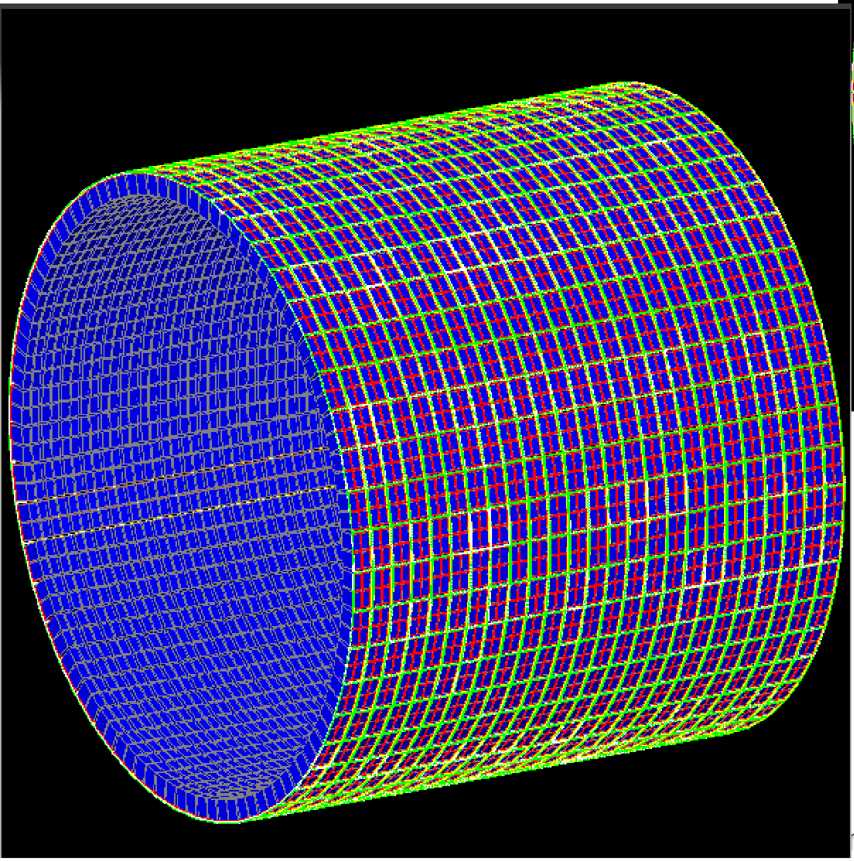

129,024 channels

LabPETII Mouse Scanner

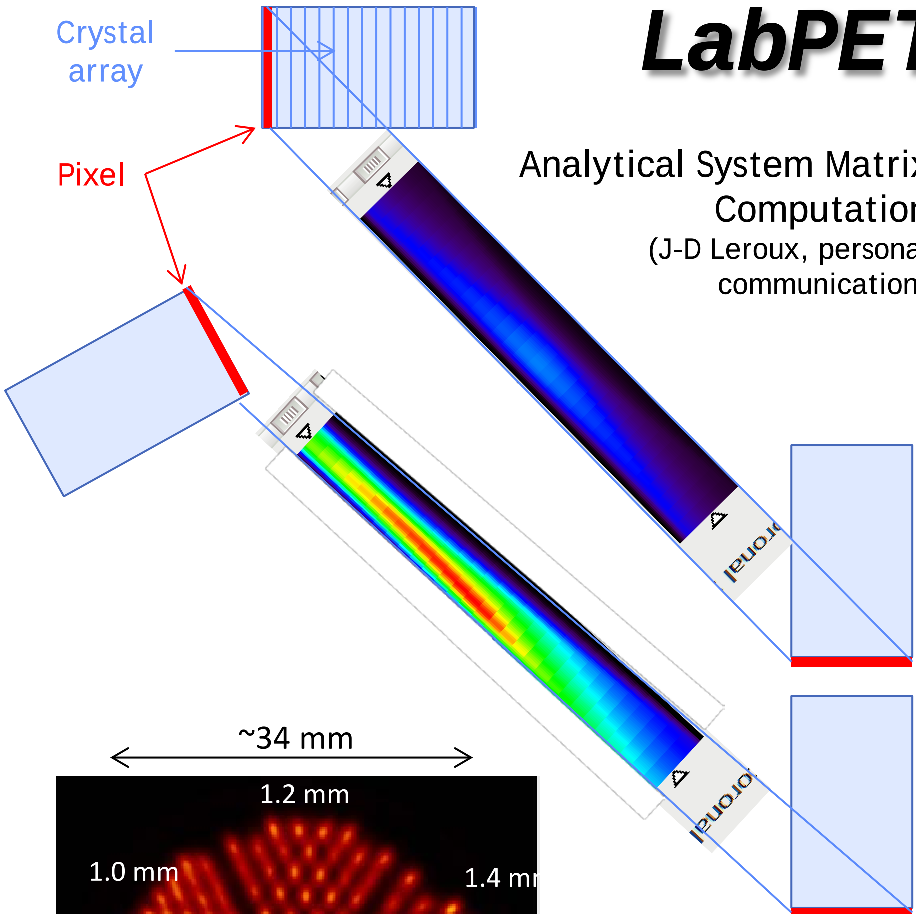

Analytical System Matrix Computation
(J-D Leroux, personal communication)

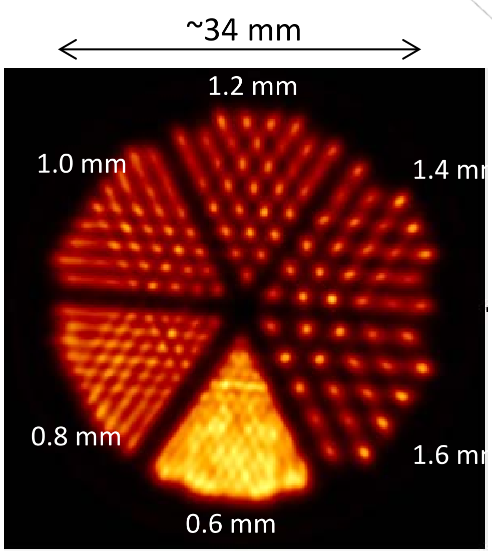

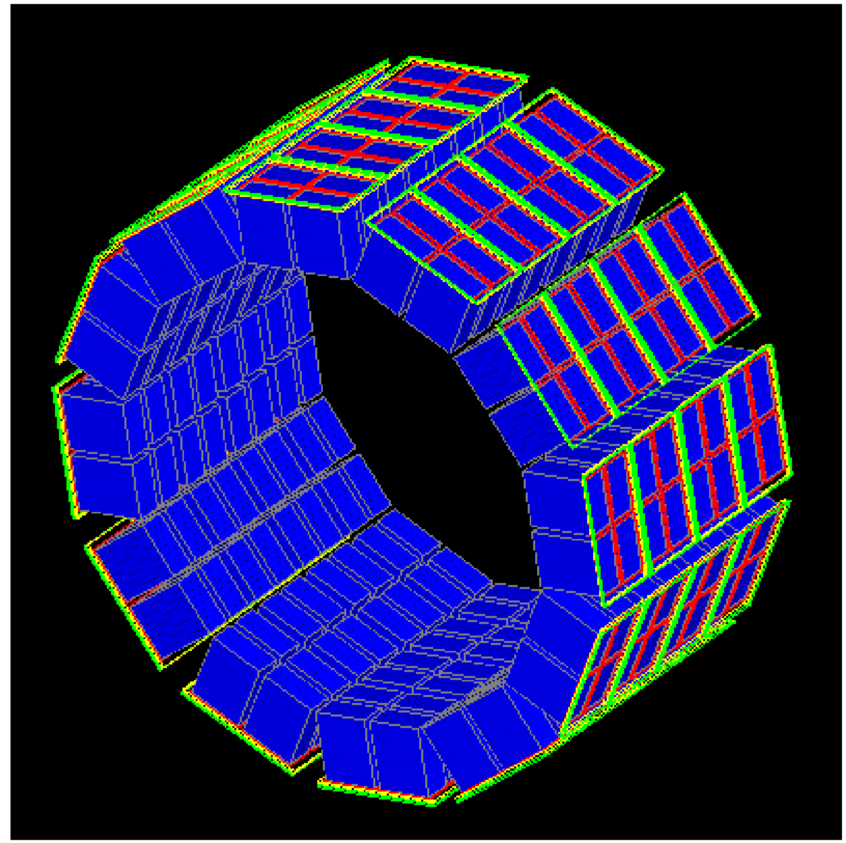

79 mm ID
30/45/60 mm FOV
51 mm axial

6144 channels
4×8 crystal arrays
4 crystal arrays / module
128-ch modules
12 modules/ring → 192 pixels/ring
4 rings of modules → 32 pixel rings
48 detector modules

- ✓ **~0.8 mm resolution achieved**
- ✓ **DOI desirable**

LabPET II (Mouse) First Image

Prototype Mouse Scanner

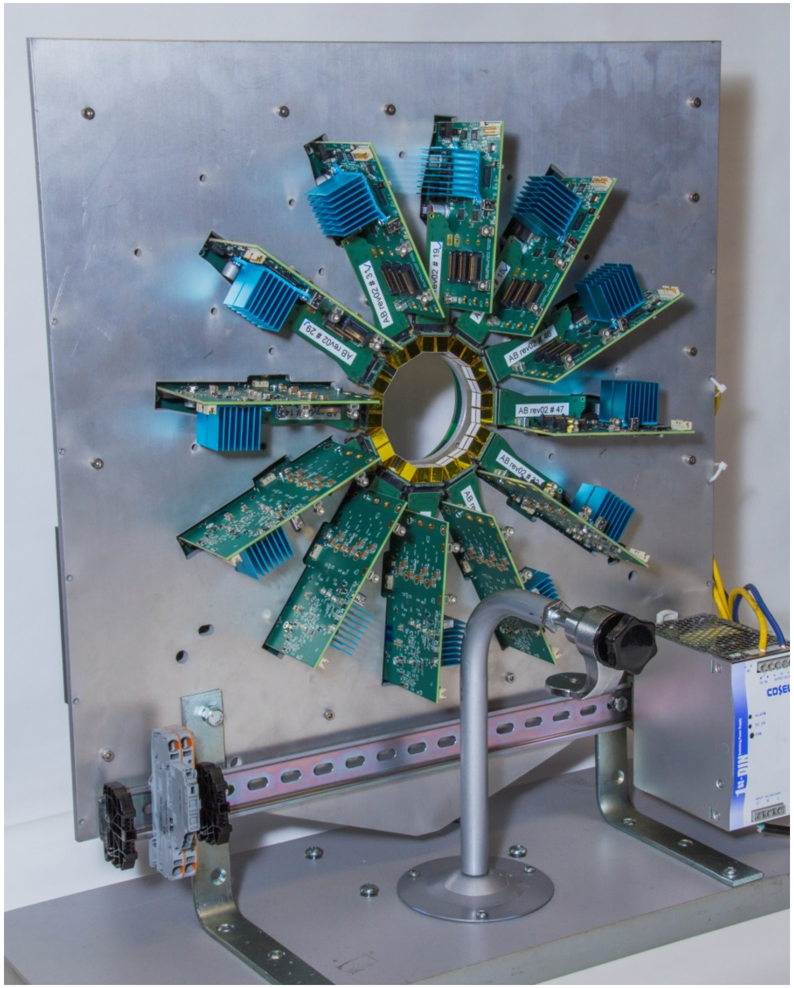

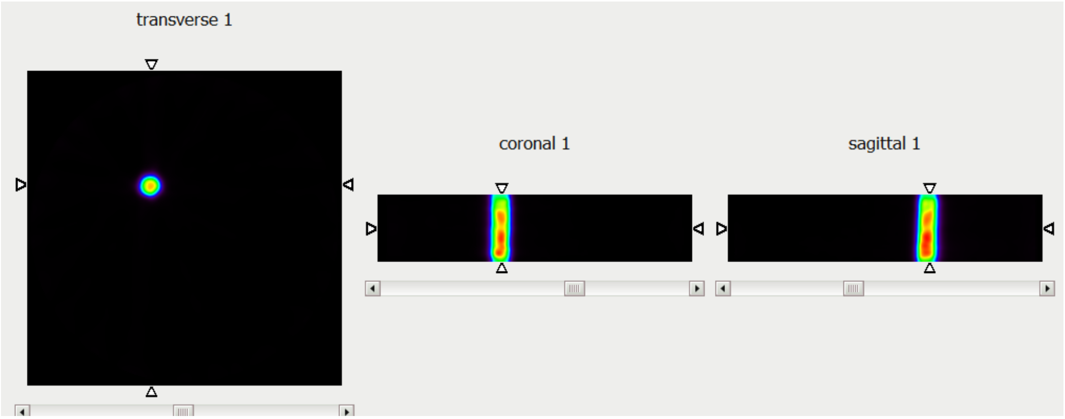

- Rod source 1.52 mm∅
- 10 MLEM iteration
- Analytical system matrix
- ~1.6 mm FWHM
- *No efficiency normalisation*
- *Still detector misalignment*

Current and Future Developments

- **Combined dual modality PET/CT**
- **Time-of-Flight PET**

Dual Modality PET/CT

CT PET

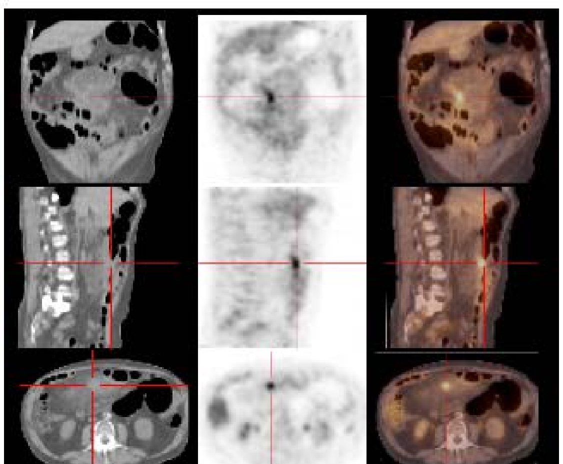

CT PET Fusion

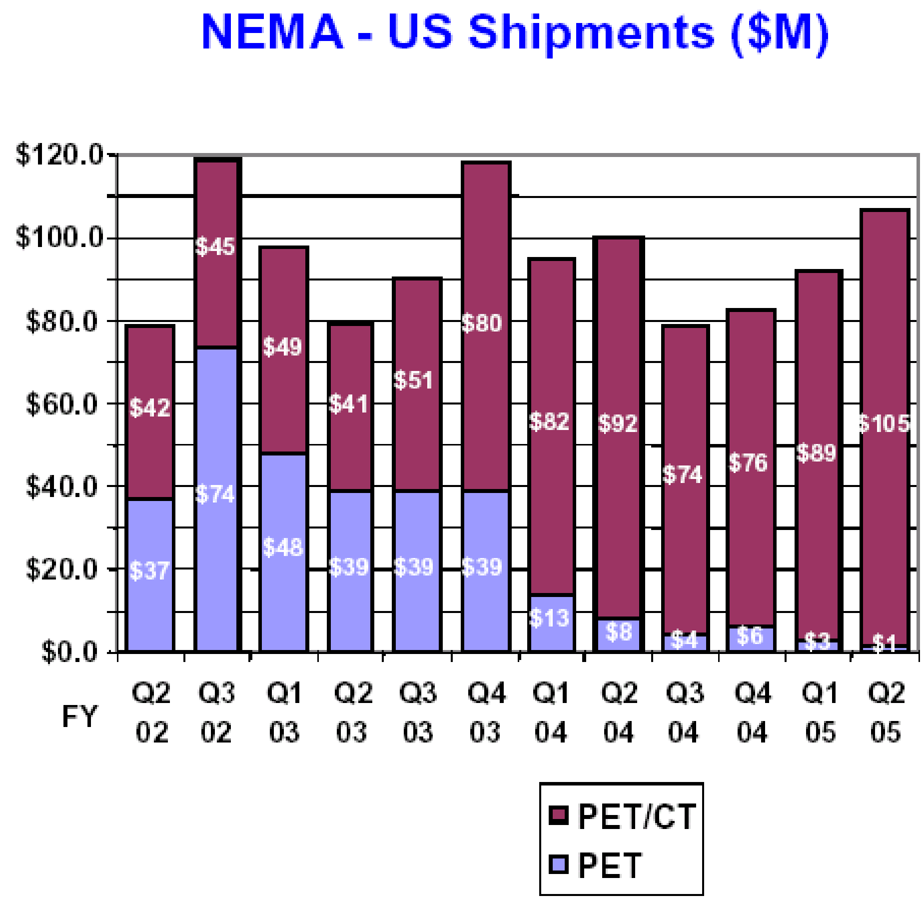

Using PET Detectors for CT ?

Motivation

- ✓ Common detection system
- ✓ Reduced cost
- ✓ Concurrent (simultaneous?) imaging of anatomy and molecular processes
- ✓ Perfect co-registration of PET and CT images in *space* and *time*
  - ⇒ Co-registered dynamic image series
  - ⇒ Correction of motion in CT image

Challenges

- ? Compromises on PET, CT, or both

Opportunity

- ✓ PET detectors are photon counting

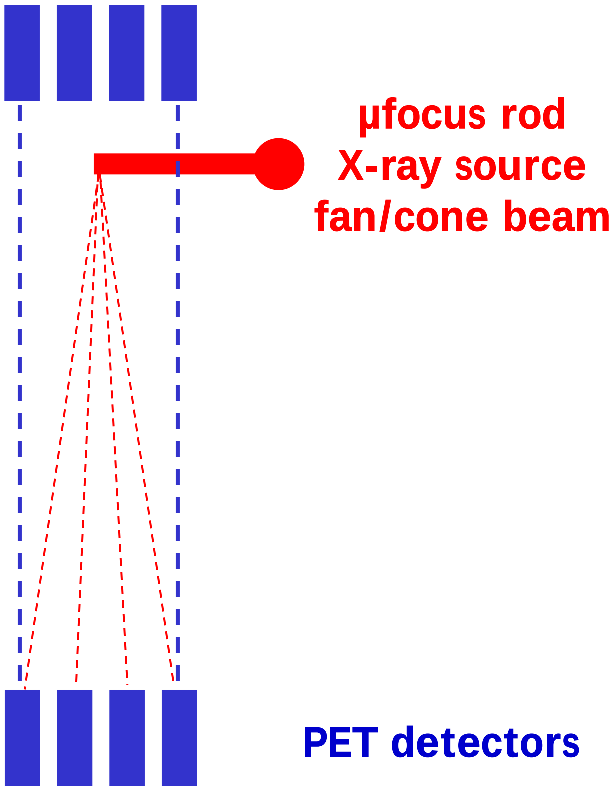

Hardware fusion of PET & CT

Spatial Resolution in μCT*

$$FWHM_{total} \approx \sqrt{FWHM_d^2 + FWHM_x^2}$$

$$FWHM_d \approx 2.35 \left(\frac{1}{M}\right) \frac{\Delta x}{2}$$

$$FWHM_x \approx M \times X_f$$

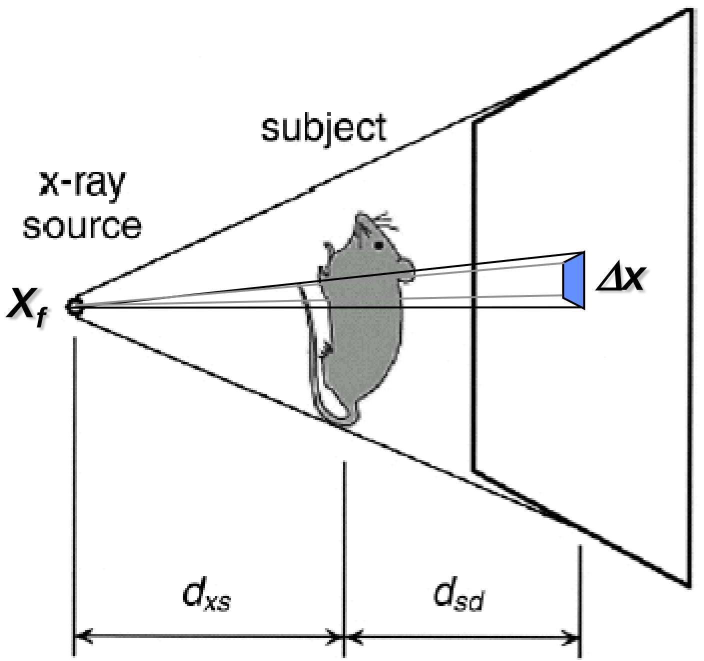

$FWHM_d$: *detector resolution*

$FWHM_x$: *projection blurring due to X-ray focal spot size*

Δx : *pixel size*

X_f : *focal spot size (FWHM)*

M : *Magnification*
$M = (d_{xs} + d_{sd}) / d_{xs}$

* M.J. Paulus et al., "High resolution X-ray computed tomography: an emerging tool for small animal cancer research", *Neoplasia* 2 (1-2), pp. 62-70, Jan-April 2000

Spatial Resolution in µCT

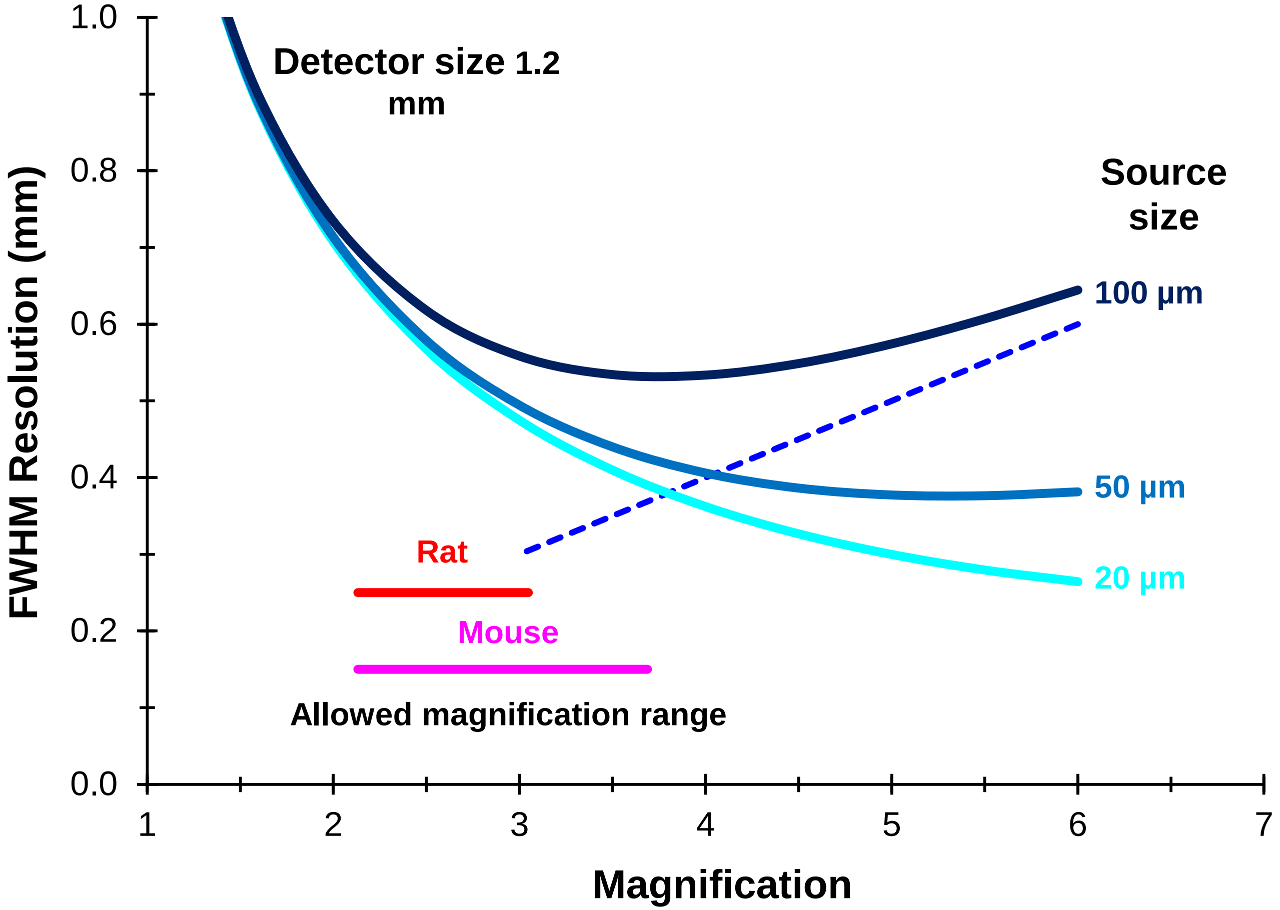

✓ **Rat: ~500 µm @ M=3.0**

✓ **Mouse: ~400 µm @ M=3.7**

→ **Microfocus X-ray source and magnification required for best performance**

→ **Range of allowed magnification with X-ray source inside PET ring**

Proof of Concept

- LabPET detectors & digital DAQ
- X-ray tube: 65 kVp, 20 μA, 50 μm focal spot
- Magnification M=2
- 16 2×2 mm^2 LYSO pixel detectors
- Parallel FBP (Nyquist cutoff)

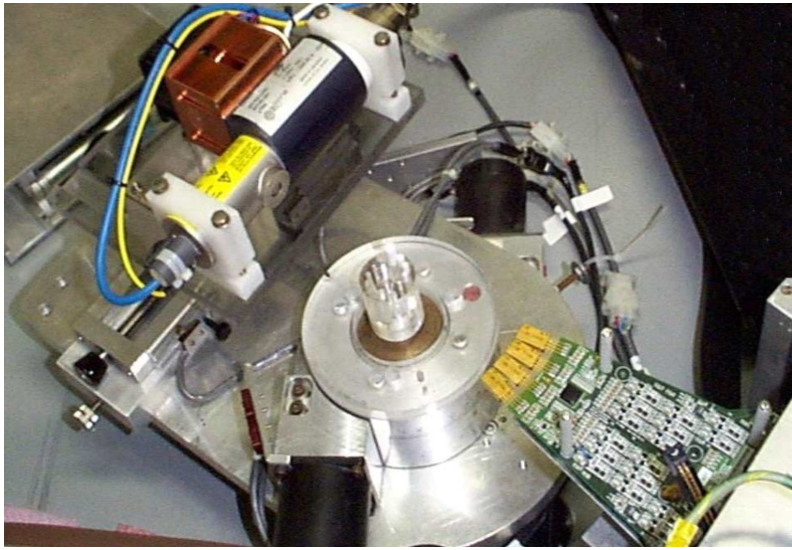

✓ **Biological tissue-like materials can be discriminated with sufficient accuracy**

	Average (HU)	Standard deviation (HU)	Density (g/cm^3)	
1. Air hole	-967.0	17.5	1.2×10^{-3}	~ Lung
2. Polystyrene	-89.5	17.6	1.06	~ Fat
3. Polyethylene	-123.6	18.4	0.93	~ Fat
4. Teflon	306.4	37.1	2.25	~ Bone
5. Nylon	58.0	15.8	1.15	~ Soft tissue
6. Polycarbonate	35.5	16.0	1.2	~ Soft tissue
Plexiglas	107.6	18.1	1.19	~ Porous bone

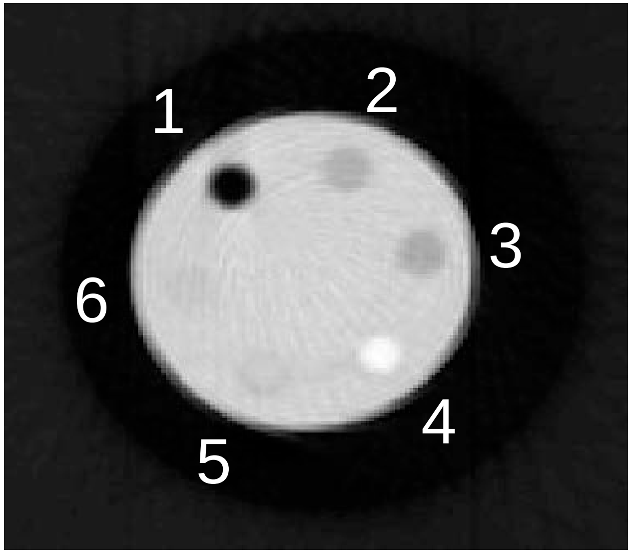

35 mm diameter phantom
5 mm inserts
1.3 mGy

Bérard et al, "Investigation of LabPET detector and electronics for photon-counting CT imaging", NIM A571 114-117, 2007)

Counting CT Imaging

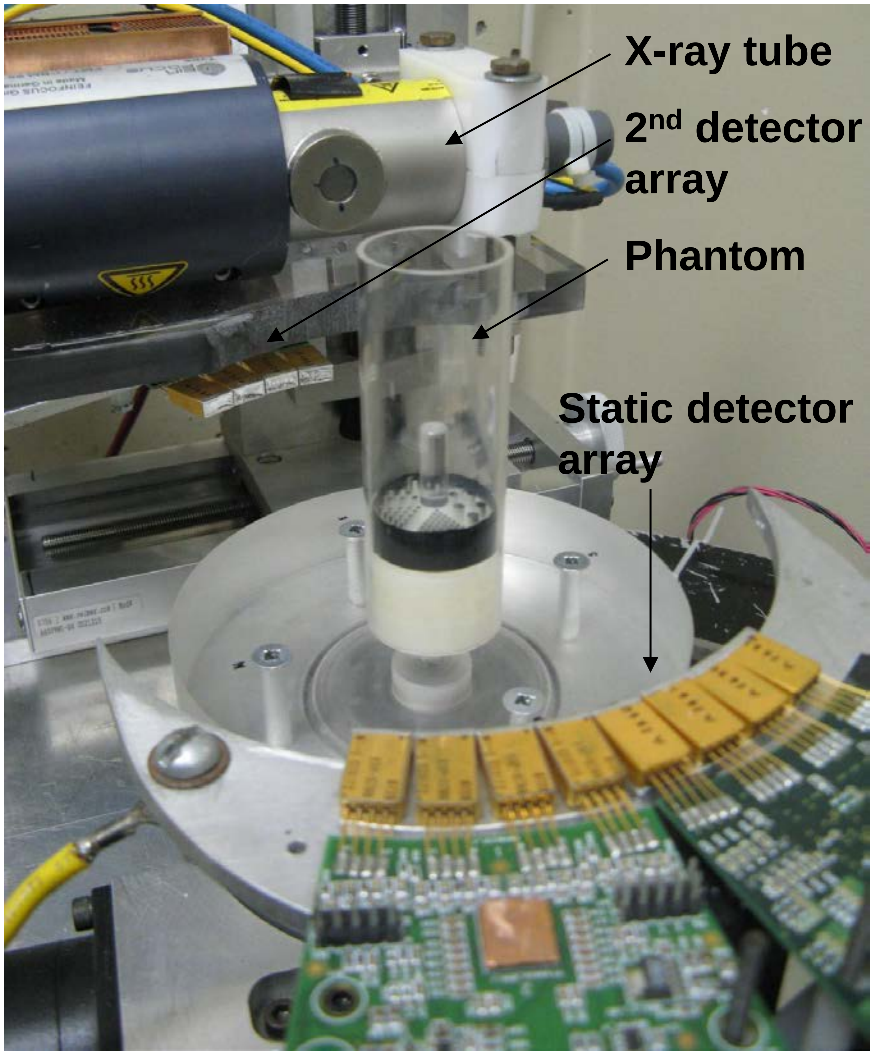

Thidaudeau et al, *Med Phys* 39:5697-5707, 2012
2009 NPSS-MIC Poster Student Paper Award

- ✓ Counting CT imaging with LabPET detectors and electronics

3D rendering of bone and tissues with corresponding axial slices obtained with CT WB scan (75 slices)

20 g mouse

Resolution: ~1.18 mm (M=2)

Acquisition Time: 500 ms (<3 min/slice)

Counting CT Imaging

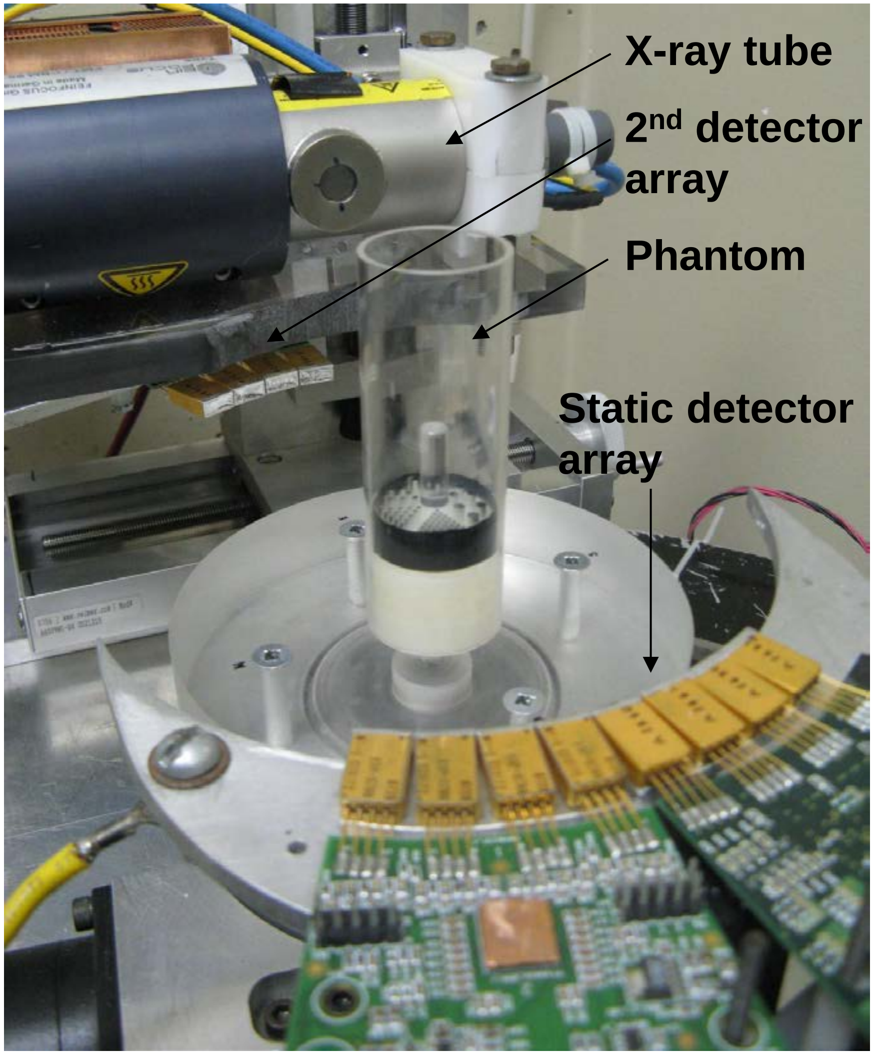

Thidaudeau et al, *Med Phys* 39:5697-5707, 2012
2009 NPSS-MIC Poster Student Paper Award

- ✓ Counting CT imaging with LabPET detectors and electronics

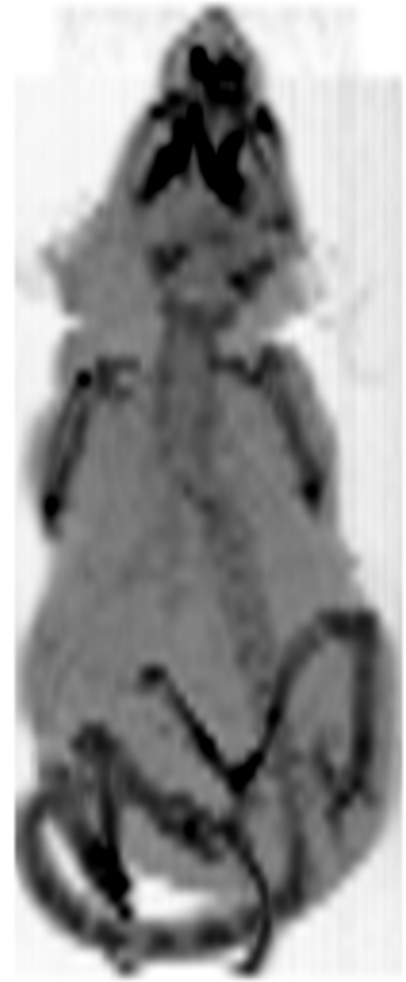

PET/Counting CT Image Fusion

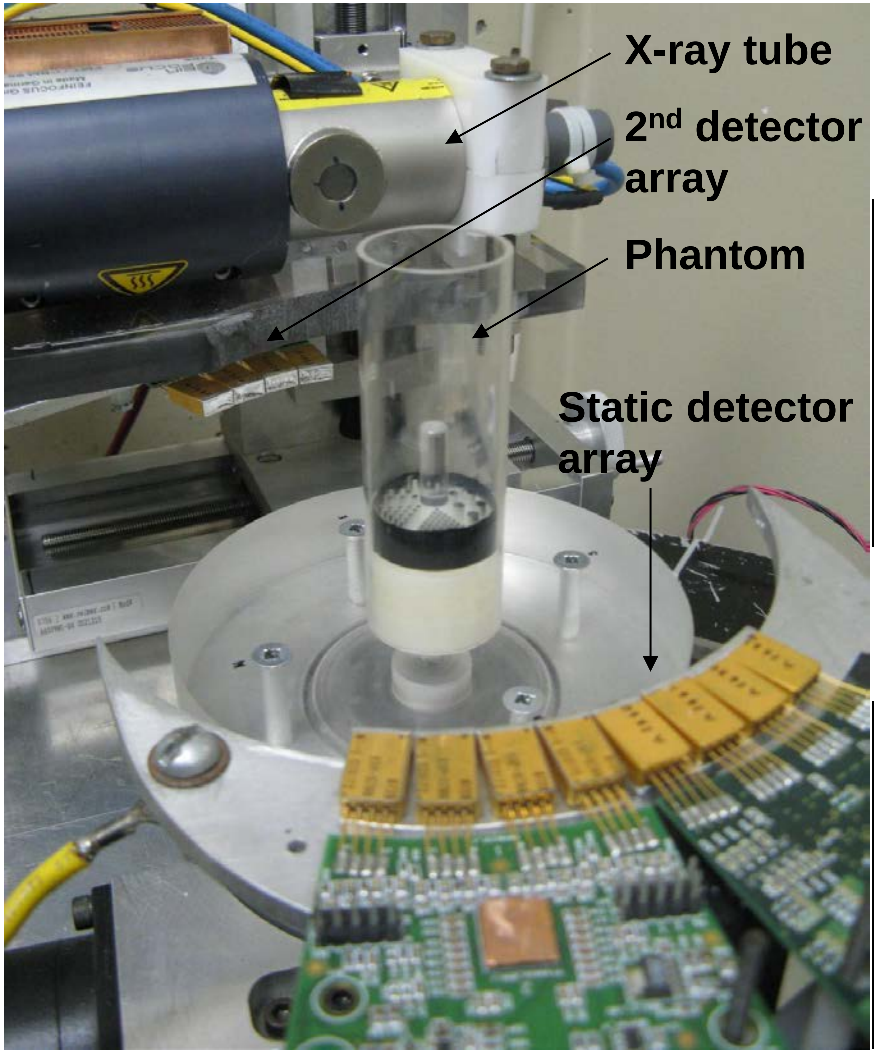

Thidaudeau et al, *Med Phys* 39:5697-5707, 2012
2009 NPSS-MIC Poster Student Paper Award

✓1st PET/CT images with PET detectors

CT | **PET** | **PET/CT**

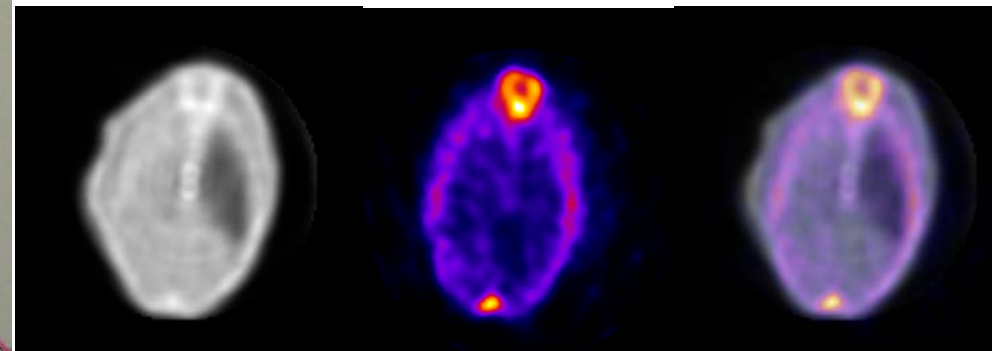

$Na^{18}F$ (2 mCi) PET/CT image fusion of slice through lungs of mouse (CT: 1 s; PET: 10 min)

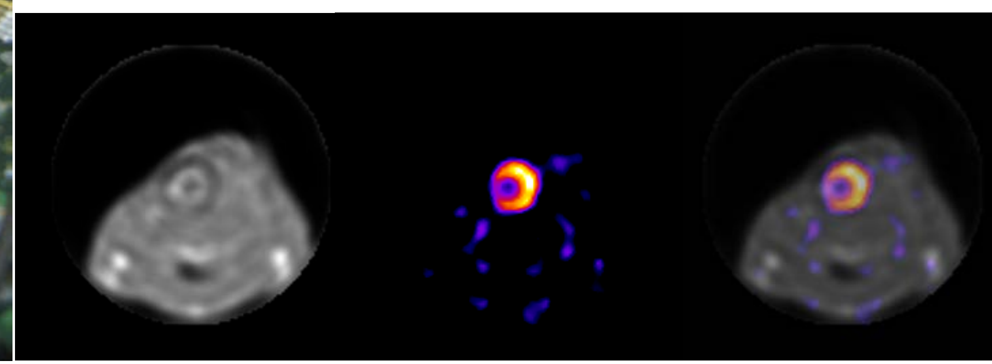

^{18}FDG (2 mCi) PET/CT image fusion of slice through heart of mouse (CT: 1 s; PET: 10 min)

Counting CT Imaging with LabPET II

LabPET I digital processing board

Custom analog front-end board with 8 x 16-channel ASIC

LabPET II detector modules (8×8 LYSO arrays) (1.2×1.2 mm^2 pixels)

μfocus 90 kV X-ray tube (65 kV, 200 μA)

Motorized rotating/translating stages)

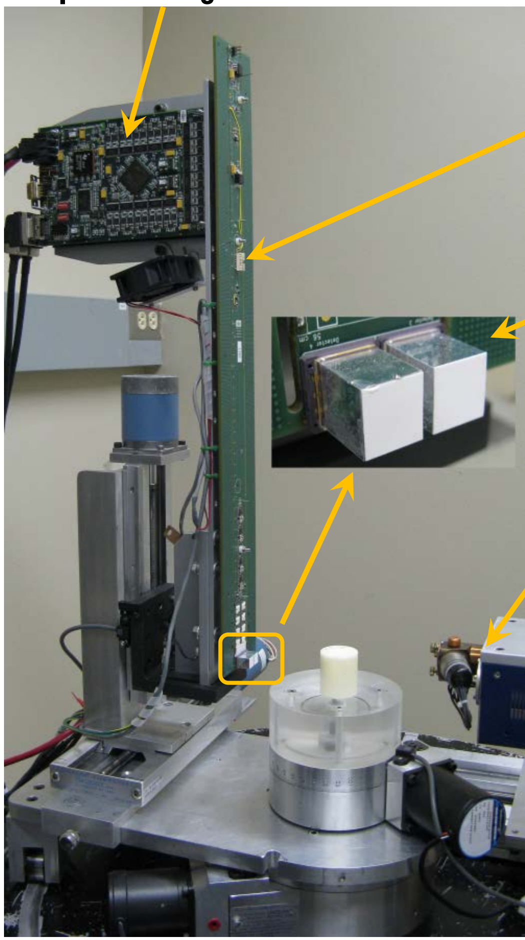

Bergeron et al, "LabPET II, an APD-based PET detector module with counting CT imaging capability", *2011 NSS/MIC*, Valencia, Spain, 23-29 Oct. 2011. ***[Finalist 2011 NPSS-MIC Oral Student Paper Award]***

✓ cCT imaging with **LabPET II** detectors and electronics

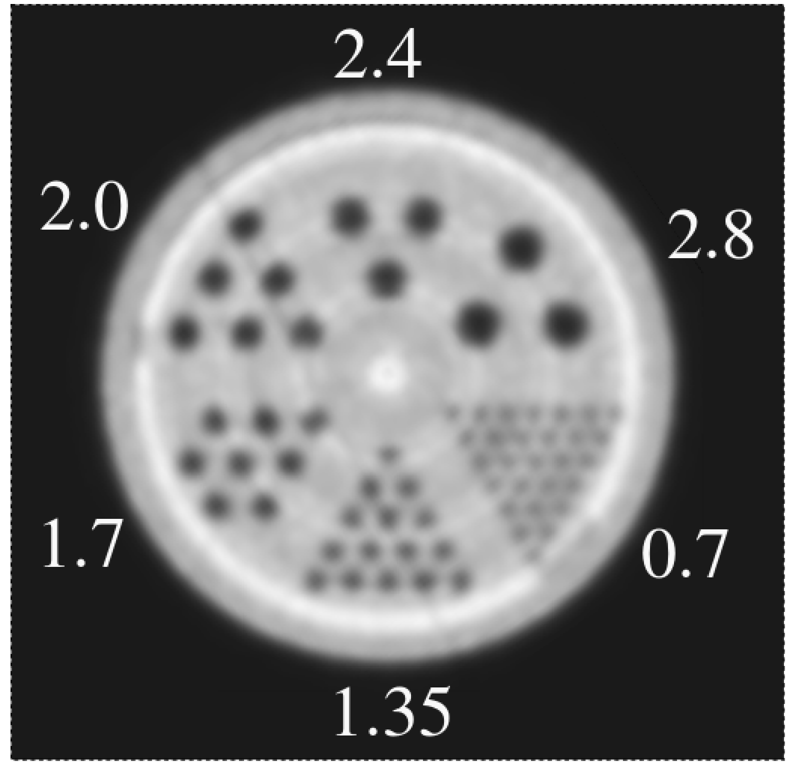

180 projections over 360°

500 ms time frame

Magnification of 2

OSEM reconstruction (10 iterations)

LabPET/CT

Under construction at CIMS

16.6 cm diam
10.3 mm axial FOV
48 modules / ring
Single ring of LabPET II modules
8 rings of detectors
384 detectors / ring
3072 detector channels

LabPET I ASICs on custom PCB
LabPET I Digital processing

µfocus X-ray tube inside PET detector ring

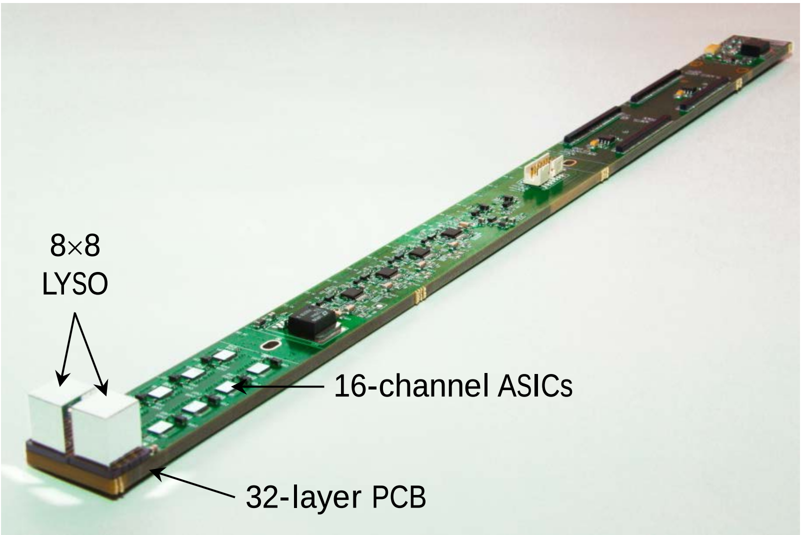

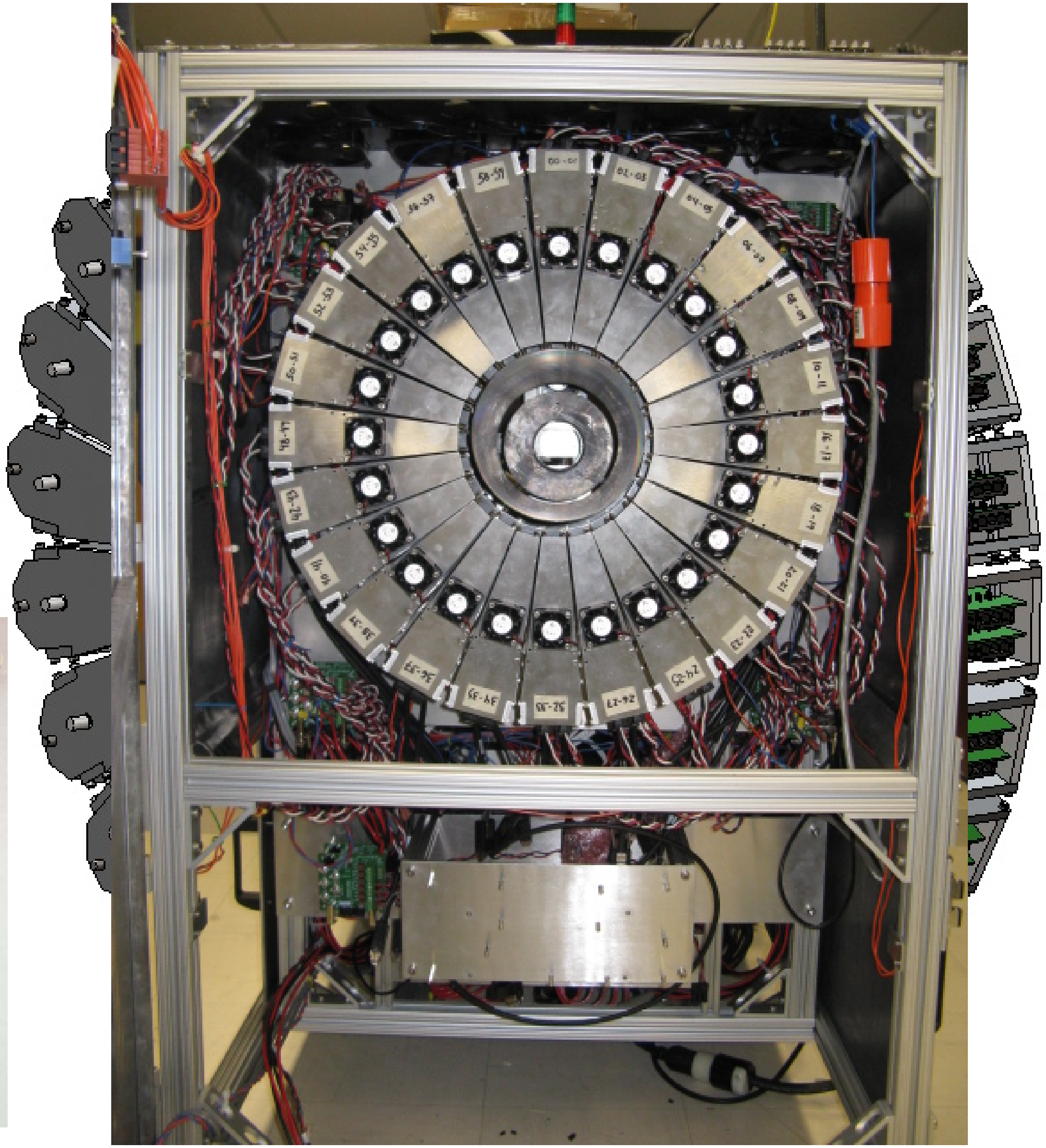

Count rate capabilities

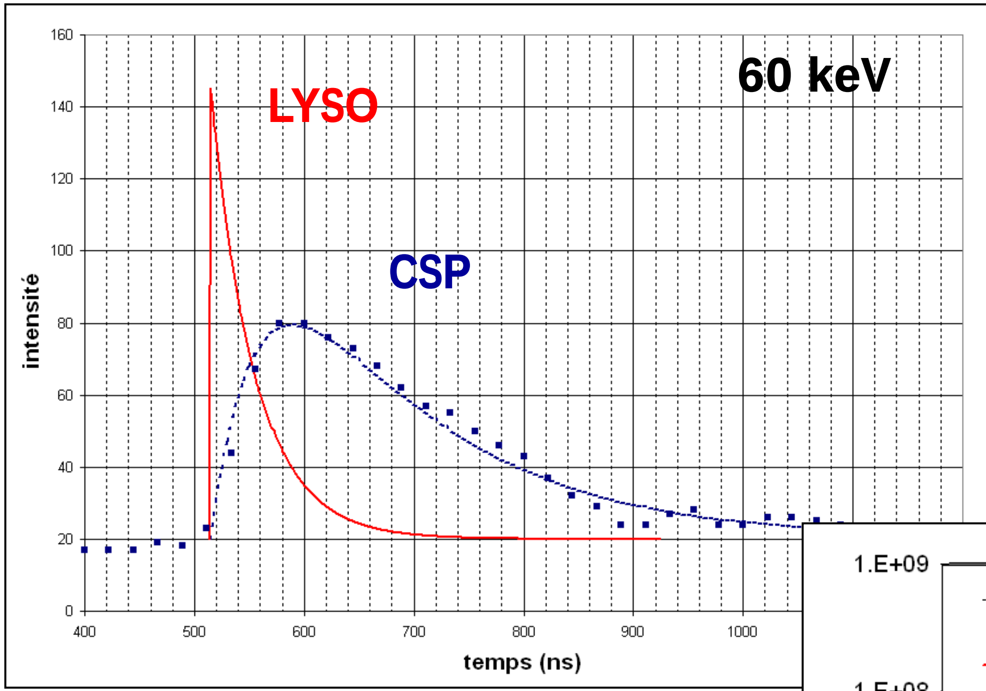

$$I = c(E) \times \left(e^{-t/\tau_p} - e^{-t/\tau_s}\right)$$

τ_p = 100 ns

τ_s = 45 ns (LYSO + APD)

~25% dead time @ ~2.8 Mcps

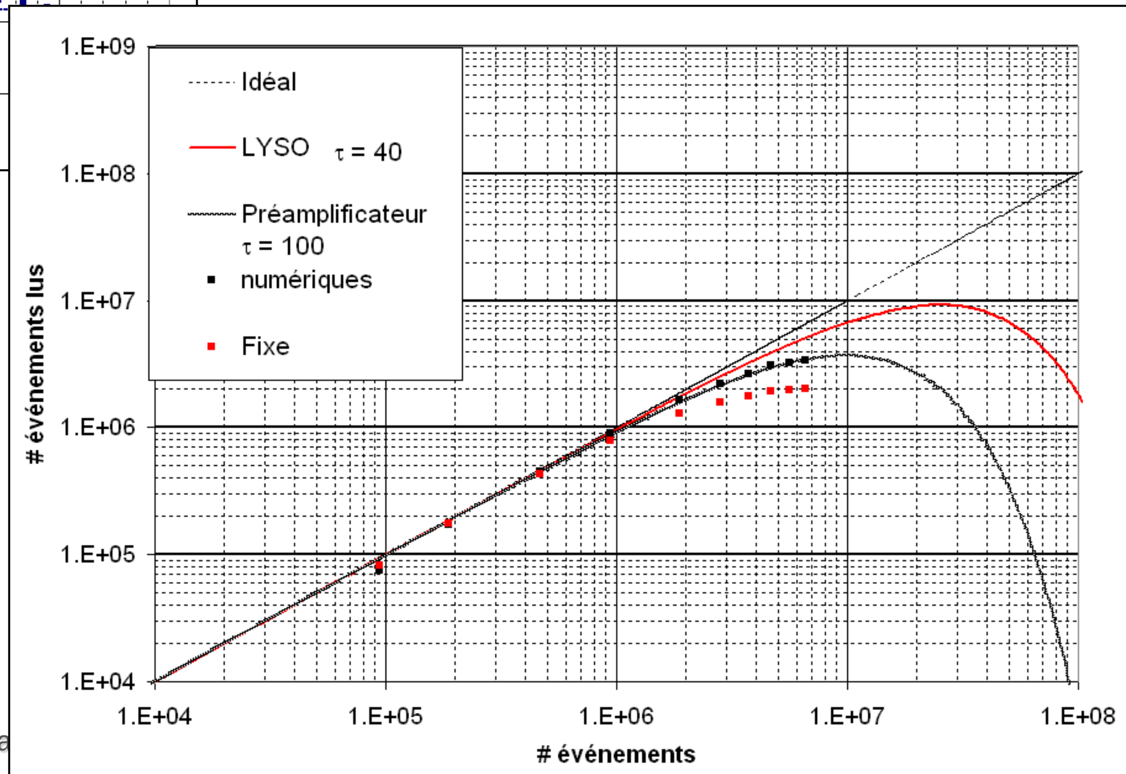

Riendeau et al, "High rate photon counting CT using parallel digital PET electronics", *IEEE TNS* 55:20-27, 2008

Time-of-Flight PET Systems

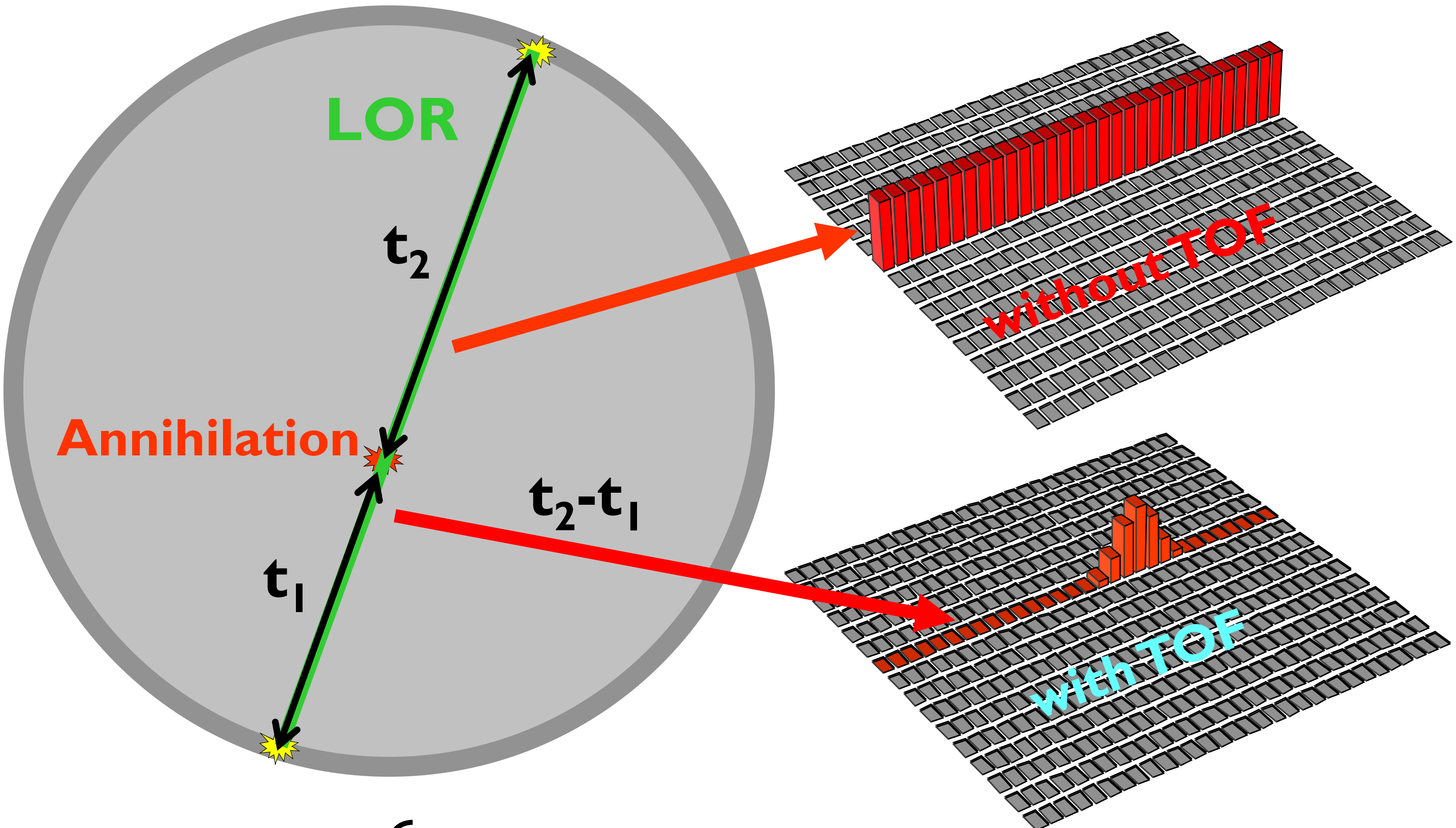

$$\Delta x = \frac{\Delta t \times c}{2} \begin{cases} \Delta t \approx 100 \text{ ps} \\ \Delta d \approx 1.5 \text{ cm} \end{cases}$$

$$c = 30 \text{ cm/ns}$$

Courtesy Matthias Egger, Philips Medical Systems

ToF Reconstruction

3D-Ramla
non-ToF

LOR Ramla
non-ToF

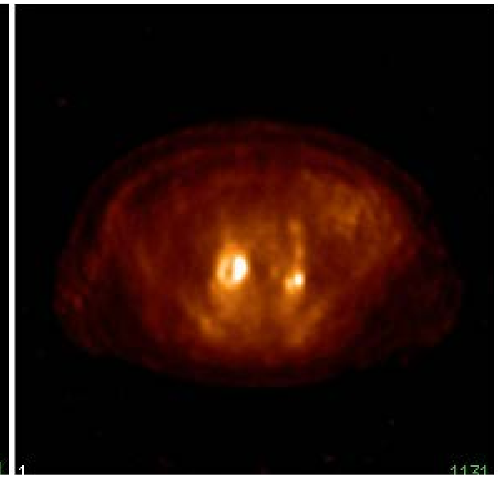

list-mode (IRX)
non-ToF

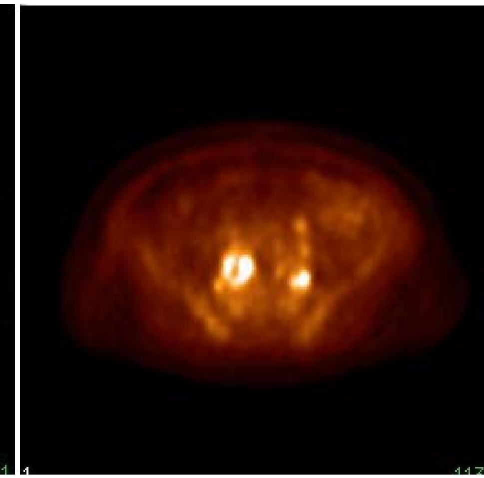

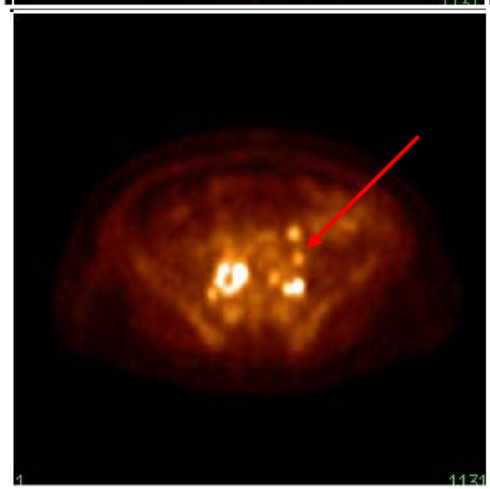

List-mode (IRX)
ToF

Rectal carcinoma metastases in mesentery and bilateral iliac chains

114 kg; BMI = 38.1
12 mCi; 2 hr post-inj

Data courtesy of J. Karp, University of Pennsylvania

Effective Sensitivity Gain with ToF-PET

$$\frac{SNR_{ToF}}{SNR_{PET}} = \left(\frac{\Delta x^2}{D^2}\right)^{-1/4} = \sqrt{\frac{D}{\Delta x}}$$

But: $SNR \propto \sqrt{\text{Nb Events}} \sim \sqrt{\text{Sensitivity}}$

$$G = \frac{D}{\Delta x} = \frac{2D}{c\Delta t} \approx \frac{\text{Object Dimension}}{\text{ToF Precision}}$$

40 cm Object
Δt = 600 ps

$$\frac{SNR_{ToF}}{SNR_{PET}} = \sqrt{\frac{40\text{ cm}}{9\text{ cm}}} = 2.1 \quad \Rightarrow \quad G = 4.4$$

4 cm Object
Δt = 60 ps

$$\frac{SNR_{ToF}}{SNR_{PET}} = \sqrt{\frac{4\text{ cm}}{0.9\text{ cm}}} = 2.1 \quad \Rightarrow \quad G = 4.4$$

Budinger TF. Time-of-Flight Positron Emission Tomography: Status Relative to Conventional PET. *J Nucl Med* 24(1):73-78, 1983.

Why faster timing in PET?

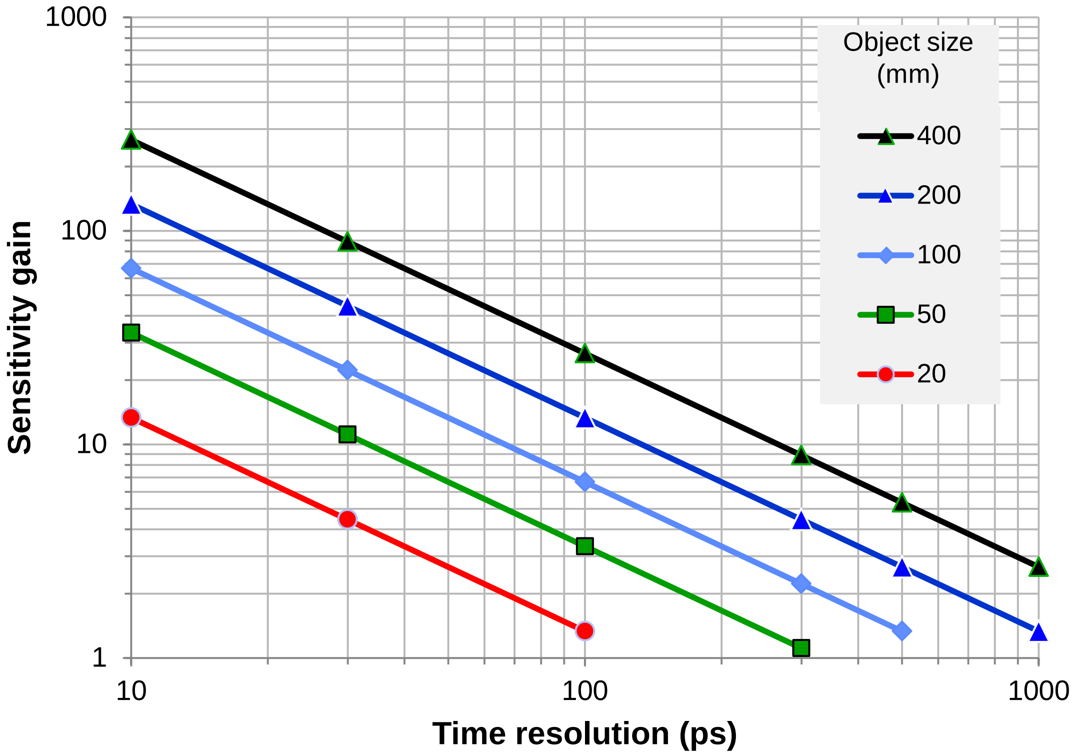

Sensitivity Gain in ToF-PET

$$G = \frac{D}{\Delta x} = \frac{2D}{c\Delta t} \approx \frac{\text{Object Dimension}}{\text{ToF Precision}}$$

- **< 300 ps** ToF resolution
  - ✓ Rejecting background & scatter events (event collimation)
  - ✓ Restoring image quality for limited angle tomography
- **~100 ps** ToF resolution
  - ✓ **×10** sensitivity gain (or equivalent dose reduction) for brain studies
  - ✓ ToF PET of small animals (rat) becomes possible
- **~30 ps** ToF resolution
  - ✓ Mouse ToF-PET imaging becomes possible
  - ✓ **~5 mm** resolution along LOR
  - ✓ Direct 3D information in whole-body PET (**no more reconstruction!**)

No more reconstruction?
Scatter Recovery in ToF-PET

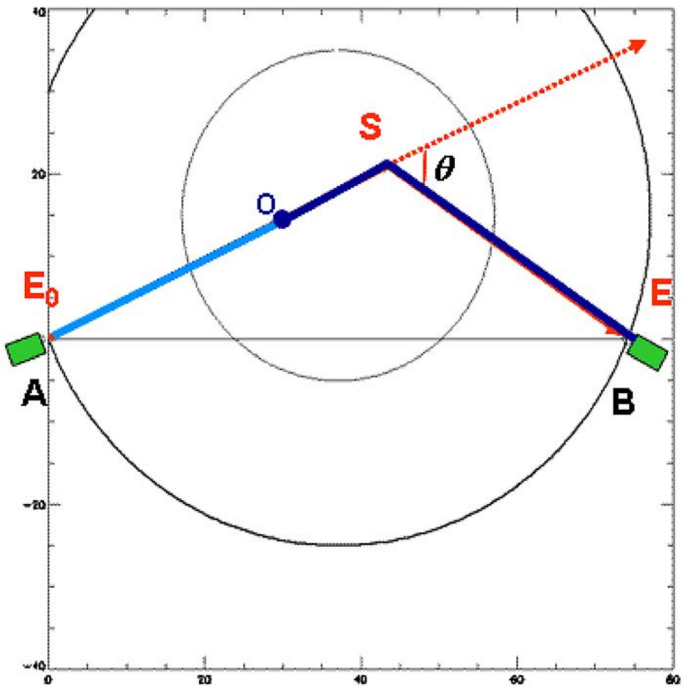

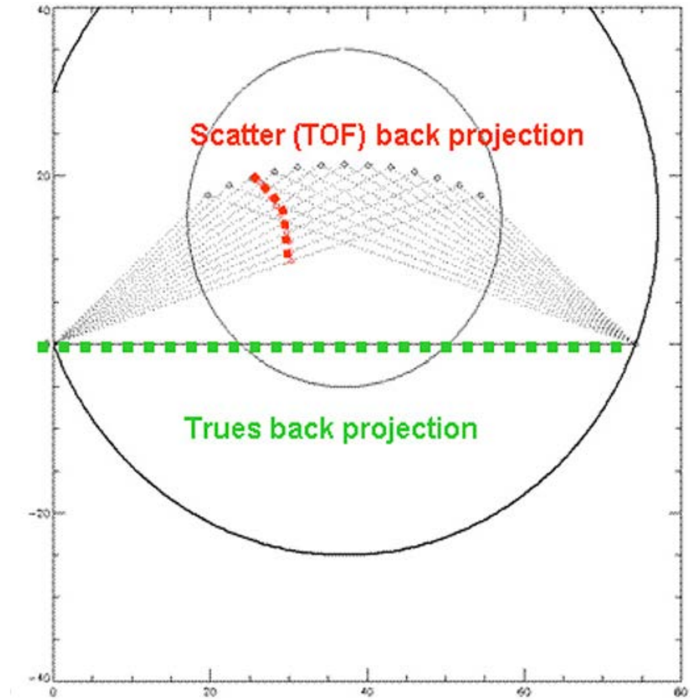

$$E = \frac{E_0}{2 - cos\theta}$$

$$\Delta T = \frac{BS + SO - AO}{c/2}$$

- Backprojection along circular arc
- Iterative reconstruction of both unscattered and scattered events
- Image of trues (unscattered) can be used as *a priori* information

Conti et al. Reconstruction of scattered and unscattered PET coincidences using TOF and energy information. *Phys Med Biol* 57:N307-N317, 2012

Scatter Reconstruction from Compton Kinematics

- ~80% single Compton interactions
- $\cos\theta = 2 - \frac{0.511}{E'}$ $\quad \theta < 90°$

$$\langle P_{AB}(\theta)\rangle = \tau \int_{TCA} \left(\int_A^S f dx\right) \cdot \rho_e(S) \cdot \frac{d\sigma_C^{KN}}{d\Omega} \cdot e^{-\left(\int_A^S \mu dl + \int_S^B \mu' dl\right)} \cdot \epsilon_{AS}\epsilon'_{BS} \left(\frac{\sigma_{AS}\sigma_{SB}}{4\pi R_{AS}^2 R_{SB}^2}\right) dV_s$$

- Backprojection along circular arc
- Object boundaries allows rejection of one arc
- LE threshold ~250 keV
- Very high *energy resolution* required

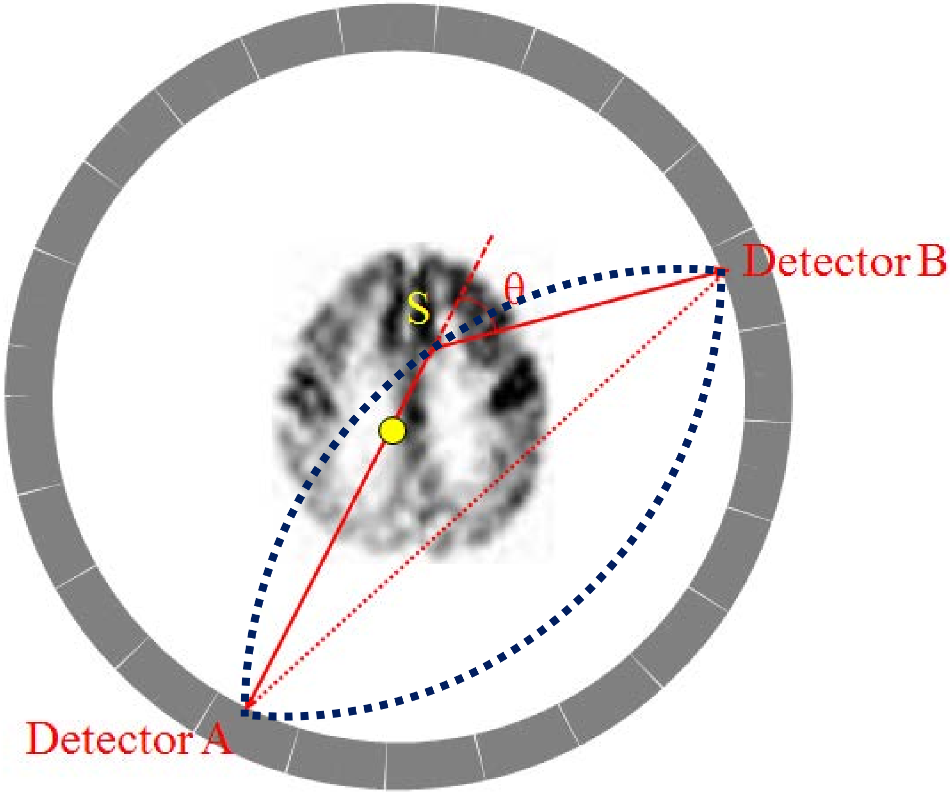

H. Sun, An Investigation into the Use of Scattered Photons to Improve 2D Positron Emission Tomography (PET) Functional Imaging Quality. *Ph. D. Thesis*, U. Manitoba, 2016

Future of Imaging Technology

High-energy physics detector

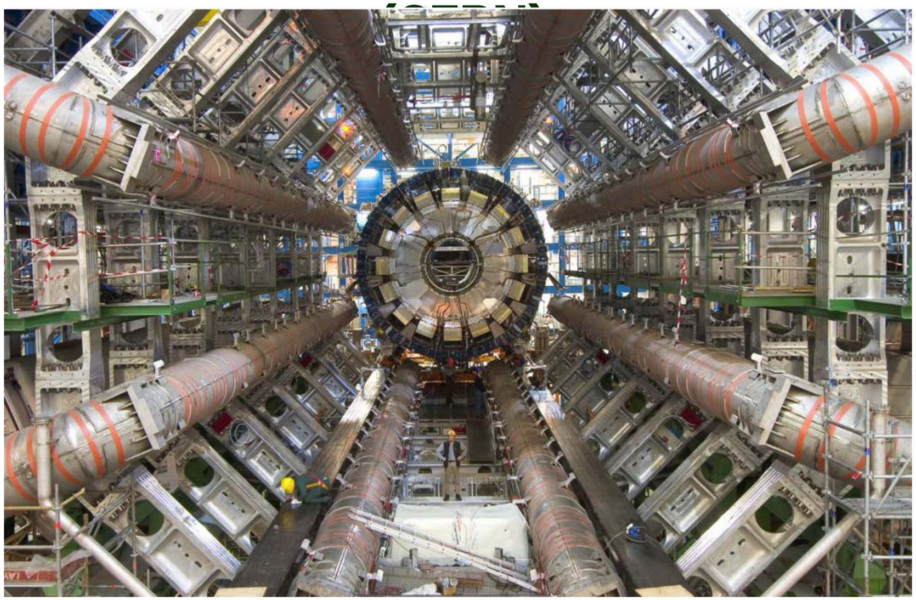

22 m∅ × 40 m
7,000 tons
4,088 Si detectors
50,000 straw detectors
400,000 scintillation detectors

Future PET/MRI scanners

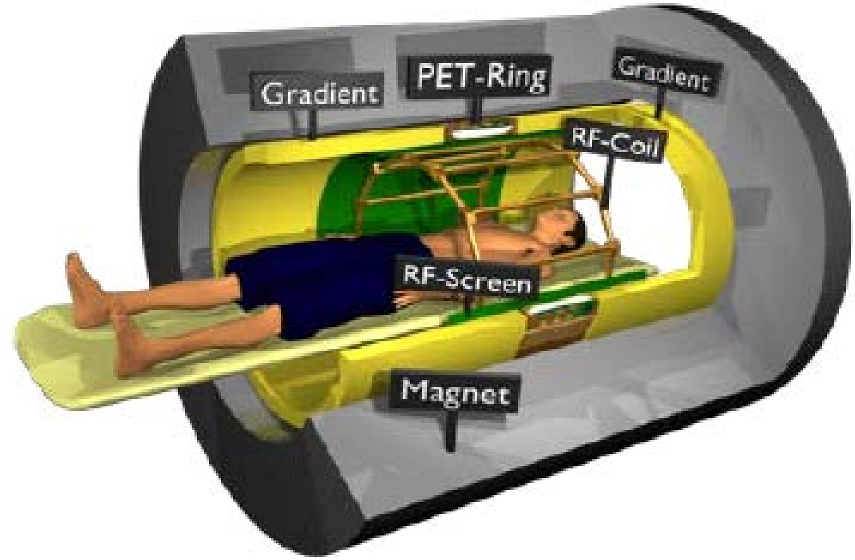

< 80 cm∅ × 25 cm
< 100 kg
~500,000 detectors
1 mm² pixels

Conclusion

- ✓ PET imaging in small animals nearing equivalent spatial definition as clinical PET imaging in humans (~10^3 gain in spatial resolution)
- ✓ Convergence of imaging modalities (PET/CT, PET/MRI...) appears inevitable for obtaining all potential benefits from PET
- ✓ ToF-PET in small animals is within reach with recent technological breakthroughs
  - ⇒ Conventional tomographic image reconstruction might be avoided
  - ⇒ Potential for scatter recovery and higher sensitivity
- ✓ Still substantial progress to be made in detectors, electronics and system integration

Acknowledgments

Special thanks to all those who have contributed :

- **Close collaborators: Prof. Réjean Fontaine**
- **AMI co-founders: Jules Cadorette and David Lapointe**
- **Students & research assistants from CIMS & GRAMS teams**
- **Commercial partners:**
  - **PerkinElmer Optoelectronics / Excelitas Technologies (Dr. Henri Dautet)**
  - **Gamma Medica / TriFoil Imaging**
  - **Marubeni & Hitachi Chemical**
  - **Canadian Microelectronics Corporation**